# Investigating a role for p63 in prostate stem cells, cancer and metastasis

## Valeria Di Giacomo

Doctoral Thesis UPF-2014

THESIS DIRECTOR

Dr. William M. Keyes

DEPARTMENT

Gene Regulation, Stem Cells and Cancer Department.
Center for Genomic Regulation (CRG), Barcelona

Alla mia famiglia,
il mio supporto
sempre e comunque

# Acknowledgments

# Contents

# Abstract

P63 is a transcription factor of the p53 family with key roles in embryonic development, stem cells and cancer. P63-deficient mice fail to form stratified and glandular epithelia, including the prostate, demonstrating a critical function for p63 in prostate development. The P63 gene encodes two different isoform groups, TA and $\Delta$N, which can act as tumor suppressors or oncogenes respectively in different tumors. In the prostate gland, $\Delta$Np63$\alpha$ is the main isoform expressed specifically in basal stem cells. There is evidence that p63+ basal stem cells are the cells-of-origin of prostate cancer. However the mature tumor has a luminal phenotype and loss of p63 expression is used as a diagnostic marker for carcinoma. To date, there have been few studies investigating the role of p63 in prostate stem cells and cancer.

First, we confirmed the expression of $\Delta$Np63$\alpha$ in basal prostate stem cells of *wild type* mice. Surprisingly we also detected $\Delta$Np63$\alpha$ in a subpopulation of cells with cancer stem cell characteristics in the PC3 human prostate metastatic cell line, which is derived from metastasis to the bone. We then performed *in vitro* and *in vivo* gain and loss of function studies in non-transformed and bone metastatic human prostate cells. We identified a role for $\Delta$Np63$\alpha$ in stem cell proliferation and self-renewal. Interestingly we discovered a new function for this isoform in favoring bone metastatic colonization through the regulation of cell adhesion and signaling to the surrounding microenvironment. Our results uncover $\Delta$Np63$\alpha$ as a critical new mediator of prostate stem cells maintenance and prostate cancer metastatic colonization to the bone.

# Resumen

P63 es un factor de transcripción de la familia de p53 con un papel clave en el desarrollo embrionario, células madre y cáncer. Ratones deficientes para P63 presentan un defecto en la formación de epitelios estratificados y glandulares, incluyendo la próstata, lo que establece una función crítica para p63 en el desarrollo de la próstata. El gen de P63 codifica para dos grupos de isoformas diferentes, TA y $\Delta$N, que pueden actuar como supresores de tumores u oncogenes, respectivamente, en diferentes tipos tumorales. En la próstata, $\Delta$Np63$\alpha$ es la isoforma principal expresada específicamente en las células madre basales. Hay pruebas de que las células madre basales p63+ son las células de origen del cáncer de próstata. Sin embargo, el carcinoma tiene un fenotipo luminal y la pérdida de expresión de p63 se utiliza como un marcador de diagnóstico. Hasta aquí no existen muchos estudios que investiguen el papel de p63 en las células madre y en el cáncer de próstata.

En primer lugar, confirmamos la expresión de $\Delta$Np63$\alpha$ en las células madre basales de próstata de ratones *wild type*. Sorprendentemente también detectamos $\Delta$Np63$\alpha$ en una subpoblación de células con características de células madre de cáncer en la línea celular metastásica de próstata humana PC3, que deriva de metástasis en el hueso. A continuación realizamos estudios de sobre-expresión y pérdida de expresión *in vitro* e *in vivo* en células de próstata humana no transformadas y en células de metástasis al hueso. Identificamos así un papel de $\Delta$Np63$\alpha$ en la proliferación y en el mantenimiento de las células madre. Sorprendentemente descubrimos una nueva función para esta isoforma en favorecer la colonización metastásica al

hueso a través de la regulación de la adhesión celular y la señalización extracelular.

Nuestros resultados establecen $\Delta$Np63$\alpha$ como un nuevo mediador crítico para el mantenimiento de las células madre de la próstata y la colonización metastásica del cáncer de próstata al hueso.

# Preface

Prostate cancer is one of the main causes of cancer death in men of western countries, with metastasis to the bone being the predominant incurable last step in the pathology. At present, perhaps the three main lines of research in prostate biology are: identification of mediators of stem cell-maintenance, uncovering the cell-of-origin of prostate cancer and understanding the mechanisms of bone metastases.

In this context, p63 is a prime candidate as a mediator of prostate stem cell-maintenance, based on its role in development and expression profiling. It has also been suggested that p63+ basal stem cells are the cells-of-origin in prostate cancer, nevertheless the mature tumor has lost the expression of p63, a loss that is used for the clinical diagnosis of carcinoma. To date, functional studies investigating a role for p63 in prostate stem cells and cancer are lacking,

In our work, we show that $\Delta Np63\alpha$ is required for adult prostate stem cell proliferation potential and self-renewal. Moreover we uncover a function for $\Delta Np63\alpha$ in prostate cancer metastatic colonization to the bone, likely through the use of similar processes it regulates in normal stem cells. Ultimately our findings help in better understanding the process of prostate stem cell maintenance and prostate cancer bone metastasis, and uncover novel mechanisms involved.

# Introduction

# 1. The p53 family of transcription factors

## 1.1 Members

The p53 family of transcription factors in vertebrates includes p53, p63 and p73 (Nedelcu and Tan, 2007).The first gene to be discovered was P53, the most frequently mutated tumor suppressor identified in human cancers, with more than 50% of malignancies associated with mutations in this gene (Hollstein et al., 1996). For this reason, the discovery of the other two members of the family created great excitement (Jost et al., 1997; Kaghad et al., 1997; Yang et al., 1998).

The differences in biological functions between p53, p63 and p73 were soon revealed by the observation that mutations in P63 and P73 in human cancers are nearly absent, in sharp contrast with what happens for P53 (Levrero et al., 2000; Osada et al., 1998; Sunahara et al., 1998). Alternatively, mutations in the P63 locus in humans cause five genetic syndromes characterized by ectodermal dysplasia, limb abnormalities and facial clefts: ectrodactyly-ectodermal dysplasia-clefting (EEC) syndrome, ankyloblepharon-ectodermal dysplasia-clefting (AEC) syndrome, limb-mammary syndrome (LMS), acro-dermato-ungual-lacrimal-tooth (ADULT) syndrome and split-hand/foot malformation (SHFM) (Celli et al., 1999; Ianakiev et al., 2000; McGrath et al., 2001; Propping and Zerres, 1993; van Bokhoven et al., 1999). Additionally, knockout (KO) mice for P53 show few developmental defects but increased tumor incidence in adulthood, instead KO mice for P63 or P73 show strong developmental defects, respectively in ectodermal derivatives and in nervous and immune systems (Mills et al., 1999; Yang et

3

al., 1999; Yang et al., 2000). These observations identify p63 and p73 as major players in development. The determination of their role in cancer has been complicated by the existence of different isoforms.

## 1.2 Isoforms

Current experimental data on p53 isoforms are fragmented and much more has been discovered for p63 and p73 (Marcel et al., 2011). The three proteins show high homology in the DNA-binding (DBD) and oligomerization (OD) domains (Deyoung and Ellisen, 2007). Transcription of P63 and P73 can be started from two different promoters, giving rise to the TA and $\Delta$N isoforms (Figure 1). TAp63 and TAp73 have a transactivation domain (TAD) at the N-terminus homologous to the one present in p53, while the $\Delta$N isoforms have a different shorter transactivation domain.  Additionally, alternative splicing in the extended C-terminal region increases the variability of p63 and p73: $\alpha$, $\beta$, $\gamma$, $\delta$ and $\varepsilon$ variants for p63 and $\alpha$, $\beta$, $\gamma$, $\delta$, $\varepsilon$, $\zeta$, and $\eta$ variants for p73 (Figure 1) (Levrero et al., 2000; Yang et al., 1998). The presence of a sterile alpha motif in the C-terminus, common in proteins regulating development, could be important for the implication of p63 and p73 in the process (Figure 1) (Thanos and Bowie, 1999).
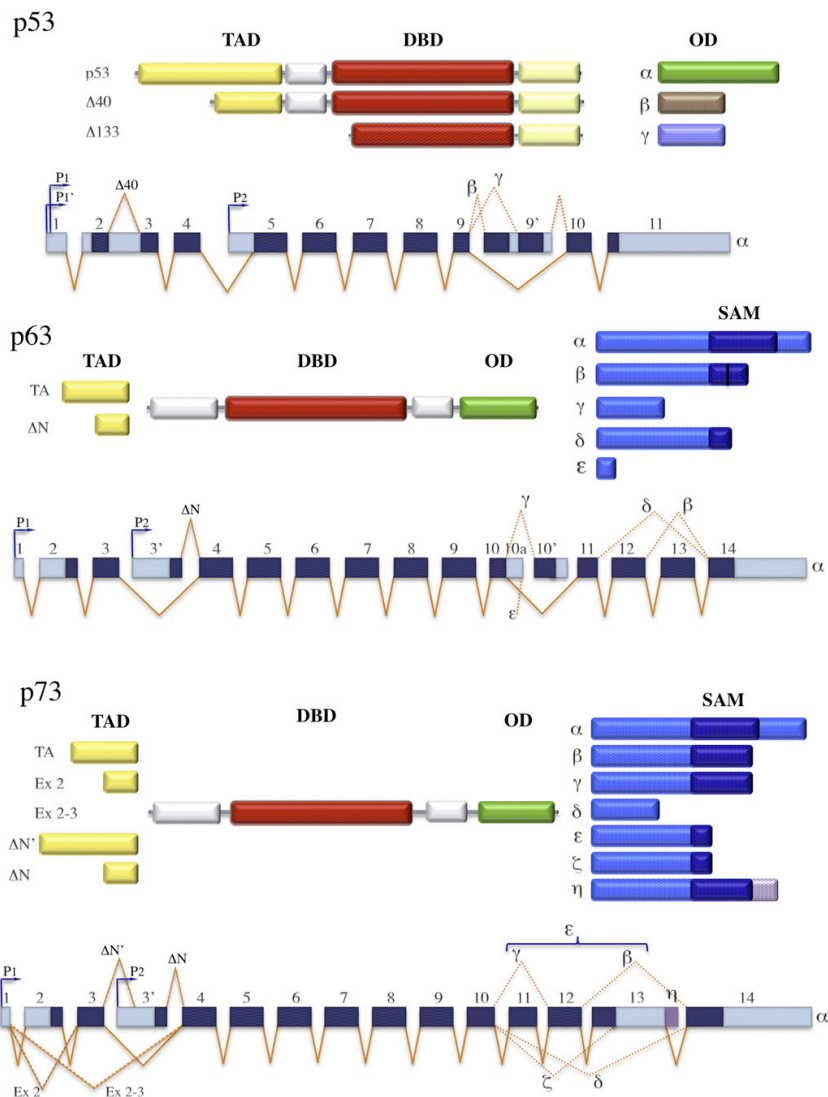
**Figure 1. Schematic representation of p53 family proteins and genes**
In the protein structure, the common transactivation domain (TAD), DNA-binding domain (DBD) and oligomerization domain (OD) are highlighted. The sterile alpha motif is also indicated in p63 and p73. The different C-termini, derived from alternative splicing, can be combined with the different N-termini, derived from transcription from two different promoters, to generate different proteins. In the gene structure, exons are in dark blue and 5' and 3' UTR are in light blue. P1 and P2 indicate the two different promoters. Taken from (Allocati et al., 2012).

P53 binds and activates targets that drive apoptosis (P21, BAX, IGFBP3), cell cycle arrest (GADD45a, 14-3-3 $\sigma$) senescence (P21, P57) and DNA damage response (PCNA, BRCA2) (Allocati et al., 2012; Levrero et al., 2000). These targets are crucial players in development, stem cells and cancer and they are directly regulated also by p63 and p73, due to their amino acid homology in the DBD domain with p53 (Jost et al., 1997; Kaghad et al., 1997; Keyes et al., 2005; Lee and La Thangue, 1999; Osada et al., 1998). At the moment, much research focuses on investigating the specific contributions of each class of isoforms to the functions of p63 and p73 in development, stem cells and cancer. TA isoforms behave as activators, due to their homology with p53 in the TA domain, and ΔN were initially identified as dominant negatives on p53 common targets (Deyoung and Ellisen, 2007). Subsequently, both TA and ΔN isoforms have been shown to also activate their own specific targets (King et al., 2003; Yang et al., 1998). There is a strong interplay between the different isoforms and, in this context, TA isoforms, more like p53, drive apoptosis and cell cycle arrest, whereas ΔN isoforms promote survival and proliferation (Deyoung and Ellisen, 2007). This explains how, in particular in cancer, ΔN isoforms perform mostly as oncogenes and TA as tumor suppressors, as it will be discussed later specifically for p63.

## 2. P63 in normal tissues

## 2.1 P63 in development

P63 is the most ancient member of the p53 family and the most highly conserved between species with 99% amino acid homology between mouse and human, and with only 8 substitutions across 483 amino acids (Yang et al., 1998).

As previously mentioned, mutations in the P63 locus 3q28 in human are associated with genetic syndromes characterized by three main developmental defects: ectodermal dysplasia, limb malformations and orofacial clefting. Moreover, two of these disorders, the limb-mammary syndrome (LMS) and acro-dermato-ungual-lacrimal-tooth (ADULT) syndrome, also present defects respectively in mammary and lacrimal glands development (Celli et al., 1999; McGrath et al., 2001; Propping and Zerres, 1993)

P63 expression during development in mouse has been detected in the proliferative basal compartment of stratified and glandular epithelia and in the ectodermal surfaces of epidermal appendages, limb buds and branchial arches. In particular the limb buds show high expression in the apical ectodermal ridge (AER), a region responsible for the signaling and patterning of the underlying mesoderm (Yang et al., 1999). Many P63-KO mice have been generated and they show prominent absence of stratified epithelia, including skin and appendages (teeth, hair and nails), and glandular tissues, such as lacrimal, salivary, mammary and prostatic glands. These mice have absent or severely truncated limbs, present with cleft lip and cleft palate

and die soon after birth from dehydration due to the skin defects (Figure 2) (Mills et al., 1999; Yang et al., 1999).
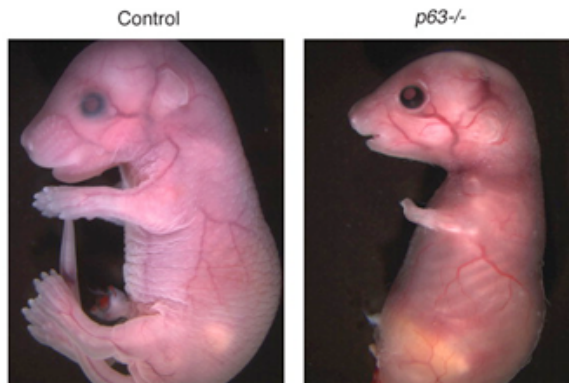


Figure 2. **Appearance of the P63-KO mouse**
Strong phenotype of the p63-KO mouse showing truncated limbs and absence of a proper stratified epidermis. Taken from (Keyes et al., 2005)

The strong phenotypes described above, led to different non-exclusive interpretations of the role of p63 in development, as a regulator of epithelial stem cell maintenance or in epithelial lineage commitment (Mills et al., 1999; Senoo et al., 2007; Yang et al., 1999).

ΔNp63 is the most highly expressed isoform in developing epithelial tissues and the phenotype of the ΔNp63-KO mouse resembles that of the complete P63-KO model with truncated limbs, craniofacial malformations and poorly developed stratified epidermis (Romano et al., 2012). On the other hand, in TAp63-KO embryos do not display any overt abnormality (Guo et al., 2009; Su et al., 2009).

## 2.2 P63 in stem cells in adult tissues

In adult life, p63 remains mainly detectable in the nuclei of the undifferentiated cells in the basal layer of stratified and glandular epithelia, including skin, oral mucosa, bronchiolar epithelium, cervical epithelium and salivary, lacrimal, mammary and prostate glands (Figure 3). The supra-basal differentiated layers of these tissues show less or no expression of p63 (Di Como et al., 2002; Parsa et al., 1999; Pellegrini et al., 2001).
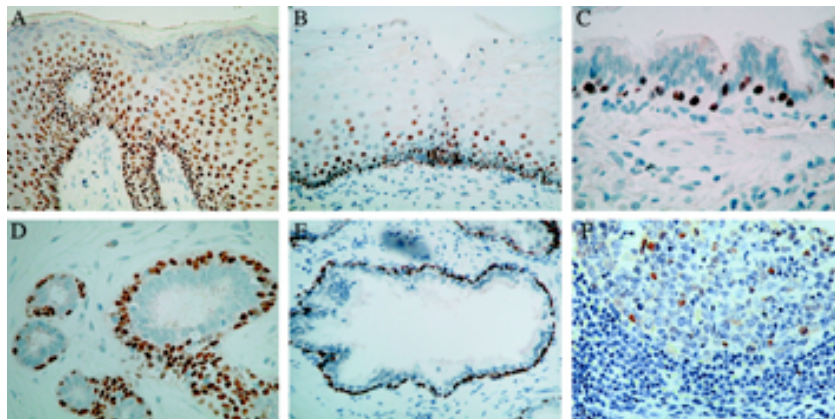


Figure 3. **P63 expression in the nuclei of cells in the basal layer of stratified and glandular epithelia**
P63 staining in the basal cells of mouse skin (A), exocervical mucosa (B), bronchium (C), breast (D) and prostate (E). Occasional cells in the germinal center of lymph nodes also display a weak p63 staining. Taken from (Di Como et al., 2002).

ΔNp63 is the most highly expressed isoform in the adult as in embryonic epithelial tissues. In an inducible knockdown mouse, in which ΔNp63 expression is shut down after birth, supra-basal keratinocytes show deregulated differentiation and basement membrane abnormalities lead to skin erosions and impaired wound healing (Koster et al., 2007; Koster et al., 2009). These observations highlight the role of ΔNp63 in the positive regulation

of adult epithelial maintenance, proper differentiation and adhesion to the extracellular matrix (ECM). Additionally, a number of studies have further shown a specific role for p63 in maintaining the epithelial stem cell population. Pellegrini and colleagues showed for the first time, in 2001, that p63 distinguish stem cells from their transient amplifying progeny in the stratified epithelium of the cornea (Pellegrini et al., 2001). Subsequently a function for $\Delta Np63\alpha$ in maintaining keratinocytes in an undifferentiated state has been demonstrated (King et al., 2003). Moreover, in the thymus and in the epidermis, p63 exerts an essential role in maintaining the proliferative potential of epithelial stem cells (Senoo et al., 2007). In accordance with the functions described above, $\Delta Np63$ has been shown to directly bind and activate targets involved in stem cell maintainance (JAG1), extracellular matrix (LAM $\gamma$2) and adhesion (ITG $\alpha$6 and $\beta$4, PERP) (Carroll et al., 2006; Vigano and Mantovani, 2007).

The TA isoform of p63 is mainly expressed in oocytes where it protects germ cell integrity and induce apoptosis in response to DNA damage (Suh et al., 2006). The role of TAp63 in epithelial tissues is not fully clear, as the level detected is normally low or absent. In an isoform-specific KO mouse model, germ line deletion of TAp63 results in an epithelial phenotype in adults, including blistering, skin ulceration and decreased hair morphogenesis and wound healing. Nevertheless, epidermis-specific ablation of TAp63 does not lead to skin abnormalities, so the phenotype derived from the germ line deletion was attributed to the role of TAp63 in maintaining dermal precursor populations (Su et al., 2009).

## 3. P63 in cancer

Mutational studies in human cancers have revealed no or few mutations (<1%) in the *p63* locus (Hagiwara et al., 1999). Two P63+/- mouse models were used to study the role of p63 in cancer, as P63-/- mice die soon after birth. P63 heterozygosity itself, or in combination with P53 deficiency, in one study identified increased tumor burden and metastasis while, in the other study, mice developed fewer spontaneous tumors that *wild type* mice and had no increased propensity to chemically-induced tumors (Flores et al., 2005; Keyes et al., 2006). In these studies, there is no discrimination between the different isoforms as the models used are deficient in both TA an ΔN. Given their different functions in cancer, explained below, the controversy generated by complete loss of p63 is comprehensible.

## 3.1 ΔNp63

In particular, the ΔNp63α isoform is over-expressed in several epithelial cancers and mostly in squamous cell carcinomas (SCCs) from head and neck, lung and skin. In addition, many different functional studies have highlighted the role of ΔNp63 as an oncogene (Graziano and De Laurenzi, 2011; Massion et al., 2003; Parsa et al., 1999; Sniezek et al., 2004). Moreover, ΔNp63α has been shown to cooperate with Ras in transforming stem cells of the skin (Keyes et al., 2011).

Nevertheless, loss of ΔNp63 has been associated with a more invasive phenotype (Koga et al., 2003; Urist et al., 2002). This apparent controversy could be explained by different functions of ΔNp63. It can promote proliferation, protect from apoptosis and

drive senescence bypass at early steps of tumorigenesis (Keyes et al., 2011; Rocco et al., 2006; Thurfjell et al., 2005; Zucchi et al., 2008). At the same time, it can maintain the epithelial characteristics of tumor cells and impair the process of epithelial to mesenchymal transition (EMT) that are necessary for invasion at later stages of cancer progression (Barbieri and Pietenpol, 2006; Barbieri et al., 2006). The role of ΔNp63 in inhibiting EMT can involve upstream and downstream molecular pathways: Snail, a mediator of tumor invasiveness, down-regulates ΔNp63 expression by binding to its promoter and in turn ΔNp63α has been shown to directly induce the expression of CD82, an inhibitor of invasiveness (Higashikawa et al., 2007; Wu et al., 2014).

## 3.2  TAp63

TAp63, on the contrary to the ΔN isoform, is well accepted to behave as a tumor suppressor. TAp63 is able to trigger death receptor complexes (CD95, TRAIL) and the mitochondrial death pathway (BAX, APAF1) in different cancer cell lines (Gressner et al., 2005). Guo and colleagues demonstrated that TA isoforms are necessary for Ras-induced senescence in mouse embryonic fibroblasts (MEFs) through induction of P21 and RB. Moreover, loss of TAp63 enhances Ras-mediated tumor formation and progression in the context of p53 deficiency *in vivo* (Guo et al., 2009). In another study, TAp63 -/- and TAp63 +/- mice develop spontaneous and aggressive carcinomas and sarcomas and there is an increase in metastatic potential when TAp63 is lost in combination with p53 (Su et al., 2010). TAp63 has been demonstrated to inhibit metastasis by indirectly controlling the

processing of miRNAs through inducing the expression of Dicer (Su et al., 2010).

## 4. The prostate gland

### 4.1 Function

The prostate is an exocrine gland of the male reproductive system. Its function is to secrete an alkaline fluid that participates to form the sperm together with spermatozoa and seminal vesicle fluid. Prostatic secretions vary among species. They are generally composed of simple sugars. In human, the protein content includes proteolytic enzymes, prostatic acid phosphatase, $\beta$-microseminoprotein, and prostate-specific antigen (PSA). The alkalinity of the sperm is required to antagonize the acidic environment of the vaginal tract and help the survival of the spermatozoa. To function properly, the prostate needs male hormones (androgens), which are responsible for male sex characteristics. The main male hormone, testosterone, is mostly produced by the testicles, others are produced by the adrenal glands (Cunha et al., 1987).

### 4.2 Development

Murine prostate develops from the urogenital sinus (UGS), an embryonic structure that appears 13 days post conception (dpc) and is divided in an epithelial and a mesenchymal component, respectively the urogenital epithelium (UGE) and the urogenital mesenchyme (UGM). The UGM will give rise to the stroma of the prostate and the UGE to the glandular epithelium (Price, 1963). These two tissue compartments must interact with each other for

prostatic development to occur normally (Cunha and Donjacour, 1987). Androgen receptors (AR) are present in both (Cunha et al., 1992). When testosterone begins to be produced by testis at 13.5 dpc, the UGE responds by forming solid prostatic buds that grow into the UGM in a precise spatial pattern that establishes the lobar subdivision of the mature gland (Sugimura et al., 1986; Timms et al., 1994). The prostatic buds consist of solid cords of epithelial cells. During the neonatal period, ductal canalization occurs and lumen formation coincides with the differentiation of the epithelium in two cell types: the luminal cells facing the lumen and basal cells in contact with the basal lamina (Hayward et al., 1996). Epithelial differentiation is accompanied by mesenchymal differentiation into stroma consisting of fibroblasts, myofibroblasts and smooth muscle cells that start surrounding the tubules. Blood vessels, nerves and immune cells are also interposed among the stroma (Cunha and Donjacour, 1987). At birth, prostatic ducts begin to bifurcate and undergo branching. This process is almost complete by two weeks after birth (Timms et al., 1994). Testosterone levels are low during this period and they rise at puberty, starting at day 21-25, causing production of secretory proteins and increase in prostatic weight (Donjacour et al., 1990).

## 4.3 Anatomy and histology

The prostate, in mouse and human, resides around the urethra on the bottom of the bladder. In mouse, the gland is divided in two anterior, two ventral and two dorsolateral lobes (Sugimura et al., 1986). In human, it consists of a peripheral, a central and a transition zone (Figure 4) (McNeal, 1981a, b).

14
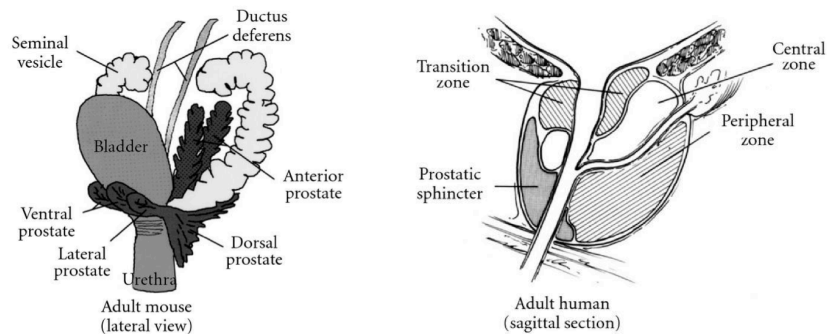
Figure 4. **Prostate anatomy**
Schematic representation of the anatomy of the mouse prostate on the left and the human prostate on the right. Taken from (Valkenburg and Williams, 2011).

Despite the anatomical differences, the histology of the gland is the same, presenting a tubular structure. Two epithelial populations of cells form the tubules: columnar luminal cells, that are androgen dependent and secrete in the lumen, and androgen-independent non-secreting basal cells, that are in contact with the basal lamina. Individual rare neuroendocrine cells are also scattered in the basal layer (Figure 5) (McNeal, 1988). The different types of cells can be distinguished by specific expression profiles. Luminal cells express cytokeratins (CK) 8 and 18, AR and PSA, basal cells express CK 5 and 14 and p63 and neuroendocrine cells are marked by synaptophysin and chromogranin A (Garabedian et al., 1998; Wang et al., 2001).
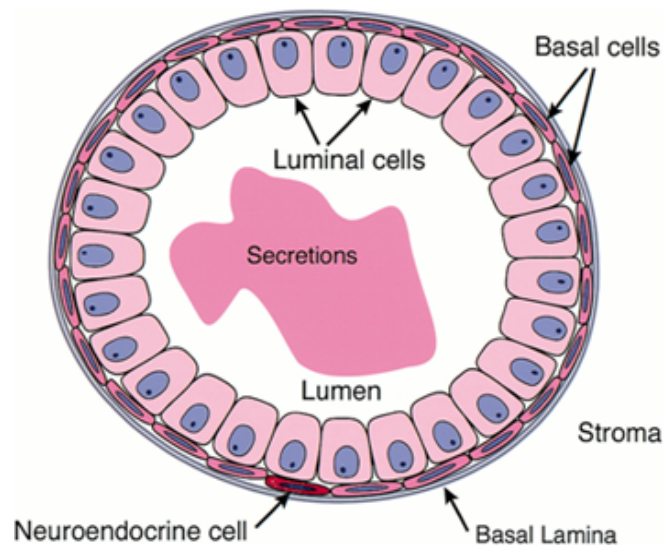
Figure 5. **Prostate histology**
Schematic representation of the tubular structure of the prostate and the different cell populations in the tubules. Taken from (Abate-Shen and Shen, 2000)

# 5. Prostate stem cells (PSCs)

## 5.1 PSCs in development

Two important mediators have been identified during prostate development: Nkx 3.1 and p63. Loss-of-function mutations in NKX3.1 cause abnormal prostatic morphogenesis and differentiation (Bhatia-Gaur et al., 1999). More strikingly, mice deficient in P63 are the first engineered animal models with prostate bud-agenesis (Mills et al., 1999; Yang et al., 1999). This observation gave an initial hint for a role of p63 in prostate stem cells during prostate development. Further confirming this, in a subsequent study, P63 -/- blastocysts were complemented with P63 +/+ marked embryonic stem cells and all of the cell lineages of the prostate derived from the transplanted P63 +/+ cells

(Signoretti et al., 2005). However, the main proof that p63, and in particular the ∆N isoform, has a role in stem cells in the developing prostate, is given by a lineage tracing study in which it has been shown that ∆Np63-expressing cells of the UGS generate all the epithelial lineages of the prostate (Pignon et al., 2013).

## 5.2 PSCs in adult life

Postnatal stem cells have been identified for different tissues, including hematopoietic system, skin and intestine. All share the characteristics of self-renewal, multi-lineage differentiation, replication quiescence, proliferation potential and localization in so-called stem cell niches (Barker et al., 2010; Fuchs et al., 2004).

The hypothesis of the existence of a stem cell population in adult prostate derives from the observation that the gland can undergo several cycles of regression and regeneration following respectively, androgen withdrawal (castration) and replacement (English et al., 1987). Moreover, tissue fragments from mouse and rat prostatic embryonic and adult epithelia, and even dissociated cells from postnatal prostate epithelium, combined with UGM, have been shown to generate prostatic structures in kidney capsule and subcutaneous engraftments in male nude mice (Cunha and Lung, 1978; Xin et al., 2003).

## 5.2.1 Methods to identify adult PSCs

Adult stem cells can be identified by testing their characteristics of self-renewal, proliferation-potential and multi-lineage differentiation.

*In vitro*, colony formation assays and three-dimensional (3D) cultures in semisolid matrix are the standard to test stem cell characteristic of cells from adult tissues or non-transformed cell lines. In the first approach, cells are plated at low density and stem cells can give rise to clonally derived colonies comprising the different cell lineages of the original tissue. Similarly, in 3D cultures, stem cells form clonally derived spheres with the different cell lineages organized in a pattern similar to the one *in vivo* (Lukacs et al., 2010a; Lukacs et al., 2008).

Specific assays for PSCs can be done *in vivo* by combining a subpopulation of epithelial cells with UGM, and injecting them in the kidney capsule or subcutaneously in male nude mice (Xin et al., 2003). Only PSCs possess the ability to generate prostatic structures in these settings. A major advantage of this *in vivo* approach is the ability to perform studies using human samples. Limitations are represented by the use of immunodeficient mice that hamper the investigation of an eventual role of inflammation and by the plasticity induced in cells in a non-physiologic environment in contact with the UGM embryonic tissue.

Recently, lineage-tracing methodology in genetically engineered mouse models (GEMMs) have been used to identify stem cells directly in a physiological setting. Subpopulations of cells selectively express the Cre recombinase that can induce the activation of a reporter gene through excision of inhibitory gene-flanking sequences. This system allows the maintenance of the expression of the reporter in the progeny of the induced population that can therefore be tracked. PSCs give rise to daughter cells of the different lineages (Choi et al., 2012; Ousset et al.; Wang et al., 2009). However, some major limits of this

procedure are the impossibility of using human samples and, the variable efficiency in labeling the cells of interest.

## 5.2.2 Identity of adult PSCs

Adult PSCs have been traditionally thought to reside in the basal layer of the gland, where they divide to form transient amplifying cells, that in turn differentiate to give rise to luminal and neuroendocrine cells (Bonkhoff and Remberger, 1996). Several observations support this theory. First of all, the position of the basal cells places them in contact with the extracellular matrix (ECM) that has been shown, for other stem cell niches, to be a reservoir of signaling molecules (Jensen et al., 1999). Second, basal cells have higher proliferation potential than luminal cells (Bonkhoff et al., 1994). Third, they express Bcl2, which protects from apoptosis and is frequently up-regulated in different stem cells (Verhagen et al., 1992). Fourth, basal cells preferentially survive following androgen withdrawal, while luminal cells undergo extensive cell death due to their dependence on androgen (English et al., 1987). Moreover, cell-surface markers used to enrich for cells with stem-like characteristics *in vitro* and *in vivo*, mostly identify subpopulations in the basal compartment of the prostate. The best recognized markers are CD44, $\alpha 2\beta 1$ integrin, CD133/prominin-1, Sca-1, CD49f/integrin $\alpha 6$, CD117/c-kit and Trop2 (Burger et al., 2005; Goldstein et al., 2008; Lawson et al., 2007; Leong et al., 2008; Richardson et al., 2004). Finally, it has been speculated that the function of p63 in prostate stem cells during development could be maintained in adult life. $\Delta Np63\alpha$ is the predominant and almost exclusive isoform expressed specifically in the nuclei of the basal cells of the adult

prostate and is enriched in stem cell populations isolated by combination of the above-mentioned markers. An important player in prostate stem cells maintenance, Bmi-1, is required for self-renewal activity and maintenance of p63+ stem cells in the adult prostate (Lukacs et al., 2010b).

However, there is still controversy as to whether p63 has a role in basal stem-like cells and if these cells are actually the unique stem cells of the adult gland. First of all, in two independent studies, P63-/- cells have been shown to differentiate into and regenerate luminal cells, even if not basal cells, in a UGS transplantation assay (Kurita et al., 2004; Signoretti et al., 2005). These results suggest a possible self-sustaining potential for luminal cells in the adult gland. Recently, lineage-tracing strategies have been developed to study the basal/luminal hierarchy. Research by Xi Wang and colleagues demonstrates that Nkx 3.1 identifies a luminal stem cell subpopulation that restores both luminal and basal compartments during prostate regeneration. These cells have been named castration-resistant Nkx 3.1-expressing cells (CARNs) (Wang et al., 2009). A different result was obtained by another group which showed that basal and luminal cells only generate cells of the same lineage during regeneration (Choi et al., 2012). Finally, Ousset and colleagues, for the first time, performed lineage-tracing experiments at different stages of postnatal prostate development and demonstrated the existence of multipotent basal progenitors and unipotent luminal progenitors, which together contribute to prostate postnatal development (Ousset et al., 2012). Similar conclusions have been reached by the same group in the mammary gland (Van Keymeulen et al., 2011). In

summary, the current model describes multipotent basal cells, backed by a possible self-sustaining population of luminal cells.

## 6. Prostate cancer

## 6.1 Epidemiology

Prostate cancer is one of the most commonly diagnosed cancers and is a major leading cause of cancer death in men in western countries. More than 95% of prostate cancers correspond to acinar adenocarcinoma characterized with a luminal phenotype, while other categories, such as ductal adenocarcinoma, mucinous carcinoma, signet ring carcinoma and the neuroendocrine subtype, are extremely rare (Grignon, 2004). As such, for the rest of the discussion with regards to prostate cancer, I will focus on acinar adenocarcinoma.

The most significant risk factor in the development of prostate cancer is aging and this most probably reflects the interplay of changes at the environmental, physiological and genetic levels (Shen and Abate-Shen, 2010). Inflammation is one of the most important environmental factors (Figure 6). A condition named proliferative inflammatory atrophy (PIA) can often be identified in aging men and regions of PIA are often located in proximity with neoplastic lesions (De Marzo et al., 1999). Among the physiological factors, the most important are oxidative stress and its cumulative impact on DNA damage, and senescence of fibroblasts, that in turn stimulate proliferation and invasiveness of epithelial cells (Figure 6) (Bavik et al., 2006; Khandrika et al., 2009; Minelli et al., 2009). Section 6.3 will be dedicated to the description of genetic determinants of prostate cancer.

## 6.2 Clinical aspects

## 6.2.1 Symptoms and diagnosis

Prostate cancer at early stages can be either non-symptomatic or associated with urinary dysfunction, due to the anatomical position of the gland (Miller et al., 2003). These symptoms could be common to benign prostatic hyperplasia (BPH) that is a physiological process characterized by controlled hyper-proliferation of epithelial and stromal cells of the prostate that generally occurs after the age of 50 (Chang et al., 2012). Specific diagnostic parameters are therefore available. A blood test for PSA is usually combined with digital rectal exam. PSA is a serine protease normally produced in prostate secretions, but is released into the blood stream as a consequence of the disruption of normal tissue architecture (Barlow and Shen, 2013). Men with elevated levels of PSA undergo biopsy to assess the histological grade of the lesion with the method of the Gleason scoring. Primary tumors often contain multiple different histologic foci, so a value from 1 to 5 is assigned to the two prevalent subtypes (most to less severe) and the sum of the two values gives the grade of the tumor (Mellinger et al., 1967). Furthermore, diagnosis of adenocarcinoma is based on the absence of staining for the basal markers CK5, CK14 and p63, and the elevated expression of the luminal marker AMACR (Grisanzio and Signoretti, 2008; Jiang et al., 2005; Luo et al., 2002).

## 6.2.2 Progression and treatments

Prostatic intraepithelial neoplasia (PIN) is widely accepted to be a precursor of malignancy and is characterized by luminal epithelial hyperplasia with nuclear atypia. Mutant cells are confined to the prostate acini and the basal cell layer is at least partially intact. The progression of the pathology can take years, as basal cells are progressively lost and luminal cells invade the stroma (Bostwick 1989; Bostwick 1989). At the moment of diagnosis, in the case in which the lesion is at the stage of localized PIN, depending on the histological grade and the life expectancy of the patient, the choices are active surveillance, with PSA measurements and biopsy-evaluation at regular intervals, or treatments such as surgery or irradiation. If carcinoma has already developed either to a locally invasive stage or metastatic disease, patients undergo androgen deprivation therapy (ADT) that consists in chemical castration (Barlow and Shen, 2013). This therapy is highly effective in reducing the tumor burden, but ultimately the disease will recur in virtually all the cases, giving rise to castration resistant prostate cancer (CRPC) (Figure 6). This is treated with chemotherapeutics, such as Docetaxel, but it remains essentially incurable (Petrylak et al., 2004; Shen and Abate-Shen, 2010). Moreover prostate cancer almost invariably metastasizes to the bone and the derived osteoblastic lesions are characterized by aberrant bone formation by osteoblasts and are responsible for patients' morbidity and mortality (Logothetis and Lin, 2005).

## 6.3 Molecular mechanisms of prostate cancer

## 6.3.1 Onset and progression

Several copy-number alterations, chromosomal rearrangements and epigenetic modifications have been associated with prostate carcinogenesis. Candidate genes have been mapped in the regions involved (Dong, 2001; Lapointe et al., 2007). Down-regulation of NKX 3.1, in the 8p21 locus, represents a frequent event in prostate cancer initiation in human. Mice mutant for this gene display epithelial hyperplasia, dysplasia and often PIN (Abdulkadir et al., 2002; Bhatia-Gaur et al., 1999; Kim et al., 2002). Another early event in tumor onset is the up-regulation of MYC, in the chromosomal region 8q24. The oncogene is overexpressed in many human PIN and carcinomas and transgenic mice display rapid formation of PIN that evolves in invasive tumor (Ellwood-Yen et al., 2003).

A crucial player in the progression of prostate cancer is the tumor suppressor PTEN, on chromosomal region 10q23. Its loss is associated with activation of the PI3K pathway and advancement of adenocarcinoma in human and mouse (McMenamin et al., 1999; Wang et al., 1998; Whang et al., 1998; Wu et al., 1998). Another frequent genomic alteration is a rearrangement that occurs in chromosome 21q and creates the TMPRSS2-ERG fusion gene. This results in the expression of N-terminally truncated ERG protein under the control of the androgen-responsive promoter of TMPRSS2 (Wang et al., 2006a). ERG is a member of the ETS family of transcription factors and in transgenic mice, the expression of the ERG

transgene synergizes with loss of PTEN to result in high-grade PIN and carcinoma (Carver et al., 2009).

The evolution to metastatic disease has been associated with up-regulation of the Polycomb group gene EZH2 (Bachmann et al., 2006). Finally, AR supports survival during tumor development and molecular mechanisms for the onset of CRPC have not yet been clarified (Stanbrough et al., 2001). Activation of developmental pathways, such as ERK/MAPK, Sonic Hedgehog (Shh) and FGF, has been suggested to provide an alternative to AR signaling in promoting survival (Acevedo et al., 2007; Karhadkar et al., 2004). Moreover, insurgence of CRPC can be linked to bone metastasis, as explained in the next section. The all process of prostate cancer development and progression is summarized in Figure 6.

## 6.3.2 Bone metastasis

As previously mentioned, bone metastases are the major cause of prostate cancer morbidity and mortality and there is a great effort in trying to elucidate the molecular mechanisms driving this process. The presence of bone metastases correlates with significantly shortened time of emergence of CRPC and it has been shown that skeletal microenvironment renders prostate cancer cells resistant to castration (Figure 6). In particular, WNT5a from bone stromal cells can induce expression of BMP-6 in prostate cancer cell lines and so stimulate cellular proliferation in androgen-deprived conditions (Lee et al., 2014). Wnt signaling is involved in osteoblastic metastasis typical of prostate cancer and Dai and colleagues demonstrated a link between the Wnt pathway and BMPs in mediating osteoblast differentiation (Dai et

al., 2008; Hall et al., 2005). Moreover, various players have been shown to be involved in skeletal colonization and cancer cells survival through adhesion and signaling to resident mesenchymal cells. Among them, IL1β and cadherin-11 seem to play crucial roles (Chu et al., 2008; Liu et al., 2013). Finally prostate cancer cells have a propensity to express molecules normally expressed by osteoblasts, such as osteocalcin, osteonectin, osteopontin, bone sialoprotein and osteoprotegerin. This phenomenon is termed osteomimicry and it is thought to contribute to preferential growth of prostate cancer cells in the bone microenvironment (Koeneman et al., 1999).
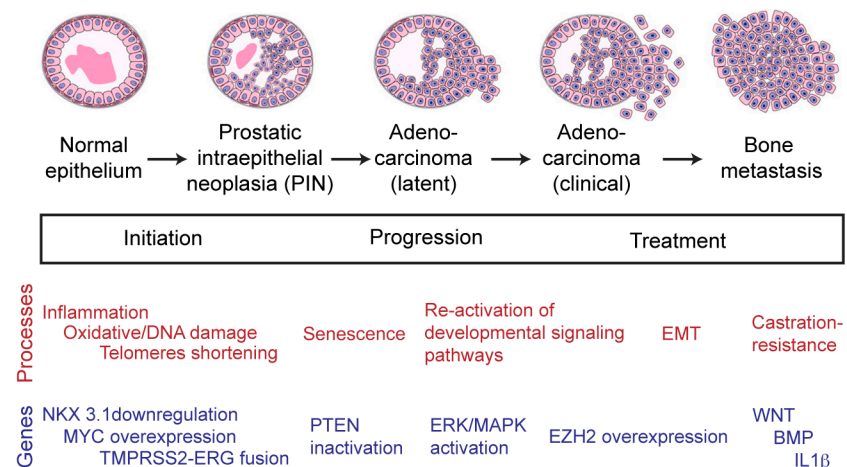


Figure 6. **Genes and processes involved in prostate cancer development**
Schematic representation of the main processes and genetic events that characterize prostate cancer onset and progression. Adapted from (Shen and Abate-Shen, 2010)

## 6.4 *In vitro* and *in vivo* models for prostate cancer

*In vitro,* primary cultures and cell lines provide a fast and efficient model for the identification of molecular mechanisms of prostate cancer. The major limitations are the difficulties in culturing

prostate epithelial cells and the restricted number of available prostate cancer cell lines. Indeed, the most widely used cell lines in prostate cancer study are derived from metastatic lesions, including LNCAP, DU145 and PC3 (Sobel and Sadar, 2005a, b). *In vivo* studies of prostate cancer are based on xenograft and genetically engineered mouse models. In xenograft models, transformed cells or tumors, mostly of human origin, are implanted subcutaneously, orthotopically or in the adrenal gland of immunodeficient mice. Intracardiac and intratibia/intrafemoral injections of cancer cells are specifically used to study the mechanisms of metastasis and bone metastasis respectively (Valkenburg and Williams, 2011). These last two models are particularly useful as there are no genetically engineered mouse models that spontaneously metastasize to the bone. However, the main limitation of all xenograft models is the use of immunocompromised mice, which hampers the study of the interaction of tumor cells with the immune system that may play an important role in the onset of primary tumor and metastasis (Buijs and van der Pluijm, 2009).

In addition, a large number of GEMMs have been developed. First generation models used transgenes that overexpress potent oncogenes. The most common one is the TRAMP (transgenic adenocarcinoma of the mouse prostate) model, which carries a minimal probasin (Pb) prostate-specific promoter driving the expression of SV40 large T and small t antigens. These mice develop primary cancer and metastasis with short latency and with features of neuroendocrine differentiation, so they do not mirror the features of slow growing epithelial acinar adenocarcinomas (Greenberg et al., 1995; Kaplan-Lefko et al.,

2003; Shappell et al., 2004). The similar LADY model uses a larger probasin promoter and expresses large T antigen only. The resulting tumors are slow growing and with a more epithelial phenotype, better mimicking those identified in human. However metastasis in these models are rare (Masumori et al., 2001; Valkenburg and Williams, 2011). GEMMs of the second generation are characterized by loss of function of candidate tumor suppressors. This is achieved by introduction of null mutations or conditional deletions. In the latter case, the expression of the Cre recombinase is under the control of a prostate-specific promoter, most commonly a modified probasin (Pb) promoter. Cre promotes specific recombination at the loxP sites flanking the target gene that is therefore excised specifically in the prostate (Wu et al., 2001). The best-studied model is the Pb-Cre; PTEN$^{flox/flox}$ mouse. This is the first case in which deletion of an endogenous gene induces metastasis and represents one of the most accurate models for prostate cancer as it progresses in a stepwise fashion as in the human disease (Wang et al., 2003). Conditional targeting of genes avoids off target effects in other tissues and allows the study of genes whose loss would result in embryonic lethality. A further improvement is represented by the generation of inducible Cre drivers, that can be switched on at specific time points by inducers such as tamoxifen, to study the effect of genes at the different stages of tumor progression (Ratnacaram et al., 2008). In summary, although transgenic mouse models have been very useful in investigating the molecular pathways of prostate cancer, they present two major limitations: the use of androgen-dependent

promoters that makes them unsuitable to study CRPC, and the absence of reliable bone metastasis.

# 7. Stem cells in prostate cancer initiation and progression

## 7.1 The cancer stem cell theory

The cancer stem cell (CSC) theory suggests there is a cellular hierarchy in the tumor as in the original normal tissue, in which rare cells with stem-like properties are able to initiate and maintain the bulk of the differentiated tumor (Figure 7). This is in opposition to the clonal evolution model where all the cells in the tumor are equally able to start and propagate the bulk of the tumor, and where the intratumoral heterogeneity is given by stochastic genetic alterations (Eaves, 2008). According to the CSC theory, the definition of tumor initiating cells (TICs) refers to those cells in the normal tissues that can be transformed by environmental and oncogenic signals, giving rise to a tumor and acting as the "cancer cell-of-origin" (Visvader, 2011). The term CSCs refers to a population of cells that is present within the tumor, can differentiate into the other tumor cell types and is responsible to maintain the tumor during cancer progression. They both share stem cell characteristics but may or may not coincide, even if the two terms are often exchanged (Figure 7) (Clarke et al., 2006; Visvader, 2011).

In some tissues, like in the intestine and the hematopoietic system, TICs have been shown to correspond to normal stem cells. They are long living, able to self renew, and so more prone to accumulate stresses and genetic alterations (Barker et al.,

2009; Passegue et al., 2004). As an alternative, more committed populations can de-differentiate and acquire a stem-like phenotype during the transformation process (Cozzio et al., 2003; Krivtsov et al., 2006). Understanding which cells initiate the disease may be useful for the development of targeted therapies.

CSCs have been identified in several malignancies, such as medulloblastoma, glioblastoma, breast, colon and hematopoietic cancers (Eaves, 2008; Visvader and Lindeman, 2012). During cancer progression, cells from the primary tumor undergo a process called epithelial to mesenchymal transition (EMT) to acquire characteristics of invasiveness and motility, enter the circulation and extravasate at distant sites (Figure 8). Once there, few cells survive, and it is suggested that they undergo an opposite mechanism of mesenchymal to epithelial transition in order to adhere to the new microenvironment and grow metastasis (Figure 8). The entire process implies characteristics of plasticity, adhesion, self-renewal and differentiation potential that have been attributed to CSCs (Brabletz, 2012; Mani et al., 2008; Ocana et al., 2012; Tsai et al., 2012). Finally, CSCs have been suggested to be more resistant to chemotherapy, and as such can contribute to the relapse of the disease (Eaves, 2008; Visvader and Lindeman, 2012). These aspects render their identification crucial for the targeting of metastatic and therapeutic-resistant diseases that are the most deadly.
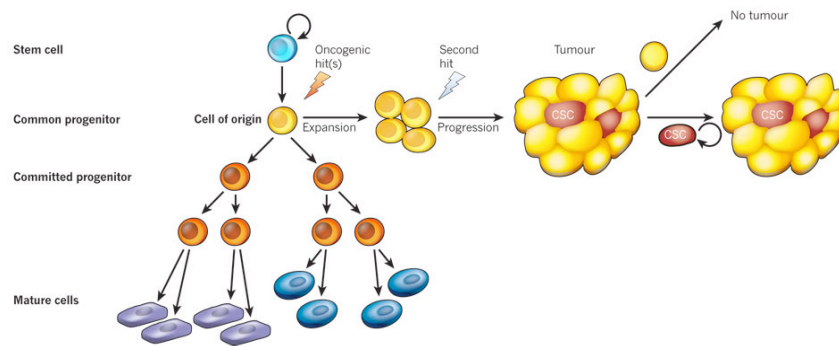
Figure 7. **The cancer stem cell model**
The cell of origin in the normal tissue is possibly a stem cell or a more committed one that is able to de-differentiate and transform as a result of an oncogenic mutation. A second hit causes the progression of the tumor that is organized with a hierarchy similar to the normal tissue, with CSCs (in red) maintaining the bulk of more differentiated cells (in yellow). Taken from (Visvader, 2011).
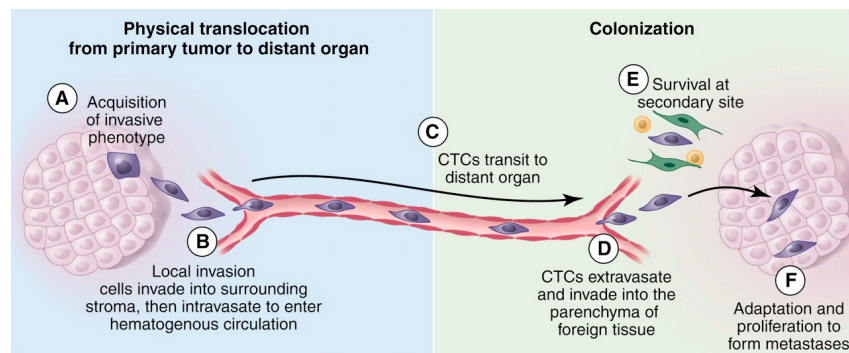


Figure 8. **The path of cancer cells from the primary tumor to distant sites of metastasis.**
Few cancer cells (in violet) in the bulk of the primary tumor (in pink) acquire an invasive phenotype through EMT (A). This way they gain motility, invade the surrounding tissue and enter the circulation (B). The circulating tumor cells (CTCs) (C) finally extravasate at distant sites (D). Once there, some are able to survive (E), interact with the resident cells in the new microenvironment (in green and yellow) and proliferate to form metastasis (F). This last step possibly implies a process of MET. Cells with characteristics of CSCs could be involved at the various stages. Adapted from (Chaffer and Weinberg, 2011).

## 7.2 Prostate TICs and CSCs

## 7.2.1 Methods of identification

TICs are identified by their ability to self renew and generate tumors following genetic alterations. The same is true for CSCs in tumors and transformed cell lines, with the exception that they already have genetic alterations.

As for PSCs, colony and sphere formation assays are the gold-standard *in vitro* assays, while kidney capsule or subcutaneous engraftments in male nude mice in combination with UGM are the best approaches *in vivo* (Lukacs et al., 2010a; Lukacs et al., 2008; Xin et al., 2003).

Lineage tracing studies in GEMMs have also been used to help identify TICs in the physiological environment. In this case, subpopulations of cells are marked by the constitutive expression of a reporter and are targeted with genetic alterations through the use of cell-specific promoters. Their tumor forming potential is assessed by following the fate of the progeny (Choi et al., 2012; Wang et al., 2009).

Advantages and limitations of xenografts and lineage tracing approaches have been previously mentioned in section 4.2.1. A further way to identify TICs is by studying the onset of tumors in the various GEMMs for prostate cancer available, described in section 5.3.

## 7.2.2 TICs in prostate cancer initiation

Given the luminal phenotype of prostate cancer, the putative cell of origin has to be either luminal or a basal progenitor that is able to differentiate into luminal progeny. The evidence for a basal

cell of origin is given by different studies. For example, mouse basal cells can be transformed by oncogenic signals in tissue reconstitution experiments, while luminal cells cannot (Lawson et al., 2010). Analogous assays demonstrated that basal human subpopulations can undergo transformation and generate prostate adenocarcinomas with a luminal phenotype after transplantation (Goldstein et al., 2010). Moreover it has been shown that Pb-Cre; PTEN[flox/flox] mice display an expansion of the p63+ subpopulation at the onset of tumor-initiation (Wang et al., 2006b). These cells have been subsequently identified as TICs through *in vitro* sphere-forming assay and *in vivo* transplantation and regeneration experiments (Mulholland et al., 2009). In a further study, it has been demonstrated that expansion of p63+ cells can be mediated by Bmi1 (Lukacs et al., 2010b). Finally, superficial markers of CSCs (CD133, $\alpha 2\beta 1$ integrin CD44) identified by combining functional *in vitro* and *in vivo* approaches, are mostly expressed in the basal layer of the prostate (Collins et al., 2005).

In contrast to the evidence reported above for a basal cancer cell of origin, a luminal TIC has been suggested in the PSA-Cre; PTEN[flox/flox] and Nkx 3.1-MYC models (Iwata et al., 2010; Korsten et al., 2009). Moreover, CARNs have been shown to behave as cells of origin for prostate cancer with lineage tracing approaches (Wang et al., 2009).

Finally, three independent lineage tracing studies demonstrated that both basal and luminal cells are capable of generating malignant lesions, although there is disagreement over which lineage is capable of generating the most aggressive tumors (Choi et al., 2012; Lu et al., 2013; Wang et al., 2013). This

discrepancy could depend on the strength of the promoter used to drive the genetic alterations, the genetic background of the mice used and the different efficiency of recombination achieved in the basal and luminal populations.

The scenario is still not resolved and there is strong evidence that prostate cancer to arise from both basal and luminal cell types.

## 7.2.3 CSCs in CRPC and metastasis

In prostate cancer, putative cancer stem cells are able to survive castration and chemotherapy driving the progression to CRPC and metastasis. Qin and colleagues used the LNCAP metastatic cell line and cells from primary prostate tumors to isolate a subpopulation of cells with CSC characteristics. This PSA$^{-/low}$ subpopulation is quiescent, refractory to androgen deprivation and chemotherapy, and has high clonogenic potential *in vitro* (Qin et al., 2012). Moreover these cells show long-term tumor-propagating capacity *in vivo* in transplantation assays, preferentially express stem cell genes, such as CD44, $\alpha2\beta1$ integrin and ALDH, and can undergo asymmetric division generating PSA+ cells (Qin et al., 2012). In an independent study on metastatic cell lines and primary cells from patients, a subpopulation of cells was identified that survive Docetaxel exposure, lacks differentiation markers and over-expresses Notch and Shh signaling pathways. They have potent tumor initiation capability in xenograft experiments *in vivo* and this characteristic was impaired by knock-down of the two pathways (Domingo-Domenech et al., 2012). In addition, collaboration between different cell types within the tumor has also been

described in the PC3 human prostate metastatic cell line. Mesenchymal cells can instruct a subpopulation of epithelial CSCs through the steps of invasion, inducing a partial and transient EMT and allowing them to reach distant sites. Once there, CSCs undergo MET, proliferate and colonize to form the lesion (Celia-Terrassa et al., 2012).

There are several lines of evidence that p63 is involved in CSCs, as it has been shown for normal prostate stem cells and TICs. Progressive loss of p63 expression during prostate tumor progression is probably linked to loss of epithelial phenotype, gain of EMT-markers and tissue-invasion (Gandellini et al., 2012; Tucci et al., 2012). Nevertheless, aberrant p63 expression in a subpopulation of cells in clinical samples of prostate adenocarcinoma has been linked with poor prognosis (Chang et al., 2011; Dhillon et al., 2009). Moreover, in a mouse model of Hedgehog-driven androgen resistant prostate cancer, p63 expression has been found in cells with characteristics of CSCs in metastatic loci within lymph node, kidney and lung (Chang et al., 2011). Also, a re-emergence of a basal cell-like signature, with expression of p63 and cytokeratins, has been observed in human bone metastasis (Ye et al., 2011). Finally, an increased expression of p63 and CSC markers, such as Shh, Notch, bcl-2 and ALDH, has been found after androgen deprivation in mice bearing prostate cancer (Tang et al., 2009). Altogether, it could be speculated that loss of p63 could be important for EMT and the acquisition of mobility during invasion, and that a reactivation of p63 expression could be linked to the onset of CRPC and metastasis, potentially mediating CSC properties.

# Objectives

Prostate cancer is a major cause of death for cancer in men in western countries and much effort is put in better understanding the biology of the normal gland and the process of tumorigenesis.

P63 has a crucial role in the prostate during development (Mills et al., 1999; Pignon et al., 2013; Signoretti et al., 2005; Yang et al., 1999). In adulthood, the $\Delta$Np63$\alpha$ isoform remains the most expressed specifically in basal stem cells of the gland and is a major candidate for their maintenance (Barbieri and Pietenpol, 2006; Di Como et al., 2002; Grisanzio and Signoretti, 2008; Signoretti et al., 2005; Wang et al., 2001). There is evidence that p63+ basal stem cells are the cells-of-origin in prostate cancer (Collins et al., 2005; Goldstein et al., 2010; Lawson et al., 2010; Mulholland et al., 2009; Wang et al., 2006). However, the mature tumor has a luminal phenotype and loss of p63 expression is used as a diagnostic marker for carcinoma (Grisanzio and Signoretti, 2008; Jiang et al., 2005).

Despite this suggested importance in prostate biology, to date, there is a lack of functional studies investigating the role of p63 in normal PSCs and cancer. The aims of my project have been to undertake such studies as follows:

✓ Study the function of p63 in normal PSCs;

✓ Investigate a putative role for p63 during cancer development;

✓ Find possible common mediators of stem cells and cancer.

**Results**

# ΔNp63 is expressed in basal PSCs in adult mice

## ΔNp63 is expressed in the basal layer of the prostate of adult mice

Expression of p63 has been detected specifically in the nuclei of cells in the basal layer of mouse adult prostate (Di Como et al., 2002; Signoretti et al., 2005; Wang et al., 2001). At first we wanted to confirm this observation, so we dissected prostates from adult *wild type* (*wt*) mice at 6-10 weeks of age (Figure 1), processed these for immunohistochemistry and stained them for p63 and the basal marker CK5 or the luminal marker CK18. As expected, we detected co-localization of p63 and CK5 in the basal layer, with p63 staining the nuclei and CK5 the cytoplasm of the cells (Figure 2A). In addition, CK18+ luminal cells were negative for p63-expression (Figure 2B).
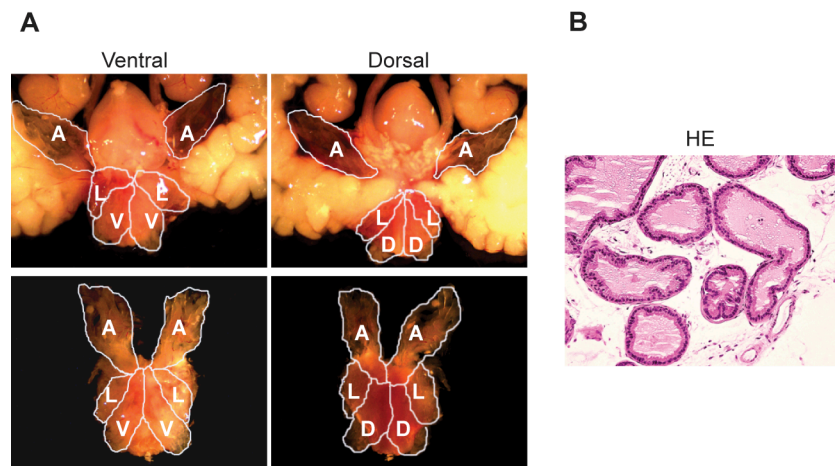


Figure 1. **Prostate dissection from adult *wt* mice**
(A) Representative images of a prostate dissected from 6-10 week-old *wild type* mice. The prostate is shown in the context of the urogenital system on the top and separately on bottom. Ventral (on the left) and dorsal (on the right) sides are displayed and the different lobes are

highlighted. Anterior lobes, A; ventral lobes, V; lateral lobes, L; dorsal lobes, D.

(B) Hematoxylin and Eosin (HE) staining of the sectioned-prostate showing the tubular structure of the gland.

**A**



**B**
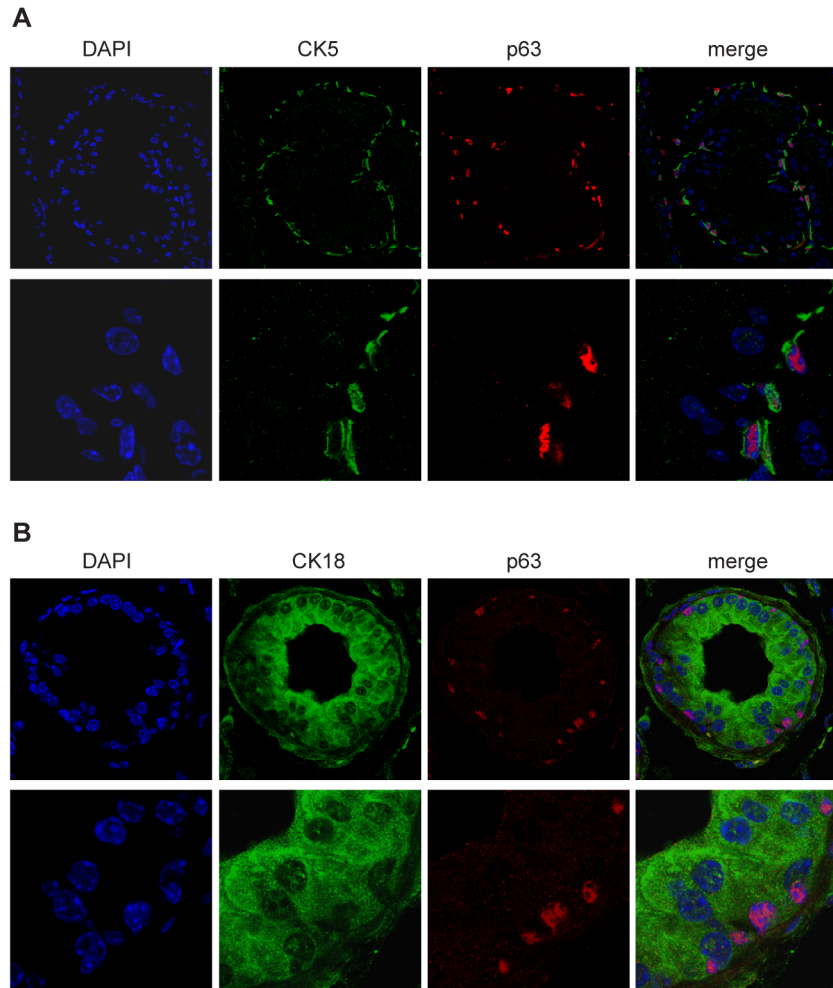


Figure 2. **P63 is expressed in the nuclei of the basal cells in the prostate of adult mice**

(A) Immunofluorescence for the basal marker CK5 and p63 shows that the two proteins are expressed respectively in the cytoplasm and the nucleus of the basal cells. On the bottom, is a higher magnification of the upper panels.

(B) Co-staining for the luminal marker CK18 and p63 showing that they do not co-localize.

**ΔNp63 expression is enriched in basal stem cells**

We wanted to confirm that p63 is enriched in the stem cell subpopulation in the basal layer, as was previously suggested (Mulholland et al., 2009). To perform this, we dissociated prostates of adult *wt* mice and sorted the cells using the prostate stem cell (PSC) markers Sca-1 and CD49f by fluorescent activated cell sorting (FACS) (Figure 3A). We obtained four populations of cells (Sca-1+ CD49f+; Sca-1- CD49f+; Sca-1+ CD49f-; Sca-1- CD49f-) and performed real time-quantitative polymerase chain reaction (RT-qPCR) for the ΔN and TA isoforms of p63 (Figure 3B). This approach identified that there was an enrichment of ΔNp63 expression in the Sca-1/CD49f double positive stem cell population (Figure 3B). It should also be pointed out that TAp63 expression was so low in this situation, that it was almost undetectable (Figure 3B).
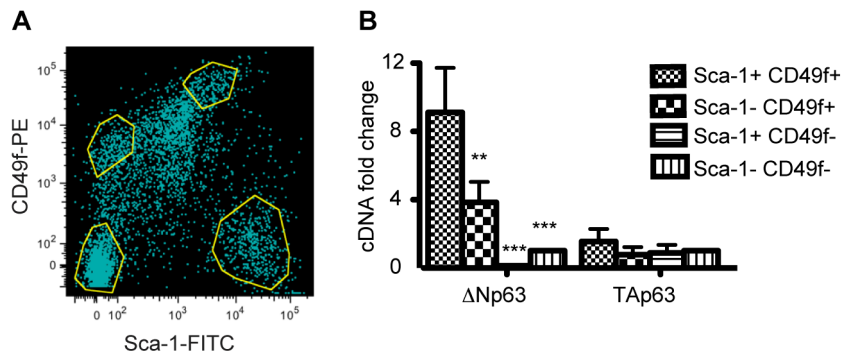


**Figure 3. ΔNp63 mRNA expression is enriched in the Sca-1+ CD49f+ basal stem cell population of mouse adult prostate**
(A) Cells dissociated from prostates of adult *wt* mice were sorted for the stem cell markers Sca-1 and CD49f. Four populations were obtained: Sca-1+ CD49f+; Sca-1- CD49f+; Sca-1+ CD49f- and Sca-1- CD49f-.
(B) RT-qPCR shows increased expression of the ΔN isoform of p63 in the Sca-1+ CD49f+ stem cell population with a significantly lower level of expression in all the other populations. All values are compared to

the Sca-1- CD49f- population. Results are shown as mean $\pm$ SEM of 3 biological replicates.

Next, we performed cytospin on the same four populations of cells isolated from the dissociated prostate gland, and stained the cells for p63 and the basal marker CK5. We found that p63 and CK5 were enriched at the protein level in the Sca-1+ CD49f+ stem cells (Figure 4).

**A**



**B**
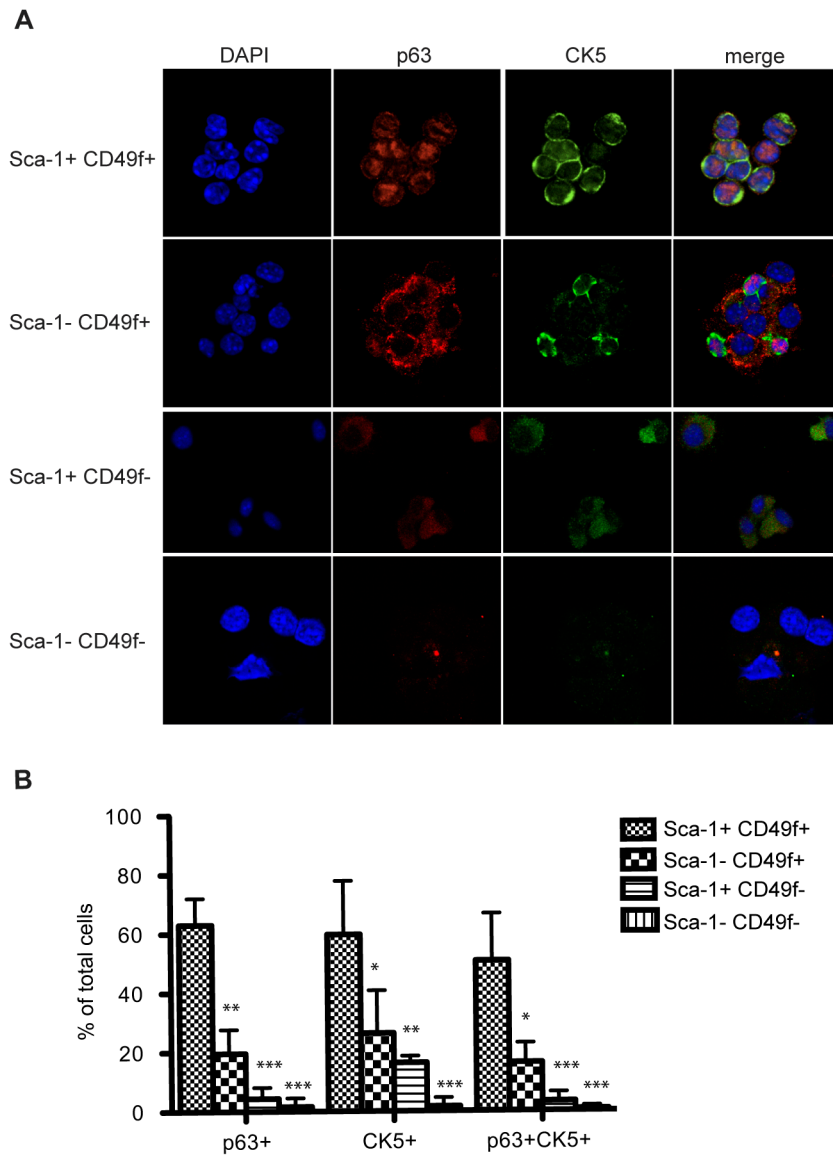


Figure 4. **P63 and CK5 expression is enriched at the protein level in the Sca-1+ CD49f+ basal stem cell population of mouse adult prostate**
Cytospin and subsequent immunofluorescent staining for p63 and CK5 were performed on Sca-1+ CD49f+; Sca-1- CD49f+; Sca-1+ CD49f- and Sca-1- CD49f- populations obtained by FACS.
(A) Representative immunofluorescent images show enrichment of expression of the two basal markers in the Sca-1+ CD49f+ stem cell population. P63 and CK5 coincide almost completely in the same cells.

47

(B) Quantification of p63+, CK5+ and p63+ CK5+ cells confirming protein enrichment in the Sca-1+ CD49f+ population and a significantly lower expression in the other populations. The results are shown as mean $\pm$ SEM from three independent experiments.

Finally we established primary cultures of prostate epithelial cells that were dissociated from adult wt mice. Colonies that could adhere and proliferate in culture, suggesting increased stem cell ability, were formed, and by immunostaining were positive for p63 and CK5 expression (Figure 5).



| Phase contrast | DAPI | CK5 | p63 |
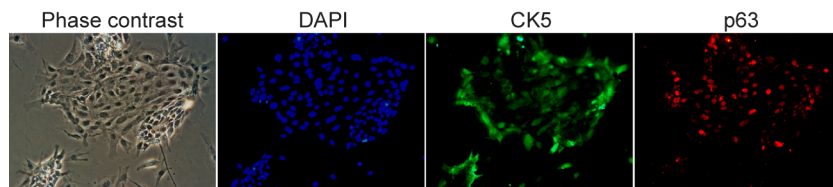
Figure 5. **P63+ CK5+ cells from mouse adult prostate are able to adhere and form colonies in culture**
Epithelial cells dissociated from prostates of adult mice were plated in culture and immunofluorescently stained for p63 and CK5 at day 5. Most of the cells attaching and giving rise to colonies were p63+ CK5+ suggesting that these basal markers identify cells with stem-like properties.

We conclude that the expression of p63, and in particular of the ΔN isoform, is enriched in a subpopulation of stem cells is the basal layer of adult mouse prostate.

# ΔNp63α is expressed in human non-transformed PSCs and in a subpopulation of putative CSCs

## ΔNp63α is expressed in the RWPE-1 human non-transformed cells and in a subpopulation of the PC3 human bone metastatic cell line

In order to choose a model suitable for functional studies of p63 in PSCs and cancer, we screened four major human prostate cell lines for p63 expression: the RWPE-1 non-transformed cells and the LNCaP, DU145 and PC3 cancer cell lines. LNCaP is derived from metastasis to the lymph nodes, DU145 from metastasis to the brain and PC3 from bone metastasis (Bello et al., 1997; Sobel and Sadar, 2005a, b). RWPE-1 has a basal phenotype and all of the cells express high levels of p63 (Harma et al., 2010; Tucci et al., 2012). The metastatic cell lines, as representatives of advanced stages of prostate cancer, are traditionally considered negative for p63 (Signoretti et al., 2000). Surprisingly however, we found expression of both the ΔN and TA isoforms of p63 by RT-qPCR in the PC3 cell line, derived from bone metastasis (Figure 6A). The levels of expression were considerable lower than RWPE-1, but consistently detectable and higher than the other two metastatic cell lines. Interestingly, the expression of p63 increased in response to stressing the cells, by culturing them at high density (Figure 6A). In order to confirm this expression, we next performed immunoprecipitation (IP) and western blot in RWPE-1 and the three metastatic cell lines. With this approach, we detected a band corresponding specifically to the ΔNα isoform of p63 in RWPE-1 and also, even if much weaker, in PC3. No p63 expression was detected for

either LNCaP or DU145 at the protein level, in agreement with the QPCR results (Figure 6B).

**A**



**B**
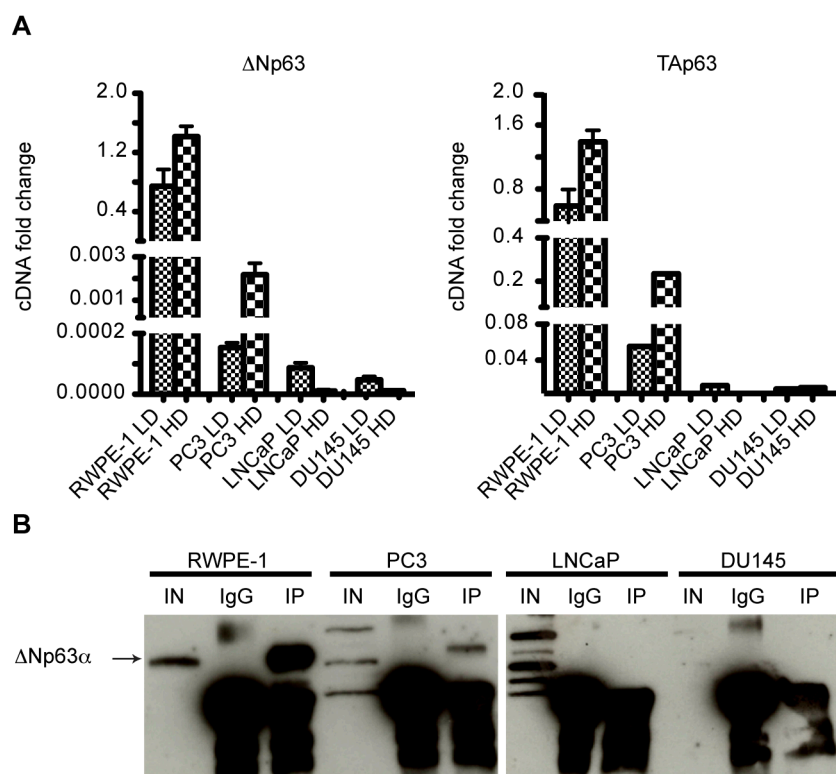


Figure 6. **ΔNp63α is expressed in the RWPE-1 human non-transformed cell line and in PC3 human bone metastatic cells and is absent in the LNCaP and DU145, deriving respectively from metastasis to lymph node and brain**
(A) RT-qPCR for the ΔN and TA isoforms of p63 in the four prostate cell lines. The mRNA expression is higher in RWPE-1, much lower but detectable in PC3 and almost absent in LNCaP and DU145. PC3 grown at high density show enrichment in expression of both isoforms. Low density, LD; high density, HD. Values are compared to those of RWPE-1 LD replicate as reference. Graphs show results as mean ± SEM of three biological replicates.
(B) IP and WB for p63 in the four prostate cell lines showing ΔNp63α expression in RWPE-1 and PC3. Input, IN; Immunoprecipitation with Immunoglobulin G control, IgG; Immunoprecipitation with the p63-specific antibody, IP.

To check whether this expression of p63 was related to a low level of expression in all of the cells, or if it was identifying specific expression in a sub-population of PC3 cells, we performed immunofluorescence for p63. Using RWPE-1 as positive control, we detected p63 expression in all RWPE-1 cells and, interestingly, in a specific subpopulation of PC3 cells (Figure 7).
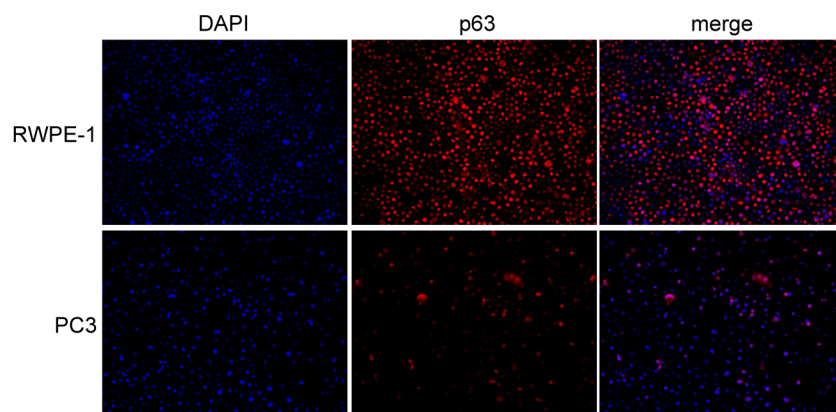


Figure 7. **P63 is expressed in all RWPE-1 and in a subpopulation of PC3 cells in culture**
Immunofluorescence for p63 on RWPE-1 (top panel) and PC3 (bottom panel) cells in culture showing expression of p63 in all RWPE-1 and in a subpopulation of PC3 cells.

To further investigate this expression of p63 in a subpopulation of cells in prostate metastases, we used intra-cardiac injection of PC3 cells to generate metastatic lesions in vivo in nude mice (Valkenburg and Williams, 2011). In order to definitively identify the PC3 cells in the developed lesion, the cells were infected with a retrovirus expressing a Cherry reporter. Following selection, the cells were injected into nude mice, and after six weeks, the metastatic lesions were dissected and stained for Cherry and p63. Importantly, we could detect p63 in a

subpopulation of the metastatic lesion, further identifying the novel expression of the protein in prostate metastatic cells (Figure 8). To confirm that this was indeed the ΔN isoform, these lesions were stained with a ΔN-specific antibody, which again identified as subpopulation of Cherry-positive cells as staining positive for p63 expression (Figure 8).
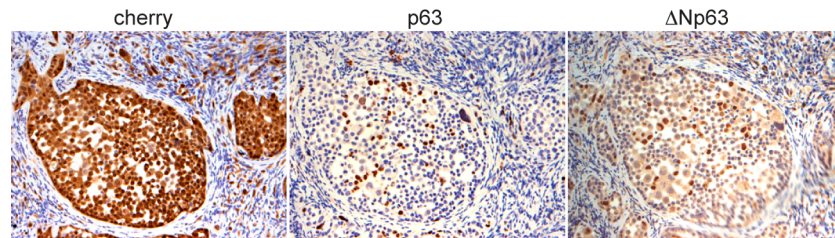


**Figure 8. ΔNp63 is expressed in a subpopulation of PC3 cells in metastatic lesions in mice**
PC3 cells were infected with a Cherry-vector and injected intra-cardiacally in adult nude mice. The derived lung metastases were identified by DAB immunostaining for Cherry. P63 and specifically ΔNp63 expression was found in a subpopulation of Cherry+ metastatic cells.

**P63+ RWPE-1 and PC3 cells have stem-like characteristics**

Considering that p63 is normally expressed in basal PSCs and that subpopulations of cells with stem-like characteristics have been described in PC3 (Celia-Terrassa et al., 2012; Li et al., 2008), we checked if both the RWPE-1 non-transformed cells and the subpopulation of p63+ PC3 metastatic cells could have properties of stem cells. The self-renewal and proliferating potential of RWPE-1 was shown *in vitro* in 3D cultures, where these cells are able to form spheres, which later undergo branching with the generation of tube-like structures, as was previously shown by Harma and colleagues (Harma et al., 2010) (Figure 9).
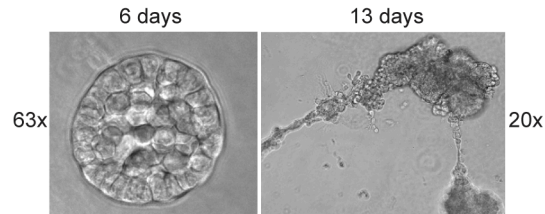
Figure 9. **RWPE-1 cells have stem-like characteristics**
Phase contrast pictures of RWPE-1 cultured in 3D in matrigel show that, in these conditions, they are able to grow spheres (left) that eventually branch and resemble the tubular structure of the prostate (right).

Similarly, as has previously been shown (Harma et al., 2010), PC3 can also form spheres when cultured in 3D (Figure 10A). We checked if these stem-cell favoring conditions would affect p63 expression, Interestingly, we found increased expression of ΔNp63 and the cancer stem cell marker CD44 in PC3 grown in serum-free 3D cultures compared to cells grown in 2D with FBS (Figure 10B).
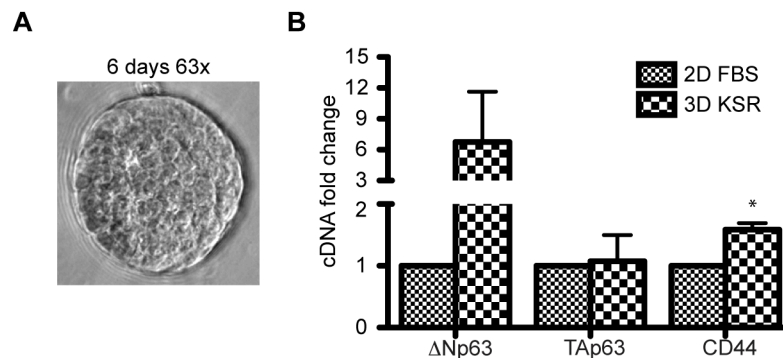


Figure 10. **The expression of ΔNp63 and of the CSC marker CD44 is enriched in PC3 cells grown in stem cell-favouring conditions**
(A) PC3 are able to form spheres when cultured in 3D
(B) PC3 cells were grown either in 2D in the presence of fetal bovine serum (FBS) or in 3D in the absence of FBS, replaced by knockout serum replacement (KSR). RT-qPCR was performed to assess the

level of expression of p63 isoforms and the CSC marker CD44. Enrichment in the expression of ΔNp63 and CD44 was detected in PC3 cells grown in 3D with KSR. Values are compared to the ones in PC3 2D FBS and results are presented as mean $\pm$ SEM of three biological replicates.

To further investigate the possibility that p63 expression might correlate with the CSC subpopulation of PC3, we purified CSCs by FACS after staining PC3 with the CSC marker CD133 (Figure 11A). By isolating these cells and performing RT-qPCR, we found an enrichment of p63, and predominantly the ΔN isoform in the CD133+ CSC population (Figure 11B).

**A**
**B**
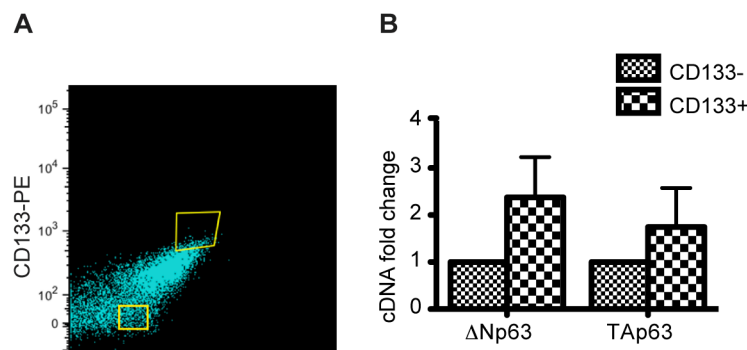


Figure 11. **ΔNp63 is enriched in the CD133+ CSC subpopulation of PC3**
(A) Sorting strategy for isolation of CD133+ PC3 cells
(B) RT-qPCR for ΔNp63 and TAp63 in PC3 CD133- and CD133+, showing enrichment, predominantly of the ΔN isoform, in the CD133+ CSC subpopulation. Values are compared to those of the PC3 CD133- population and results are represented as mean $\pm$ SEM from three independent experiments.

To confirm this result, we performed cytospin collection of CD133-positive and negative cells, and performed immunofluorescence staining for p63. In agreement with our RNA-analysis, the CD133+ cells expressed high level of p63

protein, while the CD133- cells expressed little or no detectable protein (Figure 12).
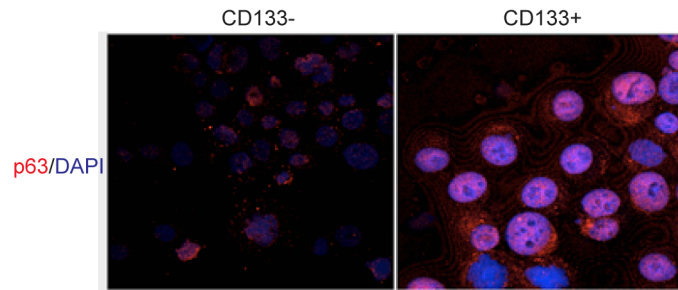


Figure 12. **P63 protein expression is enriched in the CD133+ CSC subpopulation of PC3**
PC3 cells sorted for CD133 were stained for p63 and nuclear localization of the protein was detected specifically in the CD133+ CSCs.

Together, these observations led us to the conclusion that RWPE-1 cells express high levels of $\Delta$Np63$\alpha$ in all the cells and have basal stem cell-characteristics. Furthermore $\Delta$Np63$\alpha$ is specifically expressed in a putative CSC subpopulation in the PC3 human bone metastatic cell line. We therefore chose these two cell lines as models for functional studies of $\Delta$Np63 respectively in normal PSCs and in prostate cancer.

## $\Delta$Np63 has a crucial function in PSCs and prostate cancer metastasis to the bone

### Loss of $\Delta$Np63 in RWPE-1 impairs growth capacity and self-renewal

In order to study the function of $\Delta$Np63 in normal PSCs, we designed and cloned short hairpins (shRNAs) specifically targeting the $\Delta$Np63 isoform, with which we subsequently infected the RWPE-1 cell line. The efficiency and isoform-

specificity of some of the shRNAs are shown by WB and RT-qPCR in Figure 13. Based on these parameters, we chose the shp63 4 for subsequent functional studies for ΔNp63α.
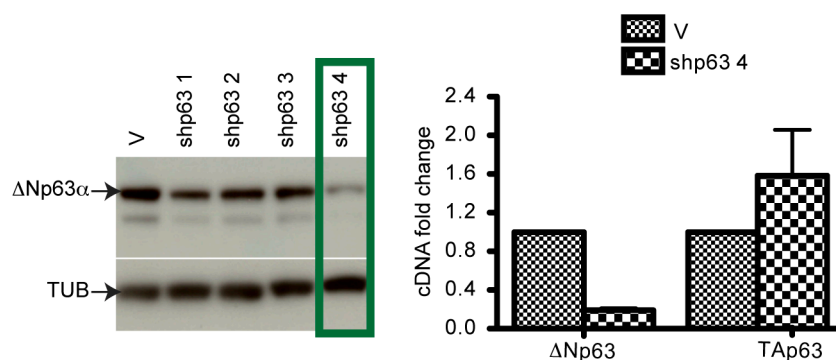


Figure 13. **Test of shRNA targeting p63**
Several shRNAs were cloned and infected into RWPE-1 cells. The efficiency of p63 knockdown was tested by WB (on the left). Isoform specificity was verified by RT-qPCR for the ΔN- and TA-isoforms. Shp63 4 was found as the most efficient and specific for ΔNp63 and it was used for subsequent studies. RT-qPCR values are compared to reference values of cells infected with vector control and results are presented as mean ± SEM of three biological replicates. Vector control, V; tubulin loading control, TUB.

The proliferation potential of the RWPE-1 cells infected with shp63 4, hereafter referred to as R-shΔN, compared to RWPE-1 infected with vector control, R-V, was tested *in vitro* through the analysis of growth curves. Proliferation potential and self-renewal were also checked by growing the cells in colony forming assay and 3D culture. Interestingly, RWPE-1 cells losing ΔNp63 expression have a slightly reduced growth rate in 2D cultures, as shown in phase contrast pictures and quantified through growth curve in (Figure 14).

**A**

**B**
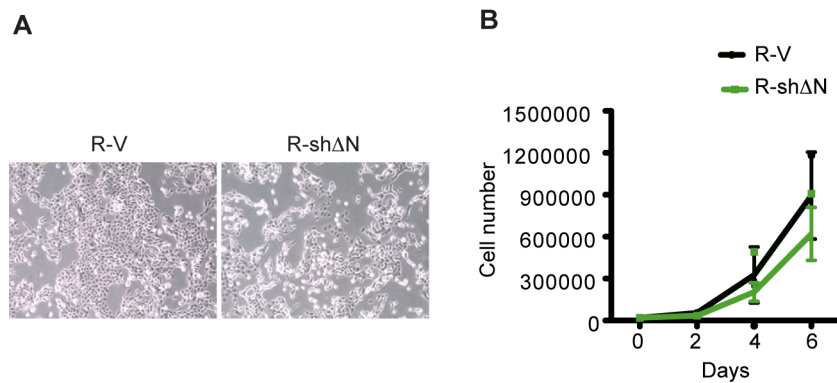


Figure 14. **RWPE-1 cells following knockdown for ΔNp63 show reduced growth rate**

RWPE-1 were infected with either vector control or shΔNp63 and plated at equal numbers.

(A) Pictures of cells at one week in culture show a slightly reduced number of cells growing when ΔNp63 is lost.

(B) Growth curve showing impairment in growth potential of R-shΔN. Results are presented as mean $\pm$ SEM of three biological replicates, each plotted as average of 3 technical replicates.

However, the growth disadvantage and self-renewal impairment of R-shΔN was most clear when the cells were plated in stem cell-favoring conditions such as colony formation assay (Gandellini et al.) (Figure 15) and 3D culture (Figure 16A). In particular, RWPE-1 infected with shΔNp63 grew less and smaller colonies in 2D, and spheres in 3D (Figures 15 and 16). In addition, upon passaging in 3D, they were practically unable to form self-renewing spheres (Figure 16A).
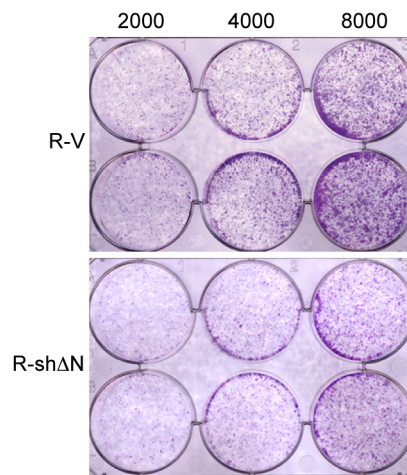
Figure 15. **Loss of ∆Np63 causes a growth disadvantage of RWPE-1 cells in focus-formation assays**
R-V and R-sh∆N were plated at low density (2000, 4000 and 8000 cells/well in duplicate) and after ten days the colonies were stained with crystal violet. Fewer and smaller colonies grew in RWPE-1 with ∆Np63 knock down.

**A**



**B**
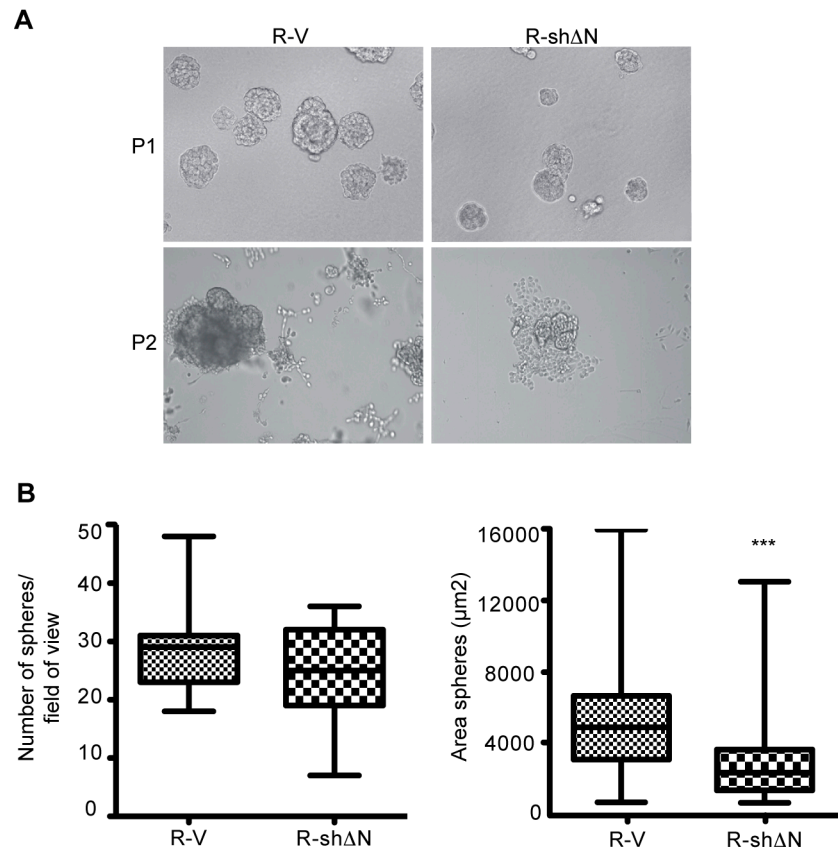


Figure 16. **R-shΔN growth is significantly impaired in stem cell-favoring 3D cultures**
(A) R-V and R-shΔN were plated in equal numbers in 3D cultures in matrigel. Representative pictures at first passage (P1) at day 6 show how RWPE-1 losing ΔNp63 grew fewer and smaller spheres (P1, top panel). The effect was even more evident in cells at the second passage (P2, bottom panel).
(B) Quantification of the number and area of the spheres at P1 after one week in culture. RWPE-1 with knockdown of ΔNp63 formed fewer and significantly smaller spheres. Values from three and two experiments are combined for quantification of number and area of around 350 spheres respectively. Whiskers plots from min–max values were used for graphic representation.

To try to study the role of p63 in PSCs *in vivo*, we attempted to use mouse genetics to ablate the expression of p63 in normal *wt* mice prostates. We used a mouse that expresses Cre

specifically in the prostate under control of the Probasin-promtoer (Pb-Cre) and crossed this to a mouse in which the p63 gene was flanked by lox-P sites ($p63^{fl/fl}$; $p63^{fl/fl}$). The aim was to obtain a mouse model with loss of p63 specifically in the adult prostate. However, after successful crossing and genotyping for the correct combination of alleles that should result in ablation of p63 expression, the mice did not present any histological defects and p63 remained expressed in most of the nuclei in the basal cells (Figure 17). We attributed the failure of the model to the fact that the probasin promoter driving Cre expression is androgen-responsive and is mostly active in the luminal cells. This inefficiency of p63 knockdown (KD) in the basal layer led us to abandon this strategy.

| | | | | | |
|---|---|---|---|---|---|
| Num mice | 6 | 12 | 12 | 3 | 3 |
| Age (weeks) | 10 | 15 | 20 | 25 | 30 |
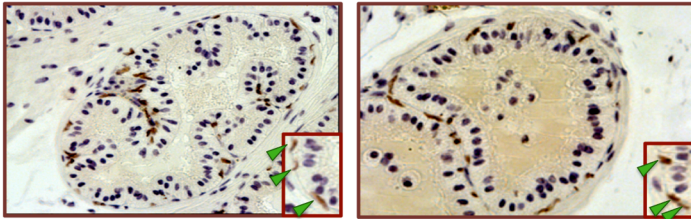


Figure 17. **Generation of a p63-specific KO mouse model**
Pb-Cre mice were crossed with a $p63^{fl/fl}$ mice to generate p63- prostate specific KO mice. On the top, the number and age of mice sacrificed and analyzed are reported. On the bottom, staining for p63 of KO and wt mice revealed that the former mostly retain p63 expression in the nuclei of the basal cells of the prostate.

In conclusion, we have shown that ΔNp63 is not only a marker of PSCs as previously described, but also has a functional role in normal PSCs proliferation and self-renewal.

**ΔNp63 does not affect PC3 growth rate *in vitro***

We then tested if the functional role we described for ΔNp63 in PSCs could be translated to the metastatic p63+ PC3 subpopulation of cells. We used the same *in vitro* approaches as in RWPE-1, comparing PC3 cells with knockdown of ΔNp63 (P-shΔN) or over-expressing ΔNp63α (P-ΔNα) to PC3 that were infected with a control vector (P-V). When examined using the same assays described above, i.e. growth curves, focus-formation assays and 3D sphere formation, there were no major differences detected in the growth rate in any condition *in vitro* (Figure 18).
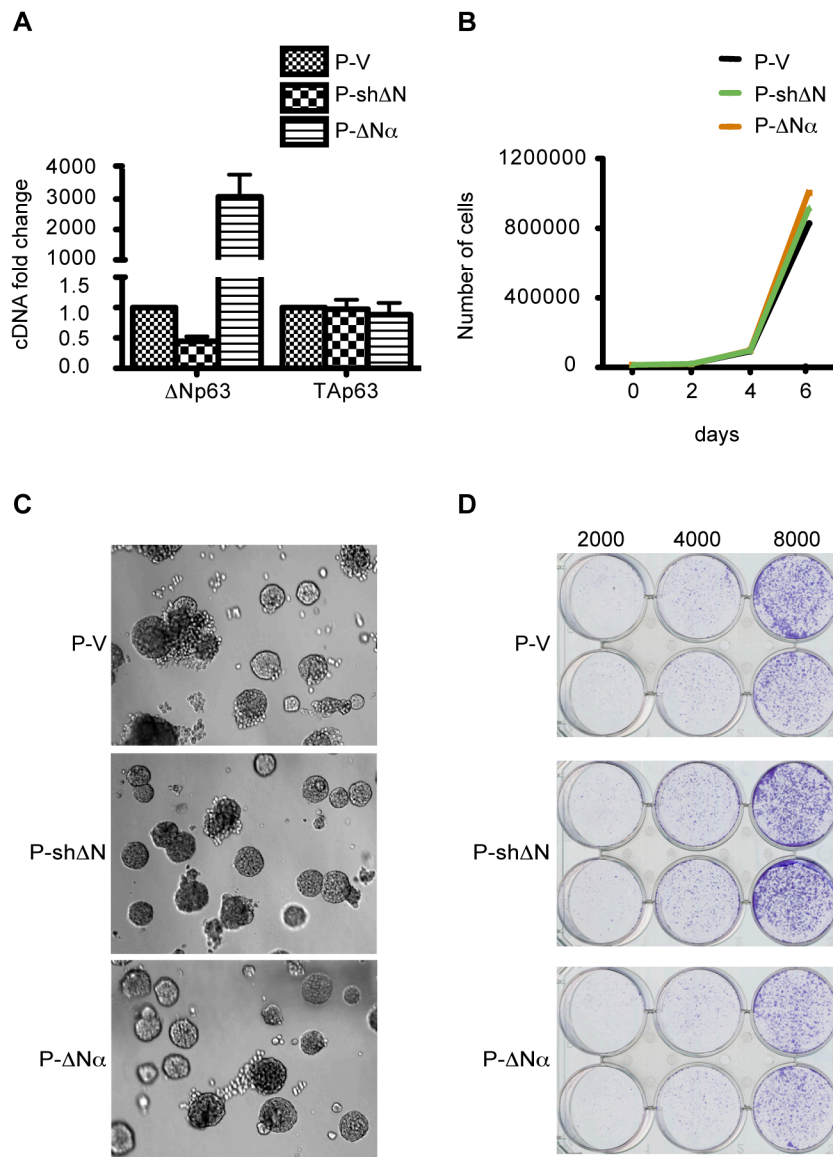
Figure 18. **ΔNp63 does not affect PC3 growth *in vitro***
PC3 cells were infected with vector control, shΔNp63 and ΔNp63α.
(A) RT-qPCR for p63 isoforms shows the efficiency and specificity respectively of the ΔNp63α overexpression and of the ΔNp63 knockdown. Values are compared to PC3-V and mean $\pm$ SEM are reported from 6 different infections.
(B-D) No difference was detected in growth rate of the cells in the three conditions of growth curve, 3D culture and FFA.

**ΔNp63α promotes metastatic colonization of PC3 to the bone**

Given the results presented above in PC3 cells *in vitro*, we next checked for a possible role for ΔNp63 in PC3 cells in a more physiological setting *in vivo*. To address this, in collaboration with Tian Tian and Laura Batlle Morera, CRG, we performed intra-cardiac injections in male nude mice of PC3 cells that had been infected with vector (P-V), or shRNA-ΔNp63 (P-shΔN) as above. These cells had also been co-infected with a luciferase-GFP (Luc-GFP) reporter vector to allow imaging of the developing tumors. First, we performed imaging of the animals immediately after injection to measure luciferase signal and to ensure that the mice had been properly injected and that the cells disseminated correctly around the body (Figure 19).
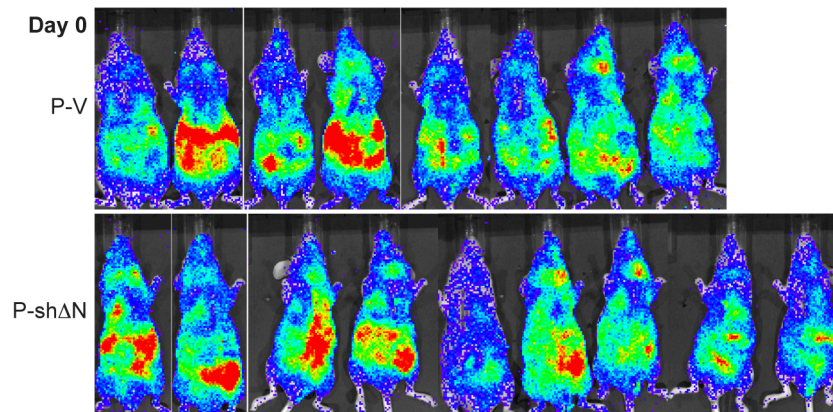


Figure 19. **Imaging of mice injected intra-cardiacally with P-V and P-shΔN cells co-infected with a Luc-GFP at day 0.**
The luciferase signal shows that cells disseminated all over the body.

Subsequently, mice were imaged every week after the second week to measure the onset and incidence of metastasis. Interestingly, we observed an earlier onset of metastases at

week four in P-V mice and a delay in the appearance of lesions, measured both as luciferase signal intensity and number of metastases, in the P-shΔN animals (Figures 20A and 20B), suggesting that an absence of ΔNp63 delayed metastatic colonization. In particular the onset of bone metastasis lesions, quantified by looking specifically at hind limbs, was delayed in the P-shΔN group (Figures 20A and 20C). The number of detectable bone metastases per mouse (but not their average signal), remained lower in the P-shΔN mice until week six. Nevertheless P-shΔN tumors eventually equalized in terms of the total and bone-specific signals, and the number of metastases (Figures 20B and 20C).

**A**



**B**



**C**
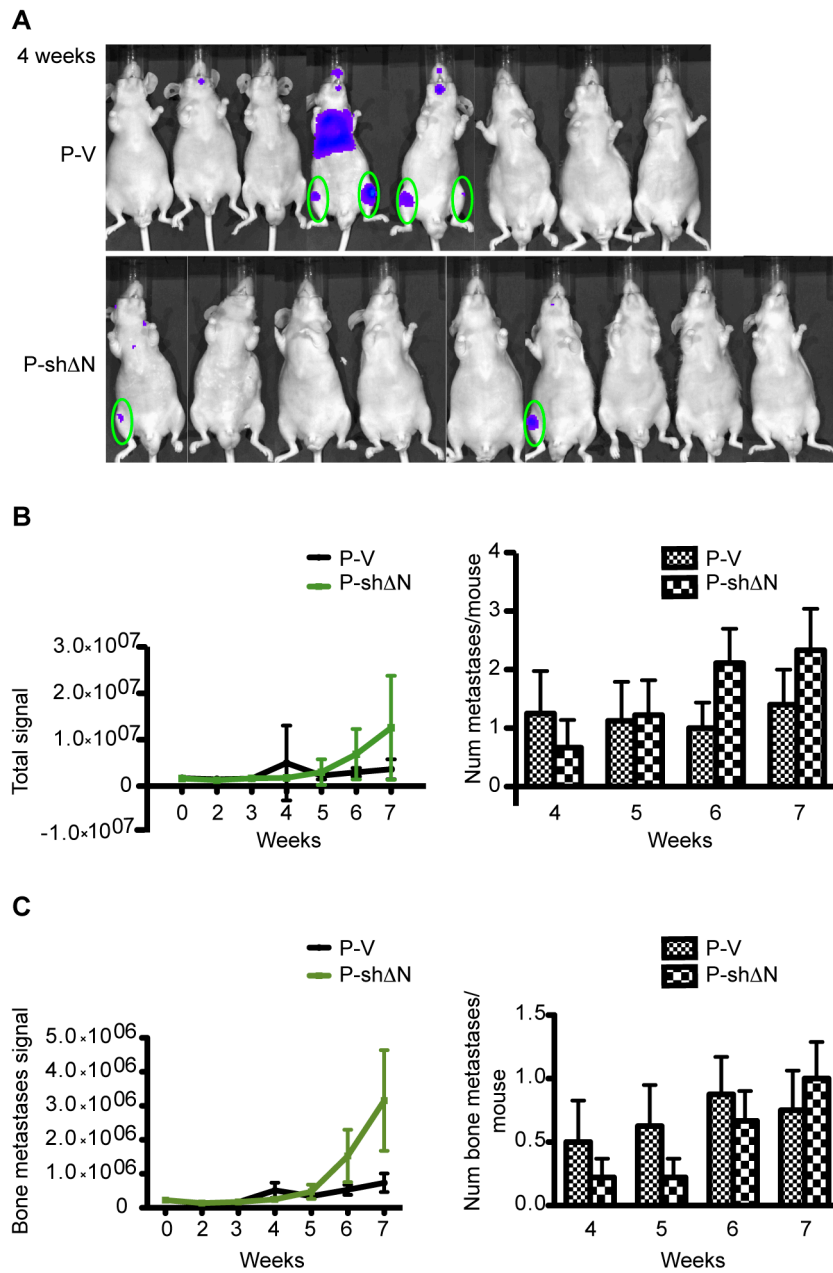


Figure 20. **Mice injected intra-cardiacally with PC3 cells with knockdown of ∆Np63 show a delay in total and bone metastases appearance**

$1x10^6$ P-V and P-sh∆N cells co-infected with a Luc-GFP construct were injected intra-cardiacally in adult male nude mice. Metastatic growth

was monitored by weakly measurement of luciferase signal. 8 mice were analyzed for the P-V group and 9 for the P-shΔN group.

(A) Imaging of the animals at week 4 shows a delay in tumor formation by P-shΔN group.

(B) Quantification of the luciferase signal and the detectable number of lesions/mouse confirms the initial delay in metastases appearance in P-shΔN mice. The differences between the two groups are not significant at any time point.

(C) Specific bone metastatic signal and the detectable number of bone lesions per mouse have been quantified by looking at hind legs (circles). There is a slightly lower luciferase signal at week 4 in the P-shΔN animals but tumors caught up at later time points. A lower number of bone lesions was evident until week 6 in the P-shΔN group. The differences were not statistically significant.

As a second approach, and to specifically investigate the role of ΔNp63α in bone metastases *in vivo,* we performed intra-tibial injections in male nude mice of P-V and P-ΔNα co-infected with the Luc-GFP reporter vector, and monitored the mice over time for the development of luciferase-positive lesions.

In a first experiment, we injected $1 \times 10^6$ cells and we observed an enhanced tumor growth in mice injected with the cells expressing ΔNp63α at weeks 2 and 3 post-injection (Figure 21). Eventually the control group equalised in luciferase signal intensity and the number of lesions at week 5 and all the mice were sacrificed at this time point (Figure 21B). This result however suggests that expression of ΔNp63α favors metastatic tumor initiation in the bone microenvironment.

66

**A**



**B**
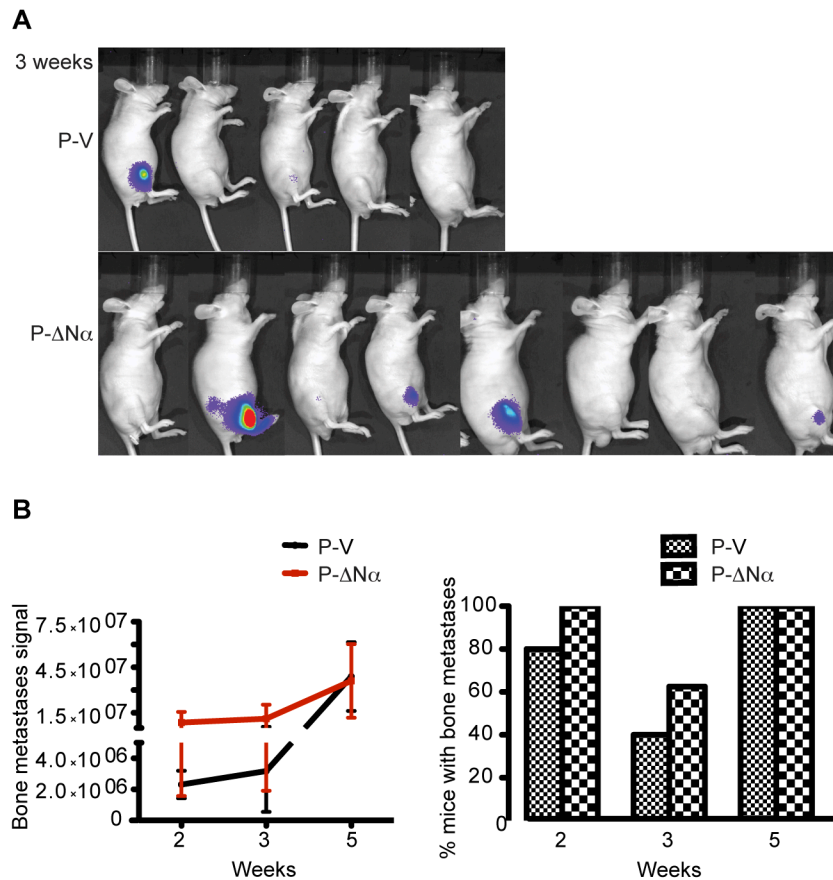


Figure 21. **Mice injected intra-tibially with P-ΔNα cells show accelerated metastasis formation compared to mice injected with P-V**
Male nude mice were injected intra-tibially with $1x10^6$ P-V + GFP-Luc and P-ΔNα + GFP-Luc cells. Bone metastasis formation was monitored weekly by luciferase imaging starting from week 2. Animals were sacrificed at week 5. 5 mice were analyzed for the V group and 8 for the ΔNp63α group.
(A) Imaging of mice at week 3 shows an accelerated tumor formation in the P-ΔNα group.
(B) Quantification of luciferase signal and number of metastases highlights an earlier onset and appearance of the lesions in the P-ΔNα mice and higher luciferase signal and number of metastasis. Luciferase signal is represented as mean $\pm$ SEM.

In order to optimize the differences between the P-ΔNα experimental group and the P-V control group, in a second intra-

tibial injection experiment, we injected a lower number of cells, $2.5 \times 10^5$, and imaged and monitored the animals as before. In this case, animals were sacrificed and samples collected at different time points, based on the appearance of the luciferase signal. This would allow us to perform histological studies of the lesions at an early time point, as the main difference between the two groups seems to be during the onset of metastasis growth. In this scenario, the increased onset and incidence of tumor growth in P-$\Delta$N$\alpha$ mice was much more evident, considering both the luciferace signal and the number of lesions (Figure 22). At week six, the difference in the percentage of mice with metastasis between the P-V and P-$\Delta$N$\alpha$ groups became significant and the last mice were sacrificed (Figure 22B).

Overall we conclude that $\Delta$Np63$\alpha$ favors metastatic colonization in the bone.

**A**



**B**



| | P-V | P-ΔNα |
|---|---|---|
| 3 weeks | 7 | 9 |
| 4 weeks | 5 | 6 |
| 5 weeks | 4 | 4 |
| 6 weeks | 4 | 2 |
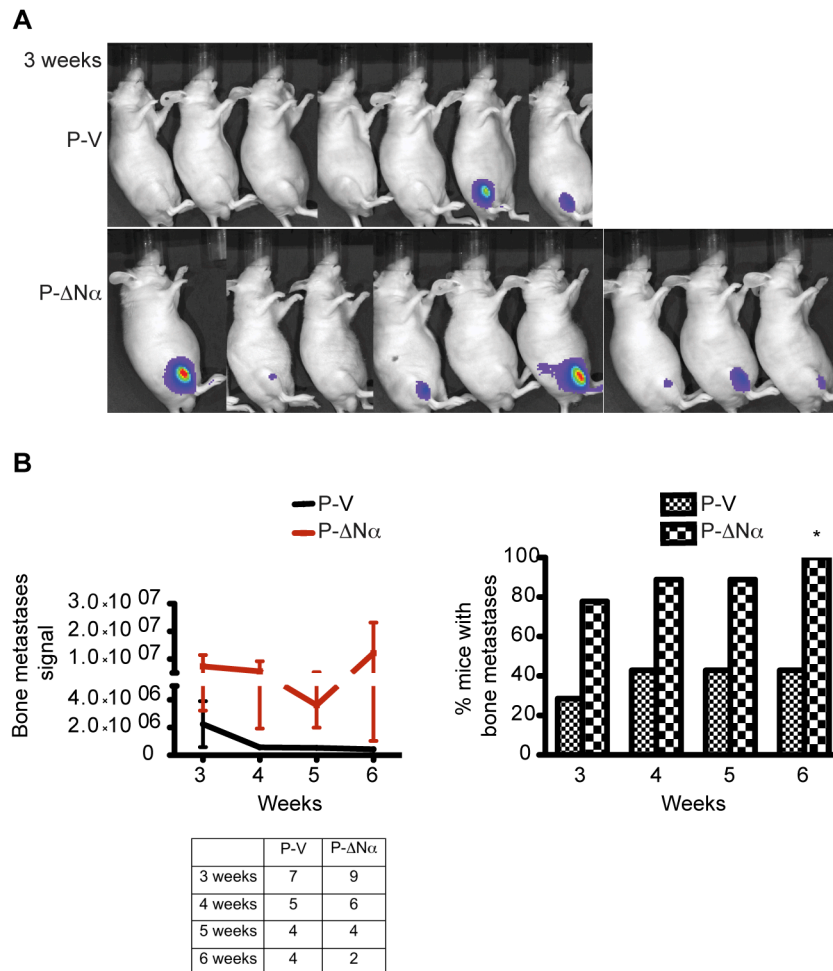
Figure 22. **ΔNp63α confers growth advantage to PC3 cells in the bone microenvironment**

Adult male nude mice were injected intra-tibially with $2.5 \times 10^5$ P-V + Luc-GFP and P-ΔNα + Luc-GFP. Bone metastasis formation was monitored weekly by luciferase imaging starting from week 3. 7 mice were analyzed for the P-V group and 9 for the P-ΔNα group. Animals were sacrificed at different time points depending on the appearance of the luciferase signal.

(A) Imaging of mice at week 3 shows an accelerated formation of metastatic lesions in the P-ΔNα group.

(B) Quantification of both luciferase signal and the percentage of animals with metastases shows an enhanced tumor formation in the P-ΔNα group. The table indicates the number of mice in which the luciferase signal was quantified at each time point. Luciferase signal is represented as mean $\pm$ SEM. The graph of the percentage of mice with

69

bone metastases refers to the total number of mice developing lesions from the beginning of the study.

## ΔNp63α expression influences the histology of bone lesions

In collaboration with the group of Jesús Ruberte at the Universitat Autonoma de Barcelona (UAB), we performed histological analyses of the bone lesions of mice that had been injected intra-tibially with $1\times10^{6}$ P-V and P-ΔNα cells (first experiment) at week 5 after injection. This analysis revealed a strong osteoclastic reaction, with destruction of the bones in both P-V and P-ΔNα tumors, as has previously been reported for PC3 cells (Angelucci et al., 2006; Chu et al., 2008; Cross et al., 2008; Margheri et al., 2005). In particular in Figure 23, HE staining indicates the loss of normal tissue structure. Further analysis using Masson's Trichrome staining highlights the damage in the mineralized parts of the bones, while staining with acidic phosphatase is indicative of the presence of activated osteoclasts and/or macrophages, both of which are increased in the metastatic lesions (Figure 23).

At this late stage of metastatic tumor progression (when tumor incidence had normalized between P-V and P-ΔNα) (Figure 21B) there were few if any major differences visible at the gross pathological level between the two samples. However, at the cellular level, the P-ΔNα appeared to have a different cellular makeup, with a predominantly more mesenchymal/stromal appearance when compared to the P-V samples (Figure 24).

| PBS | P-V | P-ΔNα |
|---|---|---|
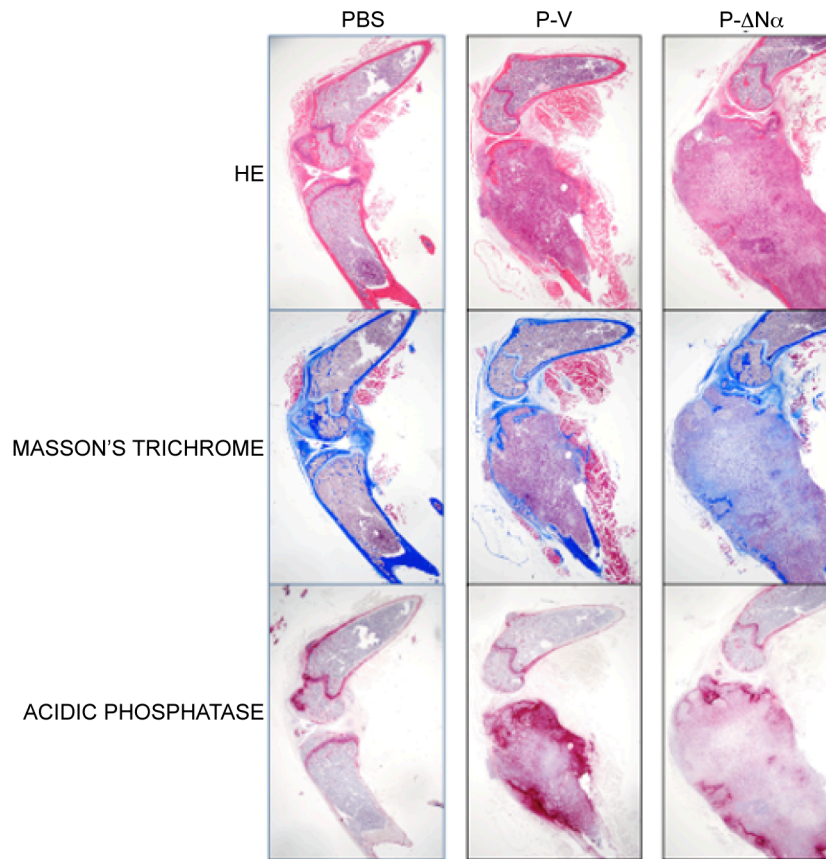


Figure 23. **Bone disruption in metastasis from P-V and P-ΔNα**
Representative images of different histological staining of tibias injected with $1x10^6$ P-V and P-ΔNα cells at week 5 post-injection. The comparison with control tibias injected with PBS shows loss of structure (HE staining on the top), destruction of mineralized bone (Masson's trichrome staining in the middle) and osteoclastic/macrophage activity (acidic phosphatase staining on the bottom) in both P-V and P-ΔNα groups of mice.

Interestingly, the detection of the metastatic cells by staining for the GFP protein marker corroborated these differences. While staining for GFP revealed a predominant composition of the tumors by the GFP-positive metastatic cells in the P-V lesions, the tumors in P-ΔNα animals were mostly negative for GFP and presented with a more mesenchymal phenotype (Figure 24).

Interestingly, this different tissue composition of the tumors in the two groups by this late stage of tumor growth might have also affected the interpretation of the luciferase signal. That is, as the luciferase signal comes specifically from the PC3 cells, it is indicative of the tumor mass in the case of the P-V metastases, but not in the case of the P-$\Delta$N$\alpha$ lesions at the later stages, when they were mostly formed by stroma. We hypothesize that the $\Delta$Np63$\alpha$ expressing cells influence the surrounding microenvironment, favoring stromal proliferation, while at the same time they could be cleared by the immune system. To address these questions, we are currently performing similar analysis on the second set of tumors that resulted from injection of fewer cells and which were collected at earlier time points (Figure 22B). The aim is to determine whether the tumors that develop earlier in response to $\Delta$Np63$\alpha$ expression manifest differently at the pathological and cellular level.
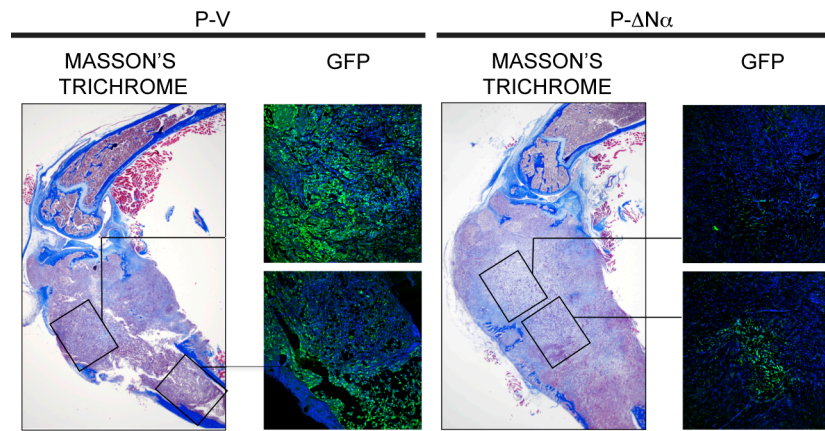
**Figure 24. ΔNp63α-expression alters bone metastasis histology**
GFP staining of tibias injected with $1x10^6$ P-V and P-ΔNα at week 5. GFP identifies the metastatic cells injected and highlights a main difference between the tumors derived from P-V and P-ΔNα. The former are formed by the GFP+ injected metastatic epithelial cells, while the latter are mainly GFP- and present with a mesenchymal phenotype.

Next, we subjected the bone-metastatic lesion to immunohistochemistry for p63 expression. An interesting observation was that p63, and in particular the ΔN isoform, was detected by fluorescent immunostaining in a subpopulation of the GFP-positive P-V cells in bone metastatic lesions (Figure 25), further supporting our initial finding that p63 is expressed in a subpopulation of prostate metastatic-cells.

However, and as expected from the previous observation that only a few GFP+ PC3 cells remained in the PC3-ΔNα lesions, almost all of the cells were negative for p63 and ΔNp63 (Figure 25). This is a further confirmation that the lesions generated by PC3 over-expressing ΔNp63α are mostly composed of a different type of cells at later stages of tumor progression.

P-V

p63    ΔNp63

P-ΔNα

p63    ΔNp63

p63 GFP    ΔNp63 GFP        p63 GFP        ΔNp63 GFP
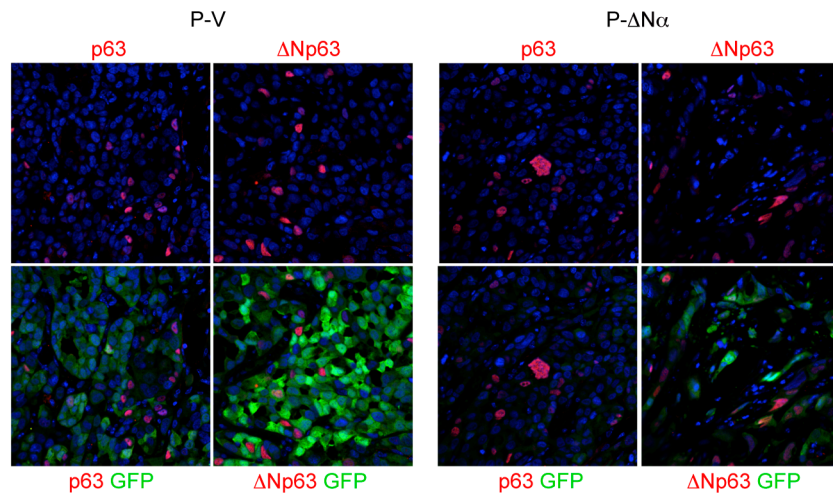
Figure 25. **Scattered ΔNp63+ metastatic cells are present in P-V bone tumors and only a few are left in P-ΔNα lesions**
Representative images of GFP and p63/ΔNp63 co-staining of tumors in tibias injected with $1 \times 10^6$ P-V (left panel) and P-ΔNα (right panel) cells at week 5. Individual double-positive (GFP+p63/ΔNp63+) cells are present in the P-V lesions. Most cells in the P-ΔNα group were double negative (GFP-p63/ΔNp63-), indicating an altered composition of the tumor.

# ΔNp63 induces epithelial stem cell and bone survival genes

## Loss of ΔNp63 expression in RWPE-1 induces loss of an epithelial stem cell signature and down-regulation of bone microenvironment genes

In order to determine how ΔNp63 might contribute to the regulation of PSC function, we performed microarray analysis on RWPE-1 cells that had been infected with shΔNp63 compared to those infected with a vector control. Analysis of the microarray, selecting for a p-value of less than 0.05, and a fold change of greater/less than 1.4 fold change identified 814 genes that were up-regulated and 472 genes that were down-regulated in response to loss of ΔNp63 expression (Figure 26A). As we have

found that expression of ΔNp63 favors PSC maintencance, we focused on the genes whose expression was decreased in response to loss of ΔNp63 expression. A number of those were validated by RT-qPCR in separate experiments (Figure 26B).

**A**



**B**
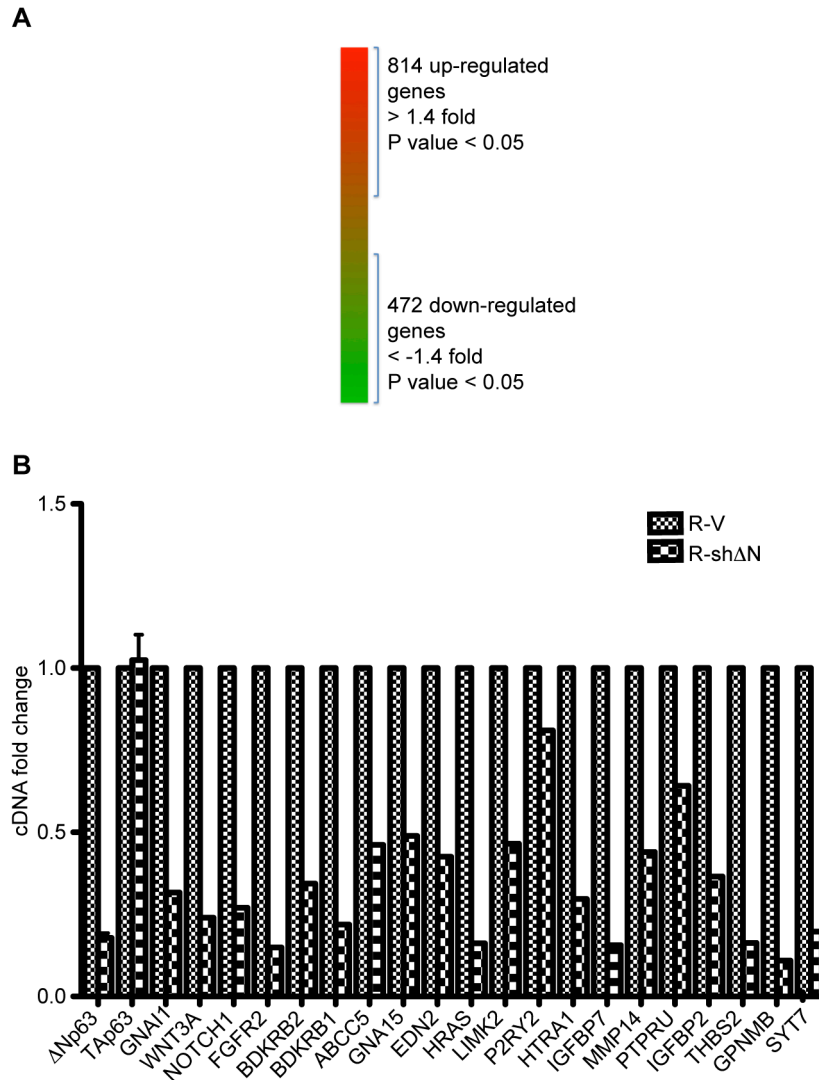


Figure 26. **Microarray analysis of R-shΔN compared to R-V**
Four technical replicates for each group were analyzed.

(A) Schematic heat map representing the microarray results, setting the fold change threshold at 1.4/-1.4 and the p value at 0.05.
(B) RT-qPCR validation of some of the targets identified in the microarrays. cDNA fold changes are compared to values in R-V. Two biological replicates are presented for ΔNp63 and TAp63, and one for the targets.

Interestingly, among the genes that were down-regulated in response to loss of ΔNp63 expression, were markers of basal cells such as CK5 and CK14, and stem cell mediators such as CD44, Notch1, CD49f and various members of the Wnt signaling pathway. Moreover, among the up-regulated genes were luminal differentiation markers such as CK8, CK18 and CK19 (Figure 27).
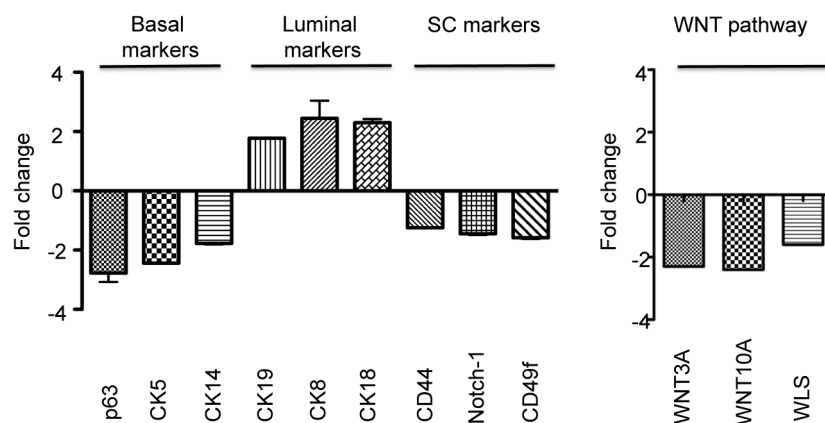


Figure 27. **Loss of ΔNp63 in RWPE-1 causes decreased expression of basal and stem cell genes and induction of luminal differentiation markers**
Analyses of the genes down-regulated in R-shΔN, compared to R-V in microarray reveal the presence of basal and stem cell markers and pathways (Wnt pathway in particular). Among the genes up-regulated in consequence of loss of ΔNp63, we found luminal differentiation markers.

To investigate the gene expression changes at a more global level, we performed gene ontology analysis on the genes that

were increased or decreased in response to knockdown of ΔNp63. Focusing on the down-regulated genes, among the biological processes mostly affected by loss of ΔNp63, were genes involved in epithelial development and stem cell division, as would be expected for loss of p63 in an epithelial cell (Figure 28A). However, we surprisingly found a loss of gene expression that gave GO signatures including "osteoblasts" "macrophages", "stromal cells" and "myofibroblasts" among others (Figure 28A). These signatures are in strong agreement with the phenotypes seen in the bone metastatic lesions where ΔNp63α is over-expressed (Figures 24 and 25). We conclude that ΔNp63 controls the expression of prostate epithelial stem cell genes and surprisingly genes whose expression is linked with the bone microenvironment.

**A**



Pathways

Tissues

Diseases

Biological processes

**B**
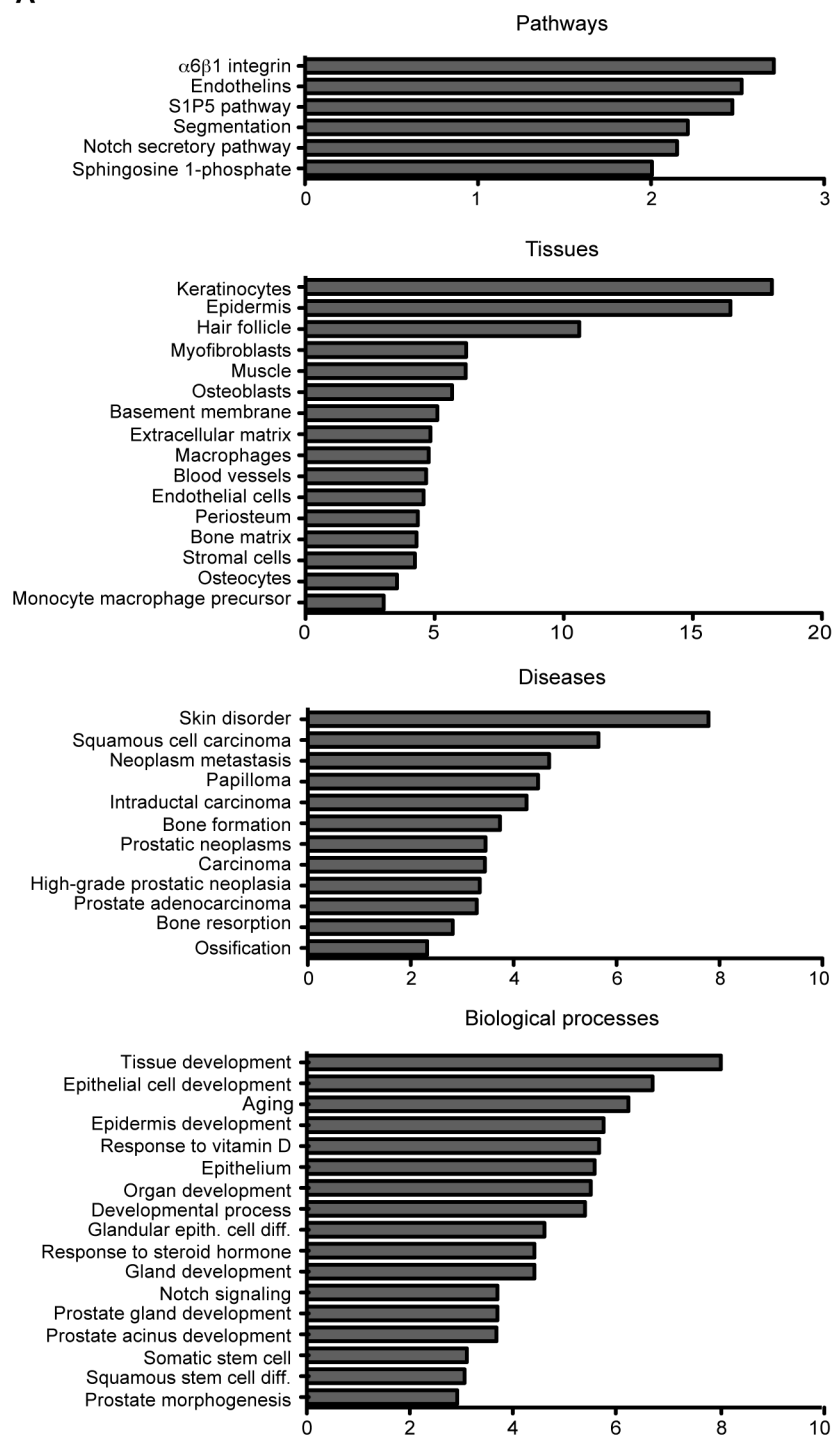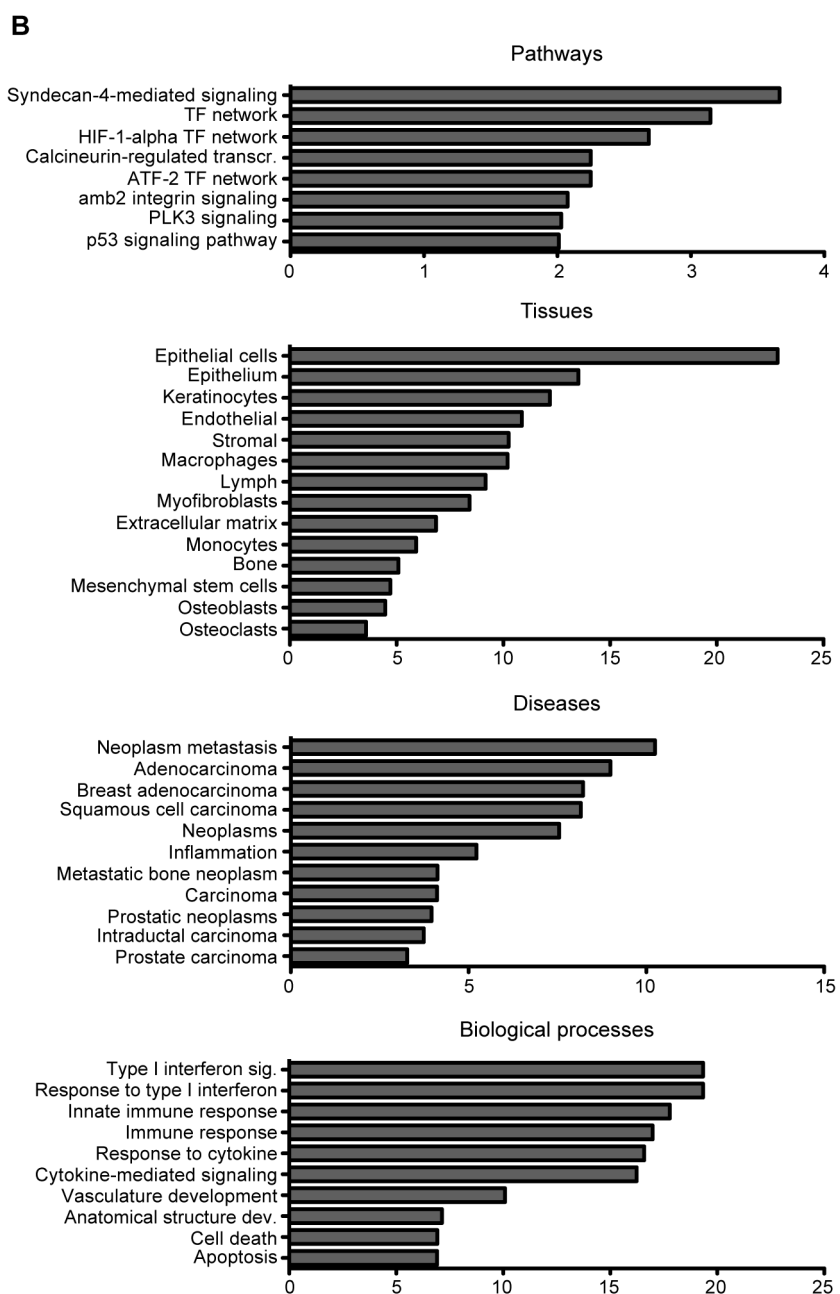


Figure 28. **Knockdown of ΔNp63 in RWPE-1 causes down-regulation of genes involved in epithelial development, stem cells and also bone microenvironment**

Gene ontology analysis of genes down (A) and up-regulated (B) in microarrays of R-shΔN compared to R-V showing the over-represented categories.

**Over-expression of ΔNp63α induces the expression of genes involved in adhesion and bone homing in PC3**

In the attempt to find the mediators of bone metastasis that are regulated by ΔNp63, we next profiled, through microarray analysis, the PC3 cells over-expressing ΔNp63α, and compared this with PC3 infected with empty vector. Surprisingly, we found very few genes whose expression was significantly affected (Figure 29A: 75 genes up-regulated; 19 down-regulated: $\pm$ 1.4 fold change, p-value 0.05). We performed Gene Ontology (GO) analysis on the small set of genes that were increased by ΔNp63α overexpression in PC3 cells (the list of genes that were downregulated was too small for similar GO analysis). Although this was a small dataset, it further pointed to roles for ΔNp63α contributing to regulation of the bone microenvironment, driving the expression genes involved in such processes as "ECM", "myofibroblasts" and "stromal cells", as well as diseases including "carcinoma" and "prostatic intraepithelial neoplasia" (Figure 29B).

**A**



75 up-regulated
genes
> 1.4 fold
P value < 0.05

19 down-regulated
genes
< -1.4 fold
P value < 0.05

**B**



Pathways

Nitric oxide
Aryl hydrocarbon rec.
TIMP pathway
Interleukin 1
MMP pathway

Tissues

Epidermis
Extracellular matrix
Myofibroblasts
Stromal cells

Diseases

Papillary carcinoma
Benign prostatic hyperplasia
Carcinoma
Systemic inflammatory response
Prostatitis
Prostatic intraepithelial neop

Biological processes

Integrin-mediated signaling
Chronic inflammatory resp.
Lipid localization
Regulation of cell prolif.
Regulation of stress response
Aging
Positive reg. of angiogenesis

Figure 29. **ΔNp63α overexpression in PC3 drives the expression of genes involved in bone microenvironment: ECM, myofibroblasts and stromal cells.**
Microarray analysis was performed on P-ΔNα, compared to P-V. Two technical replicates were analyzed for P-V and 4 for P-ΔNα.
(A) Schematic heat map representing results setting the fold change threshold at 1.4/-1.4 and the p value at 0.05
(B) Gene ontology analysis of genes up-regulated in microarrays of P-ΔNα compared to P-V showing the over-represented categories.

Interestingly among the up-regulated genes were mediators of adhesion, and bone homing and colonization including ITGβ4, IL1β and CD82 (Carroll et al., 2006; Liu et al., 2013; Nishioka et al., 2013). Moreover, genes encoding membrane transporters (SLC37A2) (Chou et al., 2013) and genes involved in drug metabolism (UGT1A6 and UGT1A8) (Rowland et al., 2013) were up-regulated in PC3 cells over-expressing ΔNp63α. All of them could be involved in survival in a hostile microenvironment such as the bone during metastatic colonization and probably in therapeutic response.

To further strengthen the observation of the regulation of these genes by ΔNp63 expression, we compared the microarray dataset in which ΔNp63 was knocked down in *wildtype* PSCs (RWPE-1) and this dataset in which ΔNp63α was overexpressed in PC3 cells (Figure 30A). Interestingly, among the 16 genes regulated accordingly to ΔNp63 in both arrays there were the same genes that have been linked with adhesion, bone homing and colonization and drug-transport (Figure 30A), and some were further validated in additional RT-qPCR experiments in both cell lines (Figure 30B).

**A**



↑ P-ΔNα
microarray

**16**

R- shΔN
microarray ↓
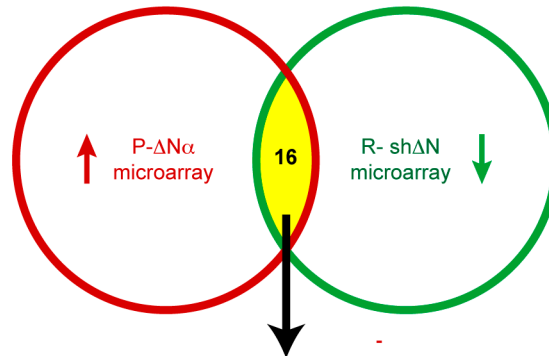
Adesion/ECM protein:
ITGβ4, DST

Bone homing and colonization:
IL1β, CD82

Membrane transporters:
SLC37A2, TMEM40, ANXA8L2

Drug metabolism:
UGT1A6 & UGT1A8, XDH, GPX2

Others:
DFNA5, KRT6A, KRT6C, NEFL, C17ORF99

**B**
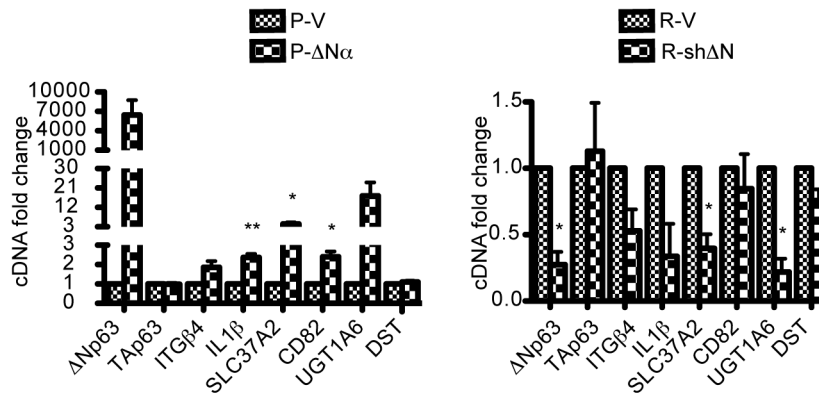


Figure 30. **ΔNp63 controls expression of genes involved both in stem cell maintenance and bone metastatic colonization**
(A) Comparison of the lists of genes up-regulated by over-expression of ΔNp63α in PC3 and down-regulated in RWPE-1 knocked-down for ΔNp63 identifies 16 genes, 11 of them involved in adhesion, ECM, bone colonization and drug metabolism.

(B) RT-qPCR for the validation of some genes changing accordingly with ΔNp63 both in PC3 and RWPE-1 validates the results observed in microarrays. Results presented as mean ± SEM from four and three biological replicates respectively for PC3 and RWPE-1

# New direct targets of p63 in the epithelial stem cell and bone survival signatures

Given the fact that p63 is a transcription factor, we wanted to check if the genes affected by ΔNp63 expression in the microarray analysis in RWPE-1 and PC3, could be direct targets. We therefore performed Chromatin immunoprecipitation for p63, followed by sequencing (ChIP-Seq) in RWPE-1 cells. To validate that the procedure worked correctly, we examined for known targets of p63, including p21 and PERP, which were indeed directly bound by p63 in these cells. Representative peaks for these are shown, along with examples of two novel p63 target genes, WNT3a and CK8 (Figure 31).
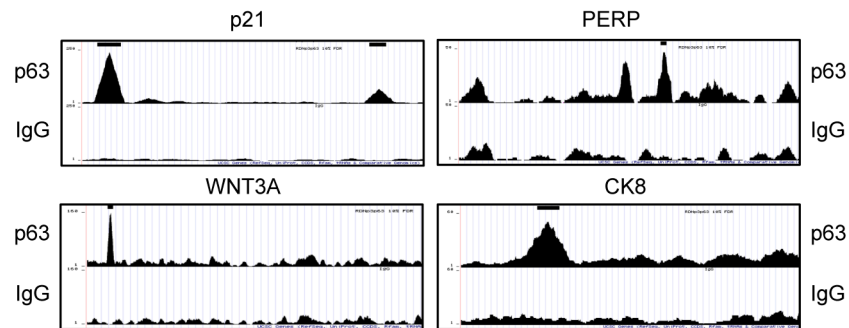


Figure 31. **Representative peaks of p63 ChIP-Seq in RWPE-1**
The known targets p21 and PERP (on the top) are represented as positive controls and two representative novel targets (WNT3A and CK8) are shown on the bottom. Peaks of p63 ChIP-Seq are compared to background peaks given by the control IgG.

Next, we overlapped the list of direct p63 targets obtained by Chip-Seq with the microarray studies to identify those direct p63 targets in PSCs that are both decreased or increased by ΔNp63 knockdown and ΔNp63α overexpression respectively in RWPE-1 and PC3 (Figure 32). Interestingly, this gave us a "10-gene signature" of genes that might be involved in PSC and bone metastasis and which are regulated by ΔNp63. This list still contained the previously mentioned genes involved in cell adhesion, bone homing and colonization and drug transport and metabolism (Figure 32). As further proof, two of these, ITGβ4 and CD82, were previously identified as direct targets of p63 in different tissues (Carroll et al., 2006; Wu et al., 2014).
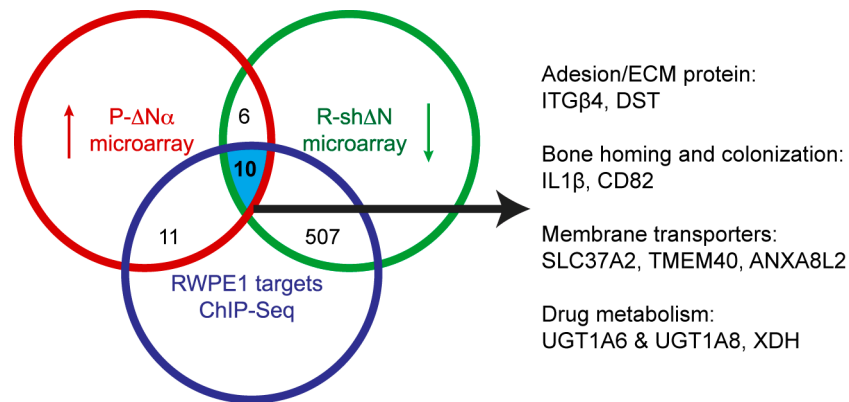


Figure 32. **Stem cell/bone metastatic genes are direct targets of p63**
Most of the genes found by list comparison of genes up-regulated by over-expression of ΔNp63α in PC3 and down-regulated in RWPE-1 knocked-down for ΔNp63 are novel direct targets of p63 identified by ChIP-Seq.

## The p63 target CD82 could mediate bone metastatic adhesion

To further investigate the mechanisms by which ΔNp63 might mediate metastasis to the bone, we concentrated on the link between ΔNp63 and IL1β and CD82, as both have previously been demonstrated to be involved in homing and adhesion to the bone.

IL1β has been previously described as a mediator of prostate cancer bone metastasis (Liu et al., 2013). As shown above (Figure 30B), both knowckdown of ΔNp63 and overexpression of ΔNp63α in RWPE-1 and PC3 respectively led to significant changes in the IL1β transcript. Next, we analyzed the levels of the protein by ELISA in the media of PC3 cells that were infected with a control vector or that over-expressed ΔNp63α. However, no difference in IL1β levels was detected in the media from cells in culture. We are now planning to perform ELISA on serum from mice injected intra-cardiacally with P-V and P-shΔN or intra-tibia with P-V and P- ΔNα to attempt to detect alterations in IL1β protein expression *in vivo.*

CD82 is traditionally described as a tumor suppressor owing to its documented inhibitory effect on invasion of primary tumors. However, it is also known to control adhesion of hematopoietic cells to the bone marrow (Larochelle et al., 2012; Liu and Zhang, 2006; Nishioka et al., 2013; Termini et al., 2014; Zhang et al., 2003). More recently it has also been identified as a direct p63 target gene (Wu et al., 2014). In order to strengthen our link between ΔNp63α and CD82 expression in the prostate, we checked through FACS analysis that CD82 was enriched at the

86

protein level in the $\Delta$Np63$\alpha$ over-expressing cells as compared to PC3 infected with vector control. Interestingly, we found that over-expression of $\Delta$Np63$\alpha$ in PC3 cells led to a 1.7 fold increase (15% to 25%) in CD82 expression, supporting our earlier data (Figure 33).



P-V          P-$\Delta$N$\alpha$

**% CD82+ cells:**     **15%**           **24.6%**
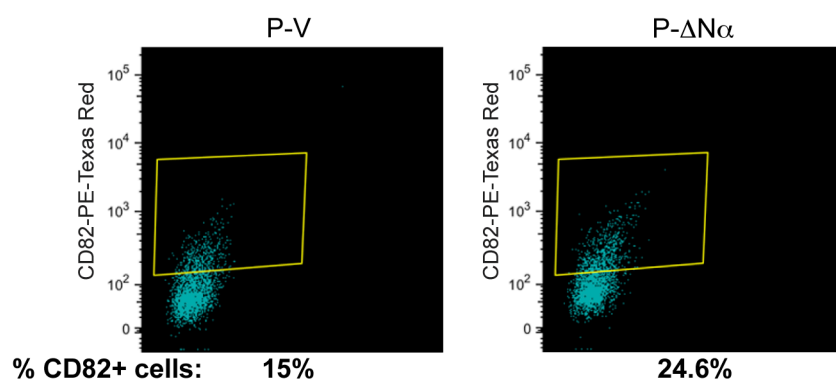
Figure 33. **CD82 protein expression is enriched in P-$\Delta$N$\alpha$ as compared to P-V**
PC3 cells infected with V or $\Delta$Np63$\alpha$ were fluorescently stained for CD82 and analyzed by FACS. CD82+ cells were constantly enriched in P-$\Delta$N$\alpha$ cells. A representative result of 3 independent experiments is shown.

As 15% of the PC3 cells contained high levels of CD82, we next took the inverse approach of sorting CD82+ cells from PC3 and checking for $\Delta$Np63 expression through RT-qPCR (Figure 34). Importantly, $\Delta$Np63 expression was increased in this population of cells (Figure 34B). We also tested the expression of the stem cell/bone signature genes from microarrays and ChIP-Seq analyses, and found that many of these were also enriched in the CD82+ population (Figure 34B).

**A**

**B**
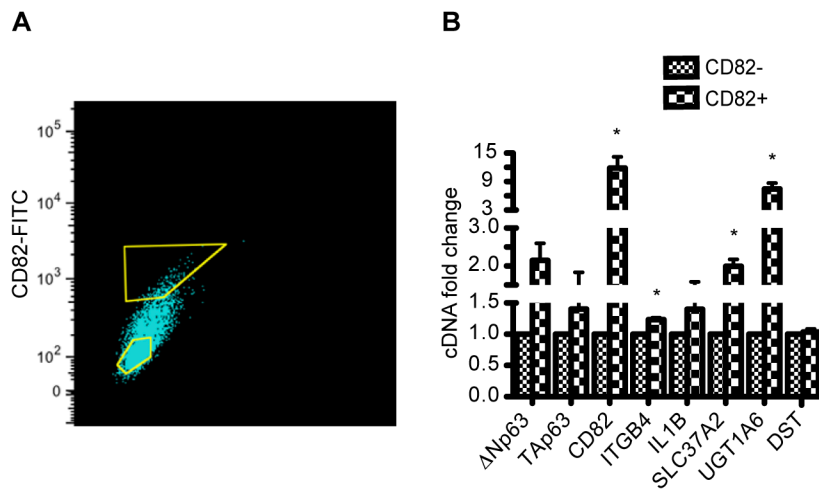


Figure 34. **Expression of ΔNp63 and its targets is enriched in PC3 CD82+ cells**
(A) CD82+ and CD82- cells were sorted from PC3.
(B) Levels of the two isoforms of p63 and of other genes directly regulated by ΔNp63 were analyzed by RT-qPCR in the two populations. ΔNp63 and most of its targets are consistently up-regulated in PC3 CD82+ cells. Values referred to PC3 CD82- and results presented as mean ± SEM from three biological replicates.

Next, to test for a possible functional role for ΔNp63α in mediating adhesion of PC3 cells in the bone microenvironment, we cultured PC3 cells that had been infected with ΔNp63α or empty vector on different substrates that are involved in bone adhesion, such as Collagen I, Fibronectin and Laminin I. In collaboration with Tian Tian, CRG, we plated out these cells and allowed them to attach for short periods of time, before washing away the non-attached cells. Quantification of the attached cells after these short time points after plating shows that PC3 cells that over-express ΔNp63α have significant advantage in adhesion on each of substrates as well as on PBS, conclusively demonstrating that ΔNp63α mediates adhesion in prostate cells. (Figure 35).
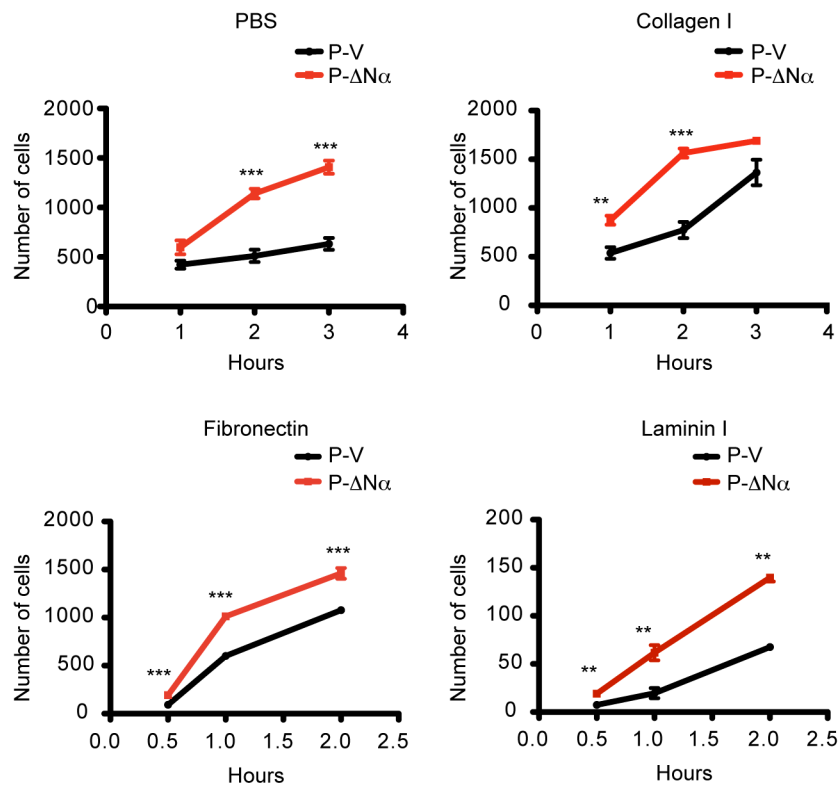
**Figure 35. ∆Np63α over-expressing cells attach better on bone adhesion substrates**

P-V and P-∆Np63α were plated in the presence of PBS, Collagen I, Fibronectin or Laminin I. Plates were washed after short time points and attached cells were fixed, stained with crystal violet and counted. The number of attached PC3 cells over-expressing ∆Np63α is significantly higher at different time points in every condition. Results are presented as mean $\pm$ SEM of three technical replicates of one representative biological replicate. One biological replicate was done for PBS and Collagen I and three biological replicates have been done for Fibronectin and Laminin I.

Next, we will investigate whether CD82 is directly involved in mediating this adhesion. We are in the process of testing several short hairpins against CD82 with which we will infect PC3 cells over-expressing ∆Np63α, to check if loss of CD82 could affect the adhesion advantage that ∆Np63α confers to PC3 *in vitro.*

Ultimately, we will also inject these same cells in which $\Delta$Np63$\alpha$ is overexpressed, but which lack CD82, intra-tibially to investigate the *in vivo* requirement of CD82 in favouring $\Delta$Np63$\alpha$-mediated bone metastasis.

**Discussion**

In our study, for the first time, we demonstrate a role for p63, and specifically the $\Delta N\alpha$ isoform, in adult basal PSCs maintenance and in metastatic colonization to the bone, possibly correlated to features of CSCs. Moreover, we identify common mediators of stemness and metastasis directly controlled by p63. These new findings could have important implications to better understand normal prostate homeostasis and the process of bone metastases formation that is the main cause of morbidity and mortality in patients with prostate cancer.

**P63 expression in prostate stem cells**

Initially, we confirmed that $\Delta Np63$ is expressed in a basal subpopulation of Sca-1+ CD49f+ stem cells in the prostate of adult mice (Barbieri and Pietenpol, 2006; Di Como et al., 2002; Grisanzio and Signoretti, 2008; Mulholland et al., 2009; Signoretti et al., 2005; Wang et al., 2001). An interesting observation is that $\Delta Np63$ expression is also present to a lesser extent in the intermediate Sca-1- CD49f+ population both at the mRNA and protein levels. This finding implies that $\Delta Np63$ could have a different dosage-sensitive role in progenitor cell populations also.

Moreover, atypical cytoplasmic staining was detected in both the Sca-1- CD49f+ and Sca-1+ CD49f- intermediate populations. From the absence of transcript expression in the Sca-1+ CD49f- cells, we speculate that $\Delta Np63$ is transported to the cytoplasm to be degraded, possibly contributing to differentiation in the Sca-1- CD49f- $\Delta Np63-$ population. Indeed, Galli and colleagues demonstrate that $\Delta Np63$ is transported to the cytoplasm and

93

degraded to allow differentiation in keratinocytes (Galli et al., 2010). This hypothesis would imply that ΔNp63- differentiated cells derive from ΔNp63+ basal stem cells in the adult prostate, as they do during development (Ousset et al., 2012; Pignon et al., 2013; Signoretti et al., 2005). In agreement with this, we show that loss of ΔNp63 in RWPE-1 induces an up-regulation of luminal differentiation genes.

Alternatively however, there might be a specific role for p63 in the cytoplasm, as described by Fotheringham and colleagues in keratinocytes, where they show that cytoplasmic p63 is involved in promoting Epstein Barr Virus-associated epithelial cancers (Fotheringham et al., 2010). In this respect, it has to be mentioned that, in a recent clinical report, cytoplasmic staining for p63 has been correlated to poor prognosis in advanced stages of prostate cancer (Dhillon et al., 2009). Moreover cytoplasmic functions have been described for the other two members of the family, p53 and p73 (Geng et al., 2010; John et al., 2011). However, in our study we concentrated on ΔNp63 as a transcription factor in the nuclei of PSCs and cancer cells, but it would be interesting to further investigate a possible cytoplasmic function for p63.

**P63 expression in CSCs**

As described, our investigation uncovered a previously unseen pattern of ΔNp63α expression in a subpopulation of metastatic cells with CSC characteristics that is specific for the PC3 bone metastatic cell line. It remains interesting that similar expression of ΔNp63α was absent from the other models of metastases to the lymph nodes and brain, further supporting our data showing

that ΔNp63α actively contributes to the attachment and survival of these cells in the bone metastatic environment. It would be interesting to assess if enforced expression of ΔNp63α in the non-bone metastatic cell lines would subsequently endow these with bone-survival properties.

Another interesting observation regarding the expression of p63 in putative metastatic CSCs is that it is enriched when the cells are stressed by culturing them in high density-culture. Given the role we discovered for ΔNp63α in prostate cell adhesion, we speculate that metastatic cells, when cultured at high density, are able to activate ΔNp63α expression to enhance attachment and prevent anoikis. Indeed our findings are in complete agreement with a previous study that identified p63 as a critical regulator of cell-adhesion and survival in breast and keratinocyte cells, through the regulation of ITGβ4 (Carroll et al, NCB). Given that ITGβ4 is one of our signature "10-gene bone metastatic list" this further reinforces the validity of our findings.

Another possibility is that ΔNp63α might promote survival through regulation of alternate metabolic pathways and detoxification of metabolic products in conditions of starvation such as high density-culture. In support of this, we found a new link for ΔNp63α in the regulation of UGT-detoxification enzymes, as well as ALDH3A1, a protein linked to the cellular response to oxidative stress and hypoxia, as among the p63 direct targets that are up-regulated in PC3 cells over-expressing ΔNp63α. In further agreement with this, roles in the regulation of cellular metabolism have been described for all of the p53 family members (Berkers et al., 2013).

Finally, Chae and colleagues demonstrated a function for $\Delta$Np63$\alpha$ in survival in high density-cultures through temporary and reversible growth inhibition (Chae et al., 2012). Accordingly, we observed that in vivo, in the metastatic lesion, a physiological setting in which cells are stressed and likely starved, the subpopulation of p63+ PC3 cells are non-proliferative, staining negative for the proliferation marker Ki67 (data not shown). In this specific context, $\Delta$Np63$\alpha$ might also exert its role in the DNA damage response and transiently block the cell cycle (Craig et al., 2010; Lin et al., 2009).

In conclusion, there is a certain plasticity in $\Delta$Np63$\alpha$ expression and it could be activated in putative CSCs to promote adhesion, metabolism, detoxification, transient and reversible cell cycle arrest and hence survival in metabolic stress conditions such as high density culture and, possibly, in a similar *in vivo* setting, in the metastatic microenvironment.

## Experimental models and approaches to study $\Delta$Np63 function in PSCs and metastases to the bone

The decision to primarily use cell lines in our work was dictated by the difficulties in maintaining, expanding and transforming primary prostate epithelial cells in culture. Although I was successfully able to establish and generate primary cultures of these cells, their long-term maintenance and propagation remains a problem in the field. However, RWPE-1 cells have been used as a valid model for basal PSCs owing to the high level of expression of $\Delta$Np63$\alpha$ and the basal stem cell phenotype and properties of these cells in culture. Subsequently we chose to use the PC3 metastatic cell line to study the role of p63 in

96

cancer after detecting that indeed, contrary to the current thinking and the published literature, p63 is expressed, albeit at very low levels, in these cells.

In our *in vitro* functional studies, we uncovered different effects of manipulation of ΔNp63-expression between the non-transformed and metastatic cell line that likely reflect the cell model used. In RWPE-1, we demonstrate a role for ΔNp63 in maintaining PSCs, whereas manipulation of ΔNp63 expression did not affect PC3 growth in normal or low density-cultures both in 2D and 3D.
This result suggests that the effect of ΔNp63 manipulation in a subpopulation of the culture is not sufficient to manifest in the context of the larger bulk of p63 negative cells. However, it also suggests that metastatic cells might be influenced by their physiological environment.

Indeed, in the PC3 cells in which ΔNp63 was knocked down for ΔNp63, there is a delay in metastasis formation *in vivo* after intra-cardiac injection in nude mice. The limited effect of loss of ΔNp63 expression in this context could again be explained by the presence of ΔNp63 in only a low percentage of cells, so the overall effect of loss of expression could be hidden in a highly aggressive metastatic cell line. However, the decrease in initiation of bone-metastasis formation suggests that ΔNp63 is involved in the very early stages of bone metastatic colonization, and that this likely involves the stem cell properties, adhesion ability and signaling to the surrounding microenvironment mediated by ΔNp63.

Another important variable that may influence the results of this study is the link between $\Delta$Np63 expression and EMT. It has been shown that loss of $\Delta$Np63 promotes loss of epithelial phenotype and EMT, which was also supported in our expression analyses in RWPE-1 cells in which $\Delta$Np63 was knocked down (Barbieri et al., 2006; Gandellini et al., 2012; Higashikawa et al., 2007; Tucci et al., 2012). As EMT might favor extravasation after intra-cardiac injection, a defect in metastases formation of PC3 with knock-down of $\Delta$Np63 could be masked by a higher amount of cells reaching distant sites. The option of intra-cardiacally injecting PC3 cells that over-express $\Delta$Np63$\alpha$ has been discarded from the beginning because these cells are theoretically impaired to undergo EMT and so exiting the blood flow and invading distant tissues to form metastatic loci would likely be significantly impaired.

Taking all these considerations into account, the intra-tibia injection of PC3 over-expressing $\Delta$Np63$\alpha$ was the most suitable experimental approach in our case and allowed us to uncover a role for $\Delta$Np63$\alpha$ in metastatic colonization.

**Functional role of $\Delta$Np63$\alpha$ in bone metastatic colonization and fate of the $\Delta$Np63$\alpha$ positive cells at later stages of metastasis**

Our functional data with overexpression of $\Delta$Np63$\alpha$ in PC3 cells clearly shows that these cells have increased metastasis-initiating capacity, giving rise to more and earlier-forming tumors. However, exactly how $\Delta$Np63$\alpha$ fully leads to this property remains to be shown. We have uncovered strong links with the regulation of cell-adhesion, but signaling to the local

microenvironment, metabolism and cell-cycle control (as discussed above) all likely contribute.

Why ΔNp63α-expressing cells may disappear at later stages of metastasis remains unknown, but again the signatures from the microarray data linking ΔNp63 with macrophage recruitment and inflammatory response suggest these processes may be involved. This further supports the role of ΔNp63α specifically in a subpopulation of colonization-initiating cells. Subsequently, other populations can form the bulk of the tumor. The predominant stromal component in ΔNp63α over-expressing tumors strongly indicates that the ΔNp63α+ PC3 cells have the ability of signaling to the surrounding bone microenvironment, instructing the formation and growth of a tumor mass with altered histology. Moreover, our microarray data in RWPE-1 cells, along with evidence from the literature (Ousset et al., 2012; Pignon et al., 2013; Signoretti et al., 2005) indicate that the ΔNp63-positive cells can differentiate into ΔNp63-negative luminal cells. This would suggest that in the context of bone metastasis, once ΔNp63+ cells have colonized, they could give rise to ΔNp63α- cells that may contribute to form the bulk of the tumor. One way to address this question would be to generate a reporter driven by the ΔNp63 promoter to track the fate of the endogenous ΔNp63-positive subpopulation. Indeed early attempts by us with such a strategy suggested that the ΔNp63-positive cells could give rise to ΔNp63-negative tumor cells (not shown). However, technical problems with the promoter reporter construct prevented us from completing and confirming these results. An alternate approach we are following, based on our later data, is to use CD82 as a surrogate marker for ΔNp63-expression, given

that this also labels a subpopulation of ΔNp63α-positive cells within the PC3 population.

**Possible osteoblastic phenotype mediated by ΔNp63α**

Bone lesions produced by both PC3 over-expressing ΔNp63α and PC3 infected with control vector show a strong osteoclastic reaction with severe disruption of the bone tissue at later stages. This is characteristic of the highly osteolytic PC3 cell line. However, this also represents a limitation of this model for the study of the histology of human prostate cancer bone metastases, as in patients, these predominantly present as osteoblastic i.e. bone forming tumors. Nevertheless, one individual lesion derived from ΔNp63α over-expressing PC3 was characterized by bone formation (data not shown). This lesion was dissected at an earlier stage compared to the others, suggesting that there could be an initial bone forming reaction by osteoblasts mediated by the expression of ΔNp63α in the metastatic cells. Indeed, our microarray data supports this idea, with many genes that are involved in stimulating osteoblasts, like BMP7, IGF2, PTHLH, TGFβ1 and WNTs being detected in the signature that is altered with ΔNp63 knock-down. In our model, it is likely that this osteoblastic phase could precede the subsequent bone disruption stages, which were detected when the majority of the ΔNp63α cells had disappeared.

To address this outstanding question, we are currently analyzing the bone metastases and pathology from the ΔNp63α-expressing tumors that we dissected at earlier timepoints.

**Novel p63 targets and a "10-gene metastatic/stem cell signature"**

We have performed extensive microarray and Chip-Seq analyses to attempt to uncover the mechanisms by which ΔNp63 might be mediating PSCs and metastatic colonization. As expected, our knockdown studies in RWPE-1 revealed a direct control by p63 of genes involved in epithelial commitment, survival and adhesion, as it was previously shown in human keratinocytes by McDade and collegues (McDade et al., 2012). Surprisingly however, as mentioned above, we also found a signature of bone-related genes that is controlled by ΔNp63 in non-transformed prostate epithelial cells. This rather intriguing finding suggests that the endogenous pathways that are normally regulated by ΔNp63 in PSCs, might also confer properties to these cells in the bone microenvironment, raising the exciting possibility that it is as a result of these genes that prostate cancer has such a predominant predisposition to metastasize to the bone.

Importantly, our analysis has identified several genes that are commonly regulated by ΔNp63 in RWPE-1 and PC3 (the "10-gene bone metastasis signature") which code for proteins involved in adhesion and xenobiotics/drug metabolism or membrane transport. Adhesion and drug resistance are main features of CSCs and both have been linked to prostate cancer bone metastasis (Domingo-Domenech et al., 2012; Lee et al., 2014; Qin et al., 2012; Visvader and Lindeman, 2012). It will be interesting to further investigate whether the expression of these 10 genes correlate with a poorer outcome in clinical profiling

studies. At present, we are focusing on the adhesion/bone colonization signaling mediated by $\Delta Np63\alpha$ possibly through induction of CD82 and IL1$\beta$.

**Summary**

Based on the work presented here, and what is already known, the general model that we propose on the role of p63 in adult PSCs and cancer, is the following: $\Delta Np63\alpha$ is the main isoform expressed in the nuclei of the basal cells of the prostate and it contributes to the maintenance of basal PSCs. These cells participate in normal tissue homeostasis, potentially giving rise to luminal differentiated cells in part through the loss of expression of $\Delta Np63\alpha$ (Figure 27) (Ousset et al., 2012). Furthermore, p63+ basal PSCs have been described as the cells of origin of prostate cancer (Collins et al., 2005; Goldstein et al., 2010; Lawson et al., 2010; Mulholland et al., 2009; Wang et al., 2006). Recapitulating the hierarchy of normal tissue, they generate a tumor mass with a p63-negative luminal phenotype (Goldstein et al., 2010; Lawson et al., 2010; Mulholland et al., 2009). Loss of $\Delta Np63$ expression is necessary for EMT, invasion through the blood stream and extravasation at distant sites (Barbieri et al., 2006; Gandellini et al., 2012; Higashikawa et al., 2007; Tucci et al., 2012). However, once there, some cells can re-activate $\Delta Np63\alpha$ expression, survive, undergo MET and specifically colonize to the bone. In this setting, $\Delta Np63\alpha$ specifically promotes adhesion, survival, and crosstalk with the new microenvironment by driving the expression of adhesion and signaling molecules such as CD82 and IL1$\beta$. Finally p63+ colonizing cells could give rise to p63- cells that participate to

form metastases together with stromal and other bone resident cells (Figure 1).
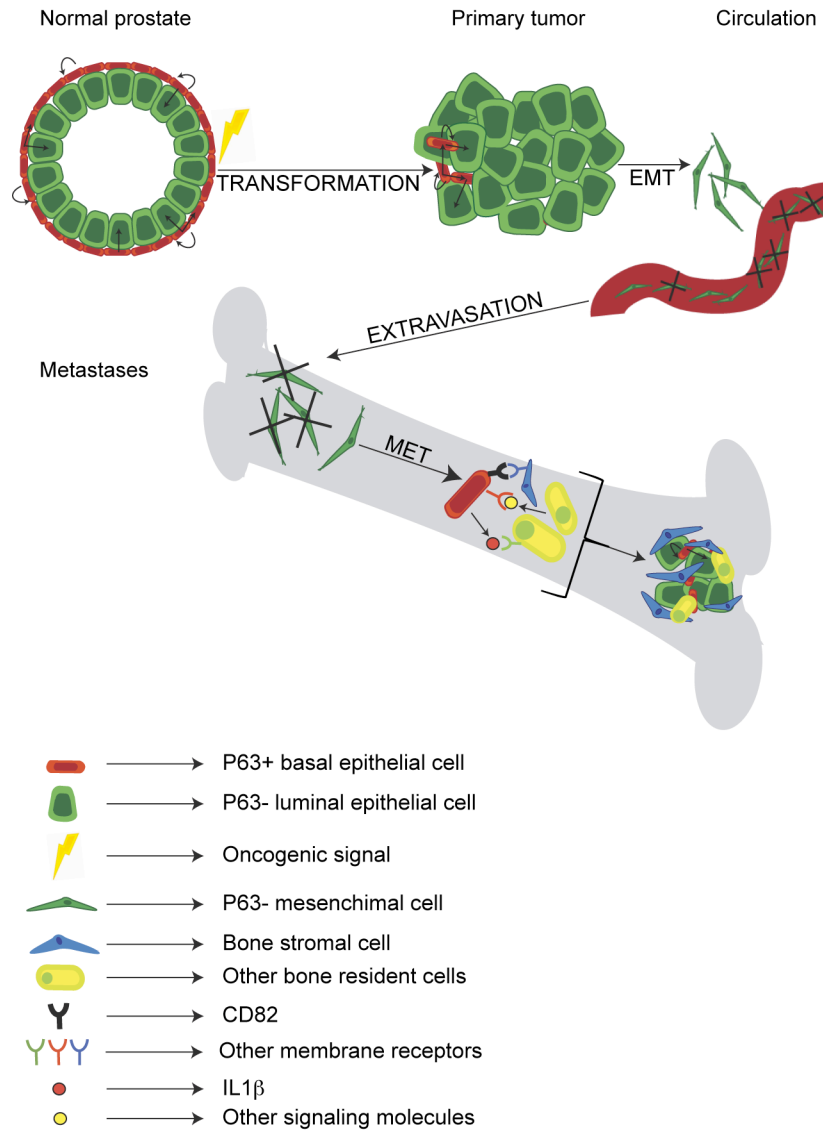


Figure 1. **Model of p63 expression and function in PSCs and cancer**
The $\Delta N\alpha$ isoform of p63 is the mostly expressed in basal PSCs and gives them the ability to self renew. These cells potentially give rise to luminal differentiated cells in part through loss of expression of $\Delta Np63\alpha$. P63+ basal PSCs can be targeted for transformation and

generate mainly p63- luminal cells that form the bulk of the primary tumor. Loss of ΔNp63 is necessary in order to undergo EMT, enter the circulation and invade distant sites. Few cells survive these processes and in prostate cancer, they predominantly colonize the bone where they re-acquire an epithelial/stem cell phenotype through MET and colonize the new microenvironment. This step could require re-activation of ΔNp63α that drives the expression of molecules, such as CD82 and IL1β, necessary for adhesion and crosstalk with bone resident cells. P63- cells could then derive from p63+ colonizing cells and participate to the formation of the metastatic lesions together with stromal and other bone resident cells.

# Conclusions

- The ΔN isoform of p63 is highly expressed in the nuclei of basal stem cells in the prostate of adult mice.

- ΔNp63α is also highly expressed in the RWPE-1 human non-transformed prostate cell line, and confers basal stem cell characteristics to these cells.

- Loss of ΔNp63 affects growth ability and self-renewal of PSCs.

- ΔNp63α is expressed in a subpopulation of cells with CSCs properties in the human prostate cancer cell line, PC3, which is derived from bone metastasis.

- ΔNp63α confers an advantage in prostate cancer metastatic colonization to the bone.

- ΔNp63 directly controls a program of stem cell gene-expression and epithelial commitment and regulates the expression of bone-related genes in PSCs.

- ΔNp63 directly controls a common signature of adhesion and signaling to the surrounding microenvironment in PSCs and bone metastatic cells.

- ΔNp63α favors cellular adhesion in prostate cells.

- CD82 is direct target and possible mediator of ΔNp63α function in adhesion and metastatic colonization.

# Materials and methods

## Mice, intra-cardiac and intra-tibia injections and imaging

Male wt C57BL/6 and Swiss Nude mice 6-10 weeks old were purchased from Charles Rivers Laboratories and housed and handled according to the Animal Facility of the Barcelona Biomedical Research Park (PRBB). C57BL/6 mice were used for prostate dissection. Swiss Nude mice were used for intra-cardiac and intra-tibia injection tumor studies. Pb-Cre4 mice were purchased from Jackson Laboratories and crossed to p63$^{flox/flox}$ mice obtained from the laboratory of Alea A. Mills (Cold Spring Harbor Laboratory, New York), to generate a p63-prostate specific KO mouse model.

For intra-cardiac injections, $1 \times 10^6$ cells were resuspended in 100 $\mu$l of PBS and injected into the left ventricle of nude mice with 1 ml syringes and 26 G x 3/8'' needles (Terumo). Luciferase signal was acquired after 30 minutes and mice without a systemic distribution of the signal were discarded. For imaging, 400 $\mu$l of 5 mg/ml Potassium Luciferin (GOLDBIO Cat#LUK1G) in DPBS w/o potassium or sodium (Gibco) were injected periotoneally in each animal and signal was acquired after 10 min with the IVIS platform. Images were analyzed with the Igor Pro Carbon software. Statistic significance was determined by two-tailed Student's t test.

For intra-tibia injections, $1 \times 10^6$ or $2.5 \times 10^5$ cells were resuspended in 20 $\mu$l of PBS and injected into the right tibias of nude mice with 1 ml syringes and 29 G x 1/2'' needles (Terumo). Left tibias were injected the same way with PBS as control. Imaging and analyses were performed as described above.

**Genotyping of transgenic mouse lines**

A piece of 0.5 cm of mouse tail was cut and lysed for DNA extraction overnight (o/n) at 55ºC in 0.5 ml of Protein K digestion solution: 100 mM Tris pH 8.0, 5 mM EDTA pH 8.0, 0.2% SDS, 200 mM NaCl, 100 $\mu$g/ml Protease K. Samples were spinned at 13000 rpm for 10 minutes in a microcentrifuge and the supernatant was transferred to a fresh tube. Genomic DNA was precipitated by adding 0.5 ml of isopropanol and spinning at 13000 rpm for 5 min. The DNA pellet was washed with 70% EtOH, air dried for 15 min and dissolved in 100 $\mu$l of TE buffer.

PCR was performed in a 25 $\mu$l reaction volume using HotMaster Taq Buffer with Magnesium and DNA polymerase 5 U/$\mu$l (5 PRIME), 0.5 $\mu$l dNTPs 10 mM, 1.25 $\mu$l transgenic mouse line specific primers (10 mM, Table 1) and 10 ng DNA. DNA fragments were analyzed by agarose gel electrophoresis.

| Mouse line | Forward/Reverse Primer |
|---|---|
| p63<sup>flox/flox</sup> | Fw: AAGTGGCAGTGAGCAGAAC<br>Rv: ACAATTCCAGTCAAACATCAA |
| Pb-Cre4 | Fw: CTGAAGAATGGGACAGGCATTG<br>Rv: CATCACTCGTTGCATCGACC |
| p63<sup>flox/flox</sup>; Pb-Cre4 | Fw: CAGAGGAGGCAACACAGGATAGA<br>Rv: CCGGGGGATCCGAATTCATCGA |

Table 1. Primers used for genotyping transgenic mouse lines

**Primary prostate epithelial cultures**

Prostates dissected from 10 Wt C57BL/6 mice were pulled and incubated in 5 mg/ml Dispase II (Larochelle et al.) in PBS at 4ºC o/n. The next day the tissue was spinned, resuspended in DMEM + 10% FBS (Gibco) and cut with scissors. Minced tissue was stirred for 30 minutes at RT and spinned. The cell pellet

obtained was washed in culture media, PrEBM + GFs (Lonza), filtered, spinned and plated at a density of 10000 cells/cm$^2$ in 12-well plates coated with collagen I  (Gibco). Plates were spinned to favour attachment. All centrifugations were performed at 1000 rpm for 5 min. Cells were cultured at 37ºC with 5% $CO_2$ and media was replaced every two days.

**Shs design, cloning and plasmids**

For shRNAs design, we used the softwares http://gesteland.genetics.utah.edu/siRNA_scales/ and http://cancan.cshl.edu/RNAi_central/RNAi.cgi?type=shRNA.

The oligonucleotides were purchased from Invitrogen and were subsequently cloned in the pLMP-GFP-Puro retroviral expression vector obtained from the laboratory of Alea A. Mills, Cold Spring Harbor Laboratory, New York. The restriction sites XhoI and EcoRI were used for the insertion. Specific shs for the ΔN isoform of human p63 were designed to target the unique sequence codifying for the transactivating domain at the N-terminus. The sequence of the shΔNp63 used in our studies is TGCTGTTGACAGTGAGCGCAAGGACAGCAGCATTGATCAAT AGTGAAGCCACAGATGTATTGATCAATGCTGCTGTCCTTTTG CCTACTGCCTCGGA.

For over-expression studies, the retroviral control pMSCV-GFP-Puro and pMSCV-GFP-Puro containing full-length mouse ΔNp63α vectors derive from Scott W. Lowe, Memorial Sloan Kettering Cancer Center, New York.

Retroviral pBABE-Cherry-Puro and pMSCV-Luc-GFP-Neo vectors were obtained from Salvador Aznar Benitah, Institute for Research in Biomedicine, Barcelona.

**Cell lines, transfection and infection**

RWPE-1 were purchased from ATCC. PC3, LNCaP and DU145 were a kind gift of Maria Paola Paronetto, Fondazione Santa Lucia, Universitá degli studi di Roma "Foro Italico". RWPE-1 were cultured in K-SFM media + 0.05 mg/ml BPE + 5 ng/ml hEGF (Gibco). PC3 were grown in DMEM + 10% FBS (Gibco) and LNCaP and DU145 in RPMI + 10% FBS (Gibco). All the cell lines were cultured at 37ºC with 5% $CO_2$ and media was replaced every two days. .

For retroviruses production, briefly, Phoenix packaging cells were transiently transfected (G. Nolan, Stanford University, Stanford, CA). Two days after, viral supernatant was collected, filtered and added to cultures. Two infections of 2 hr each were performed. After 2 days, cells were drug selected according to the different selection markers.

**FFA and 3D culture**

For FFA, 2000, 4000 and 8000 cells were cultured in duplicates in 6 well plates. At day 10 they were fixed in 4% formalin for 15 min at RT and stained with 0,5% Crystal Violet in 20% MetOH in PBS.

3D cultures were performed as previously described (Aranda et al., 2006; Debnath et al., 2003) with 1:1 collagen I (Gibco): matrigel (BD Bioscience) mix. $2.5 \times 10^3$ cells were seeded onto 8-well chamber slides (BD Falcon) and fresh media containing 5% matrigel was added every 2 days. Specific medias for every cell line were used as previously specified. Morphology was assessed by phase microscopy and the number and area of the spheres were calculated using the ImageJ program from NIH.

350 spheres from at least two experiments were counted and measured. Statistic significance was determined by two-tailed Student's t test.

**Adhesion assay**

48-well plates were coated with 200 μL substrates: PBS, Collagen I 1:100, Fibronectin 20 μg/mL, Laminin I 10 μg/mL (R&D systems), 37°C, 1 hour. Cells were plated at a concentration of 4 x $10^5$/mL in a volume of 250 μl/well and kept at 37°C with 5% $CO_2$. At 30 min, 1 hr, 2 hr and 3 hr after plating, plates were vortexed, media was removed and non-adherent cells washed with PBS and fixed with PFA 4% at RT for 10 min. Attached cells were stained with 0,5% Crystal Violet in 20% MetOH for 10 min and counted by phase microscopy at 40x in 5 randomly chosen fields per 3 wells for each condition. Statistics were performed using One-way Anova Tukey's multiple comparisons.

**Flow cytometry**

Staining for cell surface antigens was done with directly conjugated antibodies against Sca-1 (FITC) (BD Pharmigen), CD49f (PE) (BD Pharmigen) and CD133 (PE) (Miltenyi Biotec) at concentration 1:100 in staining buffer (2% FBS in PBS). CD82 was detected using the B-L2 antibody from Abcam and a secondary antibody conjugated with Alexa Fluor 488 or 568 (Invitrogen) diluted in staining buffer respectively 1:100 and 1:500. DAPI at 1 μg/ml was used as viability marker. Cells were analyzed on the LSRFortessa flow cytometer or sorted on the

FACSAria cell sorter (BD Biosciences, San Diego, CA) and data examined with FlowJo software (Tree Star, Ashland, OR).

## Cytospin

Sorted cells were resuspended in duplicates in 250 $\mu$l of media and attached to a slide by spinning at 400 rpm for 4 min in a Cytospin 4 centrifuge (Thermo Shandon). For quantification after immunocytochemistry, cells were counted and statistics were performed using Two-way Anova with Bonferroni post test.

## Immunocytochemistry

Briefly, cells after cytospin or cells in culture were washed with PBS, fixed in 4% PFA for 15 min at RT and incubated 1 hr at RT with blocking solution: PBS, 10% goat serum, 0.5% TWEEN 20 (Sigma Aldrich). Primary and secondary antibodies were diluted in blocking solution 1:10 in PBS and incubated respectively o/n at 4ºC in humid chambers and 1 hr at RT. DAPI at 1 µg/ml was used as nuclear marker. Slides were mounted with Vectashield (Vector Laboratories) and visualized through fluorescent microscopy.

Primary antibodies against p63 (4A4) and CK5 (H-40) (Santa Cruz Biotechnology) were used respectively at a concentration of 1:200 and 1:500. Secondary antibodies conjugated with Alexa Fluor 568, 594 or 647 (Invitrogen) were used 1:1000.

## Histological samples processing for stainings

Soft tissues and bones were fixed in 4% PFA o/n at 4ºC. Bones were subsequently decalcified in EDTA 10% at 4ºC for 3 weeks, adding fresh EDTA every day. All the samples were included in

paraffin and sectioned. Before every staining, sections were deparaffinized in xylene (2 times x 12 min) and re-hydrated in a decreasing series of alcohols.

**Immunofluorescent staining**

Briefly, antigen retrieval was performed boiling the sections for 20 min in EDTA buffer (10 mM Tris HCl [pH 8], 10 mM NaCl, 1 mM EDTA [pH 8] in sterile $H_2O$) [pH 9] and letting them cool to RT for 1 hr. Permeabilization was done with 0.2% TWEEN 20 (Sigma Aldrich) in PBS for 5 min at RT and blocking solution (10% goat serum, 0.1% TWEEN 20 in PBS) was added for 1 hr at RT. Primary and secondary antibodies were diluted in blocking solution 1:10 in PBS and incubated respectively o/n at 4ºC in humid chambers and 1 hr at RT. DAPI at 1 µg/ml was used as nuclear marker. Slides were mounted with Vectashield (Vector Laboratories) and visualized through confocal microscopy.

The same primary antibodies against p63 and CK5 were used at the same concentrations as reported for immunocytochemistry. Antibodies against CK18 (H-80, Santa Cruz Biotechnology), GFP (B-2, Santa Cruz Biotechnology) and ΔNp63 (p40 5-17, Millipore) were used respectively at concentration 1:100, 1:100 and 1:1000. Secondary antibodies conjugated with Alexa Fluor 488 or 568 (Invitrogen) were used 1:1000.

**DAB staining**

Antigen retrieval was done as described in the previous paragraph. Sections were then quenched with 0.3% $H_2O_2$ in PBS for 15 min at RT and permeabilized, blocked and incubated with primary antibodies as previously described. Subsequent biotin-

coupled secondary antibody incubation and avidin-peroxidase label were performed with the ABC Kit (Vectastain) and reactions were developed with DAB substrate kit for peroxidase (Vector Laboratories) according to the manufacturers' instructions. Hematoxylin counterstain was used for nuclei and images were taken in light microscopy. Sources and use of primary antibodies against p63 and ΔNp63 have been described in the previous sections. Antibody against Cherry (1C51, Abcam) was used at a concentration of 1:200.

**HE staining**

Samples were incubated in Harris' Hematoxylin (Sigma Aldrich) for 5-10 min, dipped in 0.25% HCl. and stained with eosin, prepared with Eosin Y (Merk) and Acetic Acid glacial (Panreac), for 30 sec-1 min. Then a rapid de-hydration in 96% and 100% alcohols and 2 x 5 min cycles in xylene followed. At the end the slides were mounted with DPX (Sigma Aldrich).

**Masson's trichrome staining of bones**

Before deparaffinization and re-hydration, sections were incubated in Bouin liquid o/n at RT. The day after, they were deparaffinized, re-hydrated and incubated with Weigert's iron hematoxylin (Merk) for 10 min and with scarlat acid fuchsin, prepared with Biebrich scarlet (Panreac) and Fuchsin (Merk), for 5 min. A treatment with 2.5% phosphomolybdic-phosphotungstic acid was performed for 15 min, followed by aniline blu (Panreac) staining for 15 min. The samples were finally incubated for 3-5 min in acetic acid rapidly de-hydrated before mounting with DPX (Sigma Aldrich).

**Acidic phosphatase staining of bones**

For this staining, sections were specifically deparaffinized in chloroform for 1 min and re-hydrated in a decreasing series of acetones. Subsequently, they were incubated for 16-20 h at 37°C in the dark in the following solution: 0,001 g Naphthol AS BI phosphate (Sigma Aldrich), 0.1 ml N,N-dimethylformamide, 10 ml 0.1 M Walpole's acetic acid/ sodium acetate buffer [pH 5,2], 0.002 g Fast Red Violet (Sigma Aldrich), a drop of 10% $MnCl_2$ in $H_2O$, 0.01 M sodium tartrate. At the end the sections were counterstained with Nuclear Fast Green (Merk) for 1 min, washed carefully with water, dipped in xylene and mounted with DPX (Sigma Aldrich).

**RT-qPCR**

Total RNA was isolated using TRIzol Reagent (Life Technologies) or the RNeasy Mini Kit (QIAGEN). 1 μg of RNA was reverse transcribed using the SuperScript III First-Strand kit from Invitrogen or the qScript cDNA SuperMix from Quanta. qRT-PCR reactions were performed in triplicate using SYBR Green Master Mix and a Light Cycler 480 Instrument (Larochelle et al.). All kits were used according to manufacturers' instructions. Relative levels of expression were determined using the $\Delta\Delta C_t$ method relative to the housekeeping gene β-actin. Primers are listed in table 2. Statistic significance was determined by one-sample t test.

| Gene | Forward/Reverse Primer |
|------|------------------------|
| ΔNp63 | Fw: CTGGAAAACAATGCCCAGAC<br>Rv: GAGGAGCCGTTCTGAATCTG |
| TAp63 | Fw: CCAGAGGTCTTCCAGCATA |

| | Rv: TTTCGGAAGGTTCATCCAC |
|---|---|
| CD44 | Fw: CAACAACACAAATGGCTGGT |
| | Rv: CTGAGGTGTCTGTCTCTTTCATCT |
| CD133 | Fw: TCTGGGTCTACAAGGACTTTCC |
| | Rv: GCCCGCCTGAGTCACTAC |
| GNAI1 | Fw: GCCCTCTCACTATATGCTATCCAG |
| | Rv: TTGAGGTCTTCAAACTGACATTG |
| WNT3A | Fw: AACTGCACCACCGTCCAC |
| | Rv: AAGGCCGACTCCCTGGTA |
| NOTCH1 | Fw: CGGGGCTAACAAAGATATGC |
| | Rv: CACCTTGGCGGTCTCGTA |
| FGFR2 | Fw: CTCACTCTCACAACCAATGAGG |
| | Rv: AACTAGGTGAATACTGTTCGAGAGG |
| BDKRB2 | Fw: GTTTCTGTCTGTTCGTGAGGACT |
| | Rv: ACTCCACTTGGGGGCATT |
| BDKRB1 | Fw: CTGAAGTGCAGTGGCACAAT |
| | Rv: GCATTTTGAGGGAAGAGCTG |
| ABCC5 | Fw: GCAGTAAAGCCAGAGGAAGG |
| | Rv: CAGCCTGGATGTAGACACCATA |
| GNA15 | Fw: CCTCCCACCTGGCTACCTAT |
| | Rv: AACCTCTTGGCTGCCTCA |
| EDN2 | Fw: TCCTGGCTCGACAAGGAGT |
| | Rv: CCGTAAGGAGCTGTCTGTTCA |
| HRAS | Fw: GGCATCCCCTACATCGAGA |
| | Rv: CTCACGCACCAACGTGTAGA |
| LIMK2 | Fw: ACCTCCAGAGACCTGTTTCG |
| | Rv:CCCAAACTTCCCCCAGTAG |
| P2RY2 | Fw: GCACCCTGAGAGGAGAAGC |
| | Rv: GCATTTTTCTGGGCAGGTAG |
| HTRA1 | Fw: CACTCATCAAAATTGACCACCA |
| | Rv: ATGGCGACCACGAACTCT |
| IGFBP7 | Fw: AGCTGTGAGGTCATCGGAAT |
| | Rv: CAGCACCCAGCCAGTTACTT |
| MMP14 | Fw: GCAGAAGTTTTACGGCTTGC |
| | Rv: TAGCGCTTCCTTCGAACATT |
| PTPRU | Fw: CAAAACCCTCCGGAACTACA |
| | Rv: CAAGTACTCCAGGGCCACAT |
| IGFBP2 | Fw: CCTCAAGTCGGGTATGAAGG |
| | Rv: ACCTGGTCCAGTTCCTGTTG |
| THBS2 | Fw: GTGCAGGAGCGTCAGATGT |
| | Rv: GGGTTGGATAAACAGCCATC |
| GPNMB | Fw: TCACCCAGAACACAGTCTGC |
| | Rv: CAGACCCATTGAAGGTTCGT |

| SYT7 | Fw: GAAGGACAAGCCTTGAGCAC<br>Rv: CTTCACGGGAAACAGATGGT |
|------|----------------------------------------------------|
| ITGβ4 | Fw: TCAGCCTCTCTGGGACCTT<br>Rv: TCCTTATCCACACGGACACA |
| IL1β | Fw: CCAAACCTCTTCGAGGCACA<br>Rv: ATGGCTGCTTCAGACACTTGA |
| SLC37A2 | Fw: GGCTCGTCTCTGACTACACCA<br>Rv: GGCCAATGTAGTTGTACAGGAA |
| CD82 | Fw: GAAAGCAGAACCCGCAGA<br>Rv: CCAGTGCAGCTGGTCACA |
| UGT1A6 | Fw: TGGGCCAGAAGCAGATACCA<br>Rv: GCATGACCGGCCTTTAGGAAAT |
| DST | Fw: GCCCTCTTCCTCTTGTTGCT<br>Rv: GGCTTGCTCTGAATCCCTCA |
| β-ACTIN | Fw: AAGAGAGGCATCCTCACCCT<br>Rv: TACATGGCTGGGGTGTTGAA |

Table 2. RT-qPCR primers

**IP and Western blot**

For IPs and WBs, cells were lysed in IP300 buffer (50 mM Tris HCl [pH 7.6], 300 mM NaCl, 10% glycerol, 0.2% NP40 and 1x complete protease inhibitor cocktail from Roche), sonicated 15 sec at 10% output using a Branson sonicator and centrifuged for 20 min at maximum speed to eliminate cell debris. IPs for p63 were performed using 50 µl of nProtein A Sepharose 4 Fast Flow (GE Healthcare) and 5 µg of the antibody clone H-137 from Santa Cruz. Control IPS were done the same way with normal mouse IgG sc-2025 (Santa Cruz Biotechnology). 0.5 mg of RWPE-1 lysate and 4 mg of PC3, LNCAP and DU145 protein lysates were used for immunoprecipitation. Samples were analyzed by SDS-PAGE in denaturing conditions followed by WB. WB membranes were blocked with 5% milk 1 hr at RT and stained for p63 with the 4A4 antibody from Santa Cruz Biotechnology used at a concentration of 1:200 in 2.5% milk o/n

121

at 4ºC. $\alpha$-tubulin was used as loading control and detected with the DM1A antibody (Sigma Aldrich) at a concentration of 1:5000 in 2.5% milk 1hr at RT. Anti-mouse IgG, horseradish peroxidase linked whole antibody (from sheep) GPR (GE Healthcare) was used as secondary antibody at a concentration of 1:5000 in 2.5% milk 1 hr at RT. Reactions were developed with SuperSignal West Pico Chemoluminescent Substrate (Thermo Scientific).

**ELISA**

Invitrogen ELISA Kit for IL1$\beta$ was used according to the manufacturer's instructions.

**Microarrays**

**Microarray Hybridization**

Total RNA was extracted with the RNeasy Mini Kit (QIAGEN) and 100 ng were labeled using LowInputQuick Amp Labeling kit v6.5 (Agilent 5190-2305) following manufacturer instructions. Briefly: mRNA was reverse transcribed in the presence of T7-oligo-dT primer to produce cDNA. cDNA was then in vitro transcribed with T7 RNA polymerase in the presence of Cy3-CTP to produce labeled cRNA. The labeled cRNA was hybridized to the Human Agilent SurePrint G3 gene expression 8x60K microarray (V1: ID 028004 for RWPE-1, V2: ID 039494 for PC3) according to the manufacturer's protocol. The arrays were washed, and scanned on an Agilent G2565CA microarray scanner at 100% PMT and 3 mm resolution. Intensity data was extracted using the Feature Extraction software (Agilent).

**Statistical Analysis**

Raw data was taken from the Feature Extraction output files and was corrected for background noise using the normexp method (Ritchie et al., 2007). To assure comparability across samples we used quantile normalization (Bolstad B., 2001. Probe Level Quantile Normalization of High Density Oligonucleotide Array Data. Unpublished manuscript http://bmbolstad.com/stuff/qnorm.pdf). Differential expression analysis was carried out on non control probes with an empirical Bayes approach on linear models (limma) (Smyth, 2004). Results were corrected for multiple testing according to the False Discovery Rate (FDR) method (Hochberg, 1995). All statistical analyses were performed with the Bioconductor project (http://www.bioconductor.org/) in the R statistical environment (http://cran.r-project.org/) (Gentleman et al., 2004). For gene ontology analysis we used the software Genomatix.

**ChIP-Seq**

RWPE-1 were fixed in 1% formaldehyde for 10 min at room temperature. Crosslinking was stopped in 0.125 M glycine/PBS, cells were washed in cold PBS and centrifuged 2000 rpm for 2 min and resuspended to ~3 × $10^6$ cells/ml in lysis buffer (5 mM HEPES [pH 7.9], 85 mM KCl, 0.5% NP40) + protease inhibitors and incubated on ice, 15 min. Homogenates were centrifuged at 5000 rpm, 5 min, 4°C, pellets resuspended in nuclear lysis buffer (50 mM Tris [pH 8], 10 mM EDTA [pH 8], 1% SDS) + protease inhibitors and incubated on ice, 20 min. Nuclear lysates were sonicated with a Diagenode Sonicator and centrifuged at 12000 rpm, 10 min, 4°C. Supernatants were diluted in IP buffer

(150 mM NaCl, 20 mM Tris [pH 8], 2 mM EDTA) with Protein-A beads (previously pre-blocked with sheared salmon sperm DNA and BSA and pre-cleared for >2 hr at 4°C). Pre-blocked Protein-A beads were incubated with 4A4 antibody against p63 (Santa Cruz, SC-8431) in IP buffer (2 hr, 4°C), centrifuged, washed with IP buffer, and incubated with precleared chromatin overnight at 4°C. Beads were pelleted, washed sequentially with low salt buffer (0.1% SDS, 1% Triton X-100, 2 mM EDTA, 20 mM Tris [pH 8], 150 mM NaCl), high salt buffer (0.1% SDS, 1% Triton X-100, 2 mM EDTA, 20 mM Tris [pH 8], 500 mM NaCl), LiCl buffer (0.25 M LiCl, 1% NP40, 1% $Na^{+2}$ deoxycholate, 1 mM EDTA, 10 mM Tris [pH 8]), and TE buffer. Chromatin was eluted in elution buffer (100 mM $NaHCO_3$, 1% SDS) overnight at 65°C, collected by centrifugation, and incubated with proteinase K (30 min, 37°C). DNA was extracted and PCR amplified with specific primers (Table 3).

**Library preparation and sequencing**

Libraries were prepared using the NEBNext® ChIP-Seq Library Prep Reagent Set for Illumina® kit (ref. E6200S) according to the manufacturer's protocol. Briefly, 10 ng of input and ChIP enriched DNA were subjected to end repair, addition of "A" bases to 3′ ends and ligation of PE adapters. All purification steps were performed using Qiagen PCR purification columns (refs. 50928106 and 50928006). Library size selection was done with 2% low-range agarose gels. Fragments with insert size between 180 - 380 bp were cut from the gel, and DNA was extracted using QIAquick Gel extraction kit (ref. 50928706, Qiagen) and eluted in 36 µl EB. Library amplification was performed by 17 cycles of PCR on the size selected fragments.

Final libraries were analyzed using Agilent DNA 1000 chip to estimate the quantity and check size distribution, and were then quantified by qPCR using the KAPA Library Quantification Kit (ref. KK4835, KapaBiosystems) prior to amplification with Illumina's cBot. Sequencing was done as Single Reads, 50nts on Illumina HiSeq 2000 instrument.

**Statistical Analysis**

Bowtie version 0.12.8 was used for mapping on human genome (version Ensembl 57 corresponding to GRCh37) (Langmead et al., 2009) and MACS version 1.4.1 for peak calling (Zhang et al., 2008) with standard parameters. Genes were annotated considering -25 kb from TSS with BEDTools (Quinlan and Hall, 2010) with Ensembl annotations.

| Gene | Forward/Reverse Primer |
|------|------------------------|
| p21 | Fw: CCCACAGCAGAGGAGAAAGA<br>Rv: CTGACATCTCAGGCTGCTCA |
| GAPDH | Fw: GAGCCTCCTTCCTCTCCAG<br>Rv: ACTTCCCCCTCCCCATCT |

Table 3. ChIP-Seq control primers

# References

# References

Abate-Shen, C., and Shen, M.M. (2000). Molecular genetics of prostate cancer. Genes Dev *14*, 2410-2434.

Abdulkadir, S.A., Magee, J.A., Peters, T.J., Kaleem, Z., Naughton, C.K., Humphrey, P.A., and Milbrandt, J. (2002). Conditional loss of Nkx3.1 in adult mice induces prostatic intraepithelial neoplasia. Mol Cell Biol *22*, 1495-1503.

Acevedo, V.D., Gangula, R.D., Freeman, K.W., Li, R., Zhang, Y., Wang, F., Ayala, G.E., Peterson, L.E., Ittmann, M., and Spencer, D.M. (2007). Inducible FGFR-1 activation leads to irreversible prostate adenocarcinoma and an epithelial-to-mesenchymal transition. Cancer Cell *12*, 559-571.

Adorno, M., Cordenonsi, M., Montagner, M., Dupont, S., Wong, C., Hann, B., Solari, A., Bobisse, S., Rondina, M.B., Guzzardo, V.*, et al.* (2009). A Mutant-p53/Smad complex opposes p63 to empower TGFbeta-induced metastasis. Cell *137*, 87-98.

Allocati, N., Di Ilio, C., and De Laurenzi, V. (2012). p63/p73 in the control of cell cycle and cell death. Exp Cell Res *318*, 1285-1290.

Angelucci, A., Gravina, G.L., Rucci, N., Millimaggi, D., Festuccia, C., Muzi, P., Teti, A., Vicentini, C., and Bologna, M. (2006). Suppression of EGF-R signaling reduces the incidence of prostate cancer metastasis in nude mice. Endocr Relat Cancer *13*, 197-210.

Bachmann, I.M., Halvorsen, O.J., Collett, K., Stefansson, I.M., Straume, O., Haukaas, S.A., Salvesen, H.B., Otte, A.P., and Akslen, L.A. (2006). EZH2 expression is associated with high proliferation rate and aggressive tumor subgroups in cutaneous melanoma and cancers of the endometrium, prostate, and breast. J Clin Oncol *24*, 268-273.

Barbieri, C.E., and Pietenpol, J.A. (2006). p63 and epithelial biology. Exp Cell Res *312*, 695-706.

Barbieri, C.E., Tang, L.J., Brown, K.A., and Pietenpol, J.A. (2006). Loss of p63 leads to increased cell migration and up-regulation of genes involved in invasion and metastasis. Cancer Res *66*, 7589-7597.

Barker, N., Bartfeld, S., and Clevers, H. (2010). Tissue-resident adult stem cell populations of rapidly self-renewing organs. cell stem cell *7*, 656-670.

Barker, N., Ridgway, R.A., van Es, J.H., van de Wetering, M., Begthel, H., van den Born, M., Danenberg, E., Clarke, A.R.,

Sansom, O.J., and Clevers, H. (2009). Crypt stem cells as the cells-of-origin of intestinal cancer. Nature *457*, 608-611.

Barlow, L.J., and Shen, M.M. (2013). SnapShot: Prostate cancer. Cancer Cell *24*, 400 e401.

Bavik, C., Coleman, I., Dean, J.P., Knudsen, B., Plymate, S., and Nelson, P.S. (2006). The gene expression program of prostate fibroblast senescence modulates neoplastic epithelial cell proliferation through paracrine mechanisms. Cancer Res *66*, 794-802.

Bello, D., Webber, M.M., Kleinman, H.K., Wartinger, D.D., and Rhim, J.S. (1997). Androgen responsive adult human prostatic epithelial cell lines immortalized by human papillomavirus 18. Carcinogenesis *18*, 1215-1223.

Berkers, C.R., Maddocks, O.D., Cheung, E.C., Mor, I., and Vousden, K.H. (2013). Metabolic regulation by p53 family members. Cell Metab *18*, 617-633.

Bhatia-Gaur, R., Donjacour, A.A., Sciavolino, P.J., Kim, M., Desai, N., Young, P., Norton, C.R., Gridley, T., Cardiff, R.D., Cunha, G.R.*, et al.* (1999). Roles for Nkx3.1 in prostate development and cancer. Genes Dev *13*, 966-977.

Bonkhoff, H., and Remberger, K. (1996). Differentiation pathways and histogenetic aspects of normal and abnormal prostatic growth: a stem cell model. Prostate *28*, 98-106.

Bonkhoff, H., Stein, U., and Remberger, K. (1994). The proliferative function of basal cells in the normal and hyperplastic human prostate. Prostate *24*, 114-118.

Bostwick, D.G. (1989a). Prostatic intraepithelial neoplasia (PIN). Urology *34*, 16-22.

Bostwick, D.G. (1989b). The pathology of early prostate cancer. CA Cancer J Clin *39*, 376-393.

Brabletz, T. (2012). EMT and MET in metastasis: where are the cancer stem cells? Cancer Cell *22*, 699-701.

Buijs, J.T., and van der Pluijm, G. (2009). Osteotropic cancers: from primary tumor to bone. Cancer Lett *273*, 177-193.

Burger, P.E., Xiong, X., Coetzee, S., Salm, S.N., Moscatelli, D., Goto, K., and Wilson, E.L. (2005). Sca-1 expression identifies stem cells in the proximal region of prostatic ducts with high capacity to reconstitute prostatic tissue. Proc Natl Acad Sci U S A *102*, 7180-7185.

Carroll, D.K., Carroll, J.S., Leong, C.O., Cheng, F., Brown, M., Mills, A.A., Brugge, J.S., and Ellisen, L.W. (2006). p63 regulates an adhesion programme and cell survival in epithelial cells. Nat Cell Biol *8*, 551-561.

Carver, B.S., Tran, J., Gopalan, A., Chen, Z., Shaikh, S., Carracedo, A., Alimonti, A., Nardella, C., Varmeh, S., Scardino, P.T.*, et al.* (2009). Aberrant ERG expression cooperates with loss of PTEN to promote cancer progression in the prostate. Nat Genet *41*, 619-624.

Celia-Terrassa, T., Meca-Cortes, O., Mateo, F., de Paz, A.M., Rubio, N., Arnal-Estape, A., Ell, B.J., Bermudo, R., Diaz, A., Guerra-Rebollo, M.*, et al.* (2012). Epithelial-mesenchymal transition can suppress major attributes of human epithelial tumor-initiating cells. J Clin Invest *122*, 1849-1868.

Celli, J., Duijf, P., Hamel, B.C., Bamshad, M., Kramer, B., Smits, A.P., Newbury-Ecob, R., Hennekam, R.C., Van Buggenhout, G., van Haeringen, A.*, et al.* (1999). Heterozygous germline mutations in the p53 homolog p63 are the cause of EEC syndrome. Cell *99*, 143-153.

Chae, Y.S., Kim, H., Kim, D., Lee, H., and Lee, H.O. (2012). Cell density-dependent acetylation of DeltaNp63alpha is associated with p53-dependent cell cycle arrest. FEBS Lett *586*, 1128-1134.

Chaffer, C.L., and Weinberg, R.A. (2011). A perspective on cancer cell metastasis. Science *331*, 1559-1564.

Chang, H.H., Chen, B.Y., Wu, C.Y., Tsao, Z.J., Chen, Y.Y., Chang, C.P., Yang, C.R., and Lin, D.P. (2011). Hedgehog overexpression leads to the formation of prostate cancer stem cells with metastatic property irrespective of androgen receptor expression in the mouse model. J Biomed Sci *18*, 6.

Chang, R.T., Kirby, R., and Challacombe, B.J. (2012). Is there a link between BPH and prostate cancer? Practitioner *256*, 13-16, 12.

Choi, N., Zhang, B., Zhang, L., Ittmann, M., and Xin, L. (2012). Adult murine prostate basal and luminal cells are self-sustained lineages that can both serve as targets for prostate cancer initiation. Cancer Cell *21*, 253-265.

Chou, J.Y., Sik Jun, H., and Mansfield, B.C. (2013). The SLC37 family of phosphate-linked sugar phosphate antiporters. Mol Aspects Med *34*, 601-611.

Chu, K., Cheng, C.J., Ye, X., Lee, Y.C., Zurita, A.J., Chen, D.T., Yu-Lee, L.Y., Zhang, S., Yeh, E.T., Hu, M.C.*, et al.* (2008). Cadherin-11 promotes the metastasis of prostate cancer cells to bone. Mol Cancer Res *6*, 1259-1267.

Clarke, M.F., Dick, J.E., Dirks, P.B., Eaves, C.J., Jamieson, C.H., Jones, D.L., Visvader, J., Weissman, I.L., and Wahl, G.M. (2006). Cancer stem cells--perspectives on current status and future directions: AACR Workshop on cancer stem cells. Cancer Res *66*, 9339-9344.

Collins, A.T., Berry, P.A., Hyde, C., Stower, M.J., and Maitland, N.J. (2005). Prospective identification of tumorigenic prostate cancer stem cells. Cancer Res *65*, 10946-10951.

Cooke, P.S., Young, P.F., and Cunha, G.R. (1987). Androgen dependence of growth and epithelial morphogenesis in neonatal mouse bulbourethral glands. Endocrinology *121*, 2153-2160.

Cotton, F.A., Murillo, C.A., Young, M.D., Yu, R., and Zhao, Q. (2008). Very large difference in electronic communication of dimetal species with heterobiphenylene and heteroanthracene units. Inorg Chem *47*, 219-229.

Cozzio, A., Passegue, E., Ayton, P.M., Karsunky, H., Cleary, M.L., and Weissman, I.L. (2003). Similar MLL-associated leukemias arising from self-renewing stem cells and short-lived myeloid progenitors. Genes Dev *17*, 3029-3035.

Craig, A.L., Holcakova, J., Finlan, L.E., Nekulova, M., Hrstka, R., Gueven, N., DiRenzo, J., Smith, G., Hupp, T.R., and Vojtesek, B. (2010). DeltaNp63 transcriptionally regulates ATM to control p53 Serine-15 phosphorylation. Mol Cancer *9*, 195.

Cross, N.A., Fowles, A., Reeves, K., Jokonya, N., Linton, K., Holen, I., Hamdy, F.C., and Eaton, C.L. (2008). Imaging the effects of castration on bone turnover and hormone-independent prostate cancer colonization of bone. Prostate *68*, 1707-1714.

Cunha, G.R., Alarid, E.T., Turner, T., Donjacour, A.A., Boutin, E.L., and Foster, B.A. (1992). Normal and abnormal development of the male urogenital tract. Role of androgens, mesenchymal-epithelial interactions, and growth factors. J Androl *13*, 465-475.

Cunha, G.R., and Donjacour, A. (1987a). Mesenchymal-epithelial interactions: technical considerations. Prog Clin Biol Res *239*, 273-282.

Cunha, G.R., and Donjacour, A. (1987b). Stromal-epithelial interactions in normal and abnormal prostatic development. Prog Clin Biol Res *239*, 251-272.

Cunha, G.R., Donjacour, A.A., Cooke, P.S., Mee, S., Bigsby, R.M., Higgins, S.J., and Sugimura, Y. (1987). The endocrinology and developmental biology of the prostate. Endocr Rev *8*, 338-362.

Cunha, G.R., Donjacour, A.A., and Sugimura, Y. (1986). Stromal-epithelial interactions and heterogeneity of proliferative activity within the prostate. Biochem Cell Biol *64*, 608-614.

Cunha, G.R., and Lung, B. (1978). The possible influence of temporal factors in androgenic responsiveness of urogenital tissue recombinants from wild-type and androgen-insensitive (Tfm) mice. J Exp Zool *205*, 181-193.

# References

Dai, J., Hall, C.L., Escara-Wilke, J., Mizokami, A., Keller, J.M., and Keller, E.T. (2008). Prostate cancer induces bone metastasis through Wnt-induced bone morphogenetic protein-dependent and independent mechanisms. Cancer Res *68*, 5785-5794.

Davis, L.D., Zhang, W., Merseburger, A., Young, D., Xu, L., Rhim, J.S., Moul, J.W., Srivastava, S., and Sesterhenn, I.A. (2002). p63 expression profile in normal and malignant prostate epithelial cells. Anticancer Res *22*, 3819-3825.

De Marzo, A.M., Marchi, V.L., Epstein, J.I., and Nelson, W.G. (1999). Proliferative inflammatory atrophy of the prostate: implications for prostatic carcinogenesis. Am J Pathol *155*, 1985-1992.

Deyoung, M.P., and Ellisen, L.W. (2007). p63 and p73 in human cancer: defining the network. Oncogene *26*, 5169-5183.

Dhillon, P.K., Barry, M., Stampfer, M.J., Perner, S., Fiorentino, M., Fornari, A., Ma, J., Fleet, J., Kurth, T., Rubin, M.A.*, et al.* (2009). Aberrant cytoplasmic expression of p63 and prostate cancer mortality. Cancer Epidemiol Biomarkers Prev *18*, 595-600.

Di Como, C.J., Urist, M.J., Babayan, I., Drobnjak, M., Hedvat, C.V., Teruya-Feldstein, J., Pohar, K., Hoos, A., and Cordon-Cardo, C. (2002). p63 expression profiles in human normal and tumor tissues. Clin Cancer Res *8*, 494-501.

Domingo-Domenech, J., Vidal, S.J., Rodriguez-Bravo, V., Castillo-Martin, M., Quinn, S.A., Rodriguez-Barrueco, R., Bonal, D.M., Charytonowicz, E., Gladoun, N., de la Iglesia-Vicente, J.*, et al.* (2012). Suppression of acquired docetaxel resistance in prostate cancer through depletion of notch- and hedgehog-dependent tumor-initiating cells. Cancer Cell *22*, 373-388.

Dong, J.T. (2001). Chromosomal deletions and tumor suppressor genes in prostate cancer. Cancer Metastasis Rev *20*, 173-193.

Donjacour, A.A., Cunha, G.R., and Sugimura, Y. (1987). Heterogeneity of structure and function in the mouse prostate. Prog Clin Biol Res *239*, 583-600.

Donjacour, A.A., Rosales, A., Higgins, S.J., and Cunha, G.R. (1990). Characterization of antibodies to androgen-dependent secretory proteins of the mouse dorsolateral prostate. Endocrinology *126*, 1343-1354.

Eaves, C.J. (2008). Cancer stem cells: Here, there, everywhere? Nature *456*, 581-582.

Ellwood-Yen, K., Graeber, T.G., Wongvipat, J., Iruela-Arispe, M.L., Zhang, J., Matusik, R., Thomas, G.V., and Sawyers, C.L.

(2003). Myc-driven murine prostate cancer shares molecular features with human prostate tumors. Cancer Cell *4*, 223-238.

English, H.F., Santen, R.J., and Isaacs, J.T. (1987). Response of glandular versus basal rat ventral prostatic epithelial cells to androgen withdrawal and replacement. Prostate *11*, 229-242.

Flores, E.R., Sengupta, S., Miller, J.B., Newman, J.J., Bronson, R., Crowley, D., Yang, A., McKeon, F., and Jacks, T. (2005). Tumor predisposition in mice mutant for p63 and p73: evidence for broader tumor suppressor functions for the p53 family. Cancer Cell *7*, 363-373.

Fotheringham, J.A., Mazzucca, S., and Raab-Traub, N. (2010). Epstein-Barr virus latent membrane protein-2A-induced DeltaNp63alpha expression is associated with impaired epithelial-cell differentiation. Oncogene *29*, 4287-4296.

Fuchs, E., Tumbar, T., and Guasch, G. (2004). Socializing with the neighbors: stem cells and their niche. Cell *116*, 769-778.

Galli, F., Rossi, M., D'Alessandra, Y., De Simone, M., Lopardo, T., Haupt, Y., Alsheich-Bartok, O., Anzi, S., Shaulian, E., Calabro, V.*, et al.* (2010). MDM2 and Fbw7 cooperate to induce p63 protein degradation following DNA damage and cell differentiation. J Cell Sci *123*, 2423-2433.

Gandellini, P., Profumo, V., Casamichele, A., Fenderico, N., Borrelli, S., Petrovich, G., Santilli, G., Callari, M., Colecchia, M., Pozzi, S.*, et al.* (2012). miR-205 regulates basement membrane deposition in human prostate: implications for cancer development. Cell Death Differ *19*, 1750-1760.

Garabedian, E.M., Humphrey, P.A., and Gordon, J.I. (1998). A transgenic mouse model of metastatic prostate cancer originating from neuroendocrine cells. Proc Natl Acad Sci U S A *95*, 15382-15387.

Geng, Y., Walls, K.C., Ghosh, A.P., Akhtar, R.S., Klocke, B.J., and Roth, K.A. (2010). Cytoplasmic p53 and activated Bax regulate p53-dependent, transcription-independent neural precursor cell apoptosis. J Histochem Cytochem *58*, 265-275.

Goldstein, A.S., Huang, J., Guo, C., Garraway, I.P., and Witte, O.N. (2010). Identification of a cell of origin for human prostate cancer. Science *329*, 568-571.

Goldstein, A.S., Lawson, D.A., Cheng, D., Sun, W., Garraway, I.P., and Witte, O.N. (2008). Trop2 identifies a subpopulation of murine and human prostate basal cells with stem cell characteristics. Proc Natl Acad Sci U S A *105*, 20882-20887.

Graziano, V., and De Laurenzi, V. (2011). Role of p63 in cancer development. Biochim Biophys Acta *1816*, 57-66.

Greenberg, N.M., DeMayo, F., Finegold, M.J., Medina, D., Tilley, W.D., Aspinall, J.O., Cunha, G.R., Donjacour, A.A., Matusik, R.J., and Rosen, J.M. (1995). Prostate cancer in a transgenic mouse. Proc Natl Acad Sci U S A *92*, 3439-3443.

Gressner, O., Schilling, T., Lorenz, K., Schulze Schleithoff, E., Koch, A., Schulze-Bergkamen, H., Lena, A.M., Candi, E., Terrinoni, A., Catani, M.V.*, et al.* (2005). TAp63alpha induces apoptosis by activating signaling via death receptors and mitochondria. EMBO J *24*, 2458-2471.

Grignon, D.J. (2004). Unusual subtypes of prostate cancer. Mod Pathol *17*, 316-327.

Grisanzio, C., and Signoretti, S. (2008). p63 in prostate biology and pathology. J Cell Biochem *103*, 1354-1368.

Guo, X., Keyes, W.M., Papazoglu, C., Zuber, J., Li, W., Lowe, S.W., Vogel, H., and Mills, A.A. (2009). TAp63 induces senescence and suppresses tumorigenesis in vivo. Nat Cell Biol *11*, 1451-1457.

Hagiwara, K., McMenamin, M.G., Miura, K., and Harris, C.C. (1999). Mutational analysis of the p63/p73L/p51/p40/CUSP/KET gene in human cancer cell lines using intronic primers. Cancer Res *59*, 4165-4169.

Hall, C.L., Bafico, A., Dai, J., Aaronson, S.A., and Keller, E.T. (2005). Prostate cancer cells promote osteoblastic bone metastases through Wnts. Cancer Res *65*, 7554-7560.

Harma, V., Virtanen, J., Makela, R., Happonen, A., Mpindi, J.P., Knuuttila, M., Kohonen, P., Lotjonen, J., Kallioniemi, O., and Nees, M. (2010). A comprehensive panel of three-dimensional models for studies of prostate cancer growth, invasion and drug responses. PLoS One *5*, e10431.

Hayward, S.W., Brody, J.R., and Cunha, G.R. (1996). An edgewise look at basal epithelial cells: three-dimensional views of the rat prostate, mammary gland and salivary gland. Differentiation *60*, 219-227.

Higashikawa, K., Yoneda, S., Tobiume, K., Taki, M., Shigeishi, H., and Kamata, N. (2007). Snail-induced down-regulation of DeltaNp63alpha acquires invasive phenotype of human squamous cell carcinoma. Cancer Res *67*, 9207-9213.

Hollstein, M., Shomer, B., Greenblatt, M., Soussi, T., Hovig, E., Montesano, R., and Harris, C.C. (1996). Somatic point mutations in the p53 gene of human tumors and cell lines: updated compilation. Nucleic Acids Res *24*, 141-146.

Ianakiev, P., Kilpatrick, M.W., Toudjarska, I., Basel, D., Beighton, P., and Tsipouras, P. (2000). Split-hand/split-foot malformation is

caused by mutations in the p63 gene on 3q27. Am J Hum Genet *67*, 59-66.

Iwata, T., Schultz, D., Hicks, J., Hubbard, G.K., Mutton, L.N., Lotan, T.L., Bethel, C., Lotz, M.T., Yegnasubramanian, S., Nelson, W.G*., et al.* (2010). MYC overexpression induces prostatic intraepithelial neoplasia and loss of Nkx3.1 in mouse luminal epithelial cells. PLoS One *5*, e9427.

Jensen, U.B., Lowell, S., and Watt, F.M. (1999). The spatial relationship between stem cells and their progeny in the basal layer of human epidermis: a new view based on whole-mount labelling and lineage analysis. Development *126*, 2409-2418.

Jiang, Z., Li, C., Fischer, A., Dresser, K., and Woda, B.A. (2005). Using an AMACR (P504S)/34betaE12/p63 cocktail for the detection of small focal prostate carcinoma in needle biopsy specimens. Am J Clin Pathol *123*, 231-236.

John, K., Alla, V., Meier, C., and Putzer, B.M. (2011). GRAMD4 mimics p53 and mediates the apoptotic function of p73 at mitochondria. Cell Death Differ *18*, 874-886.

Jost, C.A., Marin, M.C., and Kaelin, W.G., Jr. (1997). p73 is a simian [correction of human] p53-related protein that can induce apoptosis. Nature *389*, 191-194.

Kaghad, M., Bonnet, H., Yang, A., Creancier, L., Biscan, J.C., Valent, A., Minty, A., Chalon, P., Lelias, J.M., Dumont, X*., et al.* (1997). Monoallelically expressed gene related to p53 at 1p36, a region frequently deleted in neuroblastoma and other human cancers. Cell *90*, 809-819.

Kaplan-Lefko, P.J., Chen, T.M., Ittmann, M.M., Barrios, R.J., Ayala, G.E., Huss, W.J., Maddison, L.A., Foster, B.A., and Greenberg, N.M. (2003). Pathobiology of autochthonous prostate cancer in a pre-clinical transgenic mouse model. Prostate *55*, 219-237.

Karhadkar, S.S., Bova, G.S., Abdallah, N., Dhara, S., Gardner, D., Maitra, A., Isaacs, J.T., Berman, D.M., and Beachy, P.A. (2004). Hedgehog signalling in prostate regeneration, neoplasia and metastasis. Nature *431*, 707-712.

Keyes, W.M., Pecoraro, M., Aranda, V., Vernersson-Lindahl, E., Li, W., Vogel, H., Guo, X., Garcia, E.L., Michurina, T.V., Enikolopov, G*., et al.* (2011). DeltaNp63alpha is an oncogene that targets chromatin remodeler Lsh to drive skin stem cell proliferation and tumorigenesis. cell stem cell *8*, 164-176.

Keyes, W.M., Vogel, H., Koster, M.I., Guo, X., Qi, Y., Petherbridge, K.M., Roop, D.R., Bradley, A., and Mills, A.A. (2006). p63 heterozygous mutant mice are not prone to

spontaneous or chemically induced tumors. Proc Natl Acad Sci U S A *103*, 8435-8440.

Keyes, W.M., Wu, Y., Vogel, H., Guo, X., Lowe, S.W., and Mills, A.A. (2005). p63 deficiency activates a program of cellular senescence and leads to accelerated aging. Genes Dev *19*, 1986-1999.

Khandrika, L., Kumar, B., Koul, S., Maroni, P., and Koul, H.K. (2009). Oxidative stress in prostate cancer. Cancer Lett *282*, 125-136.

Kim, M.J., Cardiff, R.D., Desai, N., Banach-Petrosky, W.A., Parsons, R., Shen, M.M., and Abate-Shen, C. (2002). Cooperativity of Nkx3.1 and Pten loss of function in a mouse model of prostate carcinogenesis. Proc Natl Acad Sci U S A *99*, 2884-2889.

King, K.E., Ponnamperuma, R.M., Yamashita, T., Tokino, T., Lee, L.A., Young, M.F., and Weinberg, W.C. (2003). deltaNp63alpha functions as both a positive and a negative transcriptional regulator and blocks in vitro differentiation of murine keratinocytes. Oncogene *22*, 3635-3644.

Koeneman, K.S., Yeung, F., and Chung, L.W. (1999). Osteomimetic properties of prostate cancer cells: a hypothesis supporting the predilection of prostate cancer metastasis and growth in the bone environment. Prostate *39*, 246-261.

Koga, F., Kawakami, S., Fujii, Y., Saito, K., Ohtsuka, Y., Iwai, A., Ando, N., Takizawa, T., Kageyama, Y., and Kihara, K. (2003). Impaired p63 expression associates with poor prognosis and uroplakin III expression in invasive urothelial carcinoma of the bladder. Clin Cancer Res *9*, 5501-5507.

Korsten, H., Ziel-van der Made, A., Ma, X., van der Kwast, T., and Trapman, J. (2009). Accumulating progenitor cells in the luminal epithelial cell layer are candidate tumor initiating cells in a Pten knockout mouse prostate cancer model. PLoS One *4*, e5662.

Koster, M.I., Dai, D., Marinari, B., Sano, Y., Costanzo, A., Karin, M., and Roop, D.R. (2007). p63 induces key target genes required for epidermal morphogenesis. Proc Natl Acad Sci U S A *104*, 3255-3260.

Koster, M.I., Marinari, B., Payne, A.S., Kantaputra, P.N., Costanzo, A., and Roop, D.R. (2009). DeltaNp63 knockdown mice: A mouse model for AEC syndrome. Am J Med Genet A *149A*, 1942-1947.

Krivtsov, A.V., Twomey, D., Feng, Z., Stubbs, M.C., Wang, Y., Faber, J., Levine, J.E., Wang, J., Hahn, W.C., Gilliland, D.G.*, et*

*al.* (2006). Transformation from committed progenitor to leukaemia stem cell initiated by MLL-AF9. Nature *442*, 818-822.

Kurita, T., Medina, R.T., Mills, A.A., and Cunha, G.R. (2004). Role of p63 and basal cells in the prostate. Development *131*, 4955-4964.

Lapointe, J., Li, C., Giacomini, C.P., Salari, K., Huang, S., Wang, P., Ferrari, M., Hernandez-Boussard, T., Brooks, J.D., and Pollack, J.R. (2007). Genomic profiling reveals alternative genetic pathways of prostate tumorigenesis. Cancer Res *67*, 8504-8510.

Larochelle, A., Gillette, J.M., Desmond, R., Ichwan, B., Cantilena, A., Cerf, A., Barrett, A.J., Wayne, A.S., Lippincott-Schwartz, J., and Dunbar, C.E. (2012). Bone marrow homing and engraftment of human hematopoietic stem and progenitor cells is mediated by a polarized membrane domain. Blood *119*, 1848-1855.

Lawson, D.A., Xin, L., Lukacs, R.U., Cheng, D., and Witte, O.N. (2007). Isolation and functional characterization of murine prostate stem cells. Proc Natl Acad Sci U S A *104*, 181-186.

Lawson, D.A., Zong, Y., Memarzadeh, S., Xin, L., Huang, J., and Witte, O.N. (2010). Basal epithelial stem cells are efficient targets for prostate cancer initiation. Proc Natl Acad Sci U S A *107*, 2610-2615.

Lee, C.W., and La Thangue, N.B. (1999). Promoter specificity and stability control of the p53-related protein p73. Oncogene *18*, 4171-4181.

Lee, G.T., Kang, D.I., Ha, Y.S., Jung, Y.S., Chung, J., Min, K., Kim, T.H., Moon, K.H., Chung, J.M., Lee, D.H*., et al.* (2014). Prostate cancer bone metastases acquire resistance to androgen deprivation via WNT5A-mediated BMP-6 induction. Br J Cancer *110*, 1634-1644.

Leong, K.G., Wang, B.E., Johnson, L., and Gao, W.Q. (2008). Generation of a prostate from a single adult stem cell. Nature *456*, 804-808.

Levrero, M., De Laurenzi, V., Costanzo, A., Gong, J., Wang, J.Y., and Melino, G. (2000). The p53/p63/p73 family of transcription factors: overlapping and distinct functions. J Cell Sci *113 ( Pt 10)*, 1661-1670.

Li, H., Chen, X., Calhoun-Davis, T., Claypool, K., and Tang, D.G. (2008). PC3 human prostate carcinoma cell holoclones contain self-renewing tumor-initiating cells. Cancer Res *68*, 1820-1825.

Lin, Y.L., Sengupta, S., Gurdziel, K., Bell, G.W., Jacks, T., and Flores, E.R. (2009). p63 and p73 transcriptionally regulate genes involved in DNA repair. PLoS Genet *5*, e1000680.

Liu, Q., Russell, M.R., Shahriari, K., Jernigan, D.L., Lioni, M.I., Garcia, F.U., and Fatatis, A. (2013). Interleukin-1beta promotes skeletal colonization and progression of metastatic prostate cancer cells with neuroendocrine features. Cancer Res *73*, 3297-3305.

Liu, W.M., and Zhang, X.A. (2006). KAI1/CD82, a tumor metastasis suppressor. Cancer Lett *240*, 183-194.

Logothetis, C.J., and Lin, S.H. (2005). Osteoblasts in prostate cancer metastasis to bone. Nat Rev Cancer *5*, 21-28.

Lu, T.L., Huang, Y.F., You, L.R., Chao, N.C., Su, F.Y., Chang, J.L., and Chen, C.M. (2013). Conditionally ablated Pten in prostate basal cells promotes basal-to-luminal differentiation and causes invasive prostate cancer in mice. Am J Pathol *182*, 975-991.

Lukacs, R.U., Goldstein, A.S., Lawson, D.A., Cheng, D., and Witte, O.N. (2010a). Isolation, cultivation and characterization of adult murine prostate stem cells. Nat Protoc *5*, 702-713.

Lukacs, R.U., Lawson, D.A., Xin, L., Zong, Y., Garraway, I., Goldstein, A.S., Memarzadeh, S., and Witte, O.N. (2008). Epithelial stem cells of the prostate and their role in cancer progression. Cold Spring Harb Symp Quant Biol *73*, 491-502.

Lukacs, R.U., Memarzadeh, S., Wu, H., and Witte, O.N. (2010b). Bmi-1 is a crucial regulator of prostate stem cell self-renewal and malignant transformation. cell stem cell *7*, 682-693.

Luo, J., Zha, S., Gage, W.R., Dunn, T.A., Hicks, J.L., Bennett, C.J., Ewing, C.M., Platz, E.A., Ferdinandusse, S., Wanders, R.J.*, et al.* (2002). Alpha-methylacyl-CoA racemase: a new molecular marker for prostate cancer. Cancer Res *62*, 2220-2226.

Mani, S.A., Guo, W., Liao, M.J., Eaton, E.N., Ayyanan, A., Zhou, A.Y., Brooks, M., Reinhard, F., Zhang, C.C., Shipitsin, M.*, et al.* (2008). The epithelial-mesenchymal transition generates cells with properties of stem cells. Cell *133*, 704-715.

Marcel, V., Dichtel-Danjoy, M.L., Sagne, C., Hafsi, H., Ma, D., Ortiz-Cuaran, S., Olivier, M., Hall, J., Mollereau, B., Hainaut, P.*, et al.* (2011). Biological functions of p53 isoforms through evolution: lessons from animal and cellular models. Cell Death Differ *18*, 1815-1824.

Marcel, V., Petit, I., Murray-Zmijewski, F., Goullet de Rugy, T., Fernandes, K., Meuray, V., Diot, A., Lane, D.P., Aberdam, D., and Bourdon, J.C. (2012). Diverse p63 and p73 isoforms regulate Delta133p53 expression through modulation of the internal TP53 promoter activity. Cell Death Differ *19*, 816-826.

Margheri, F., D'Alessio, S., Serrati, S., Pucci, M., Annunziato, F., Cosmi, L., Liotta, F., Angeli, R., Angelucci, A., Gravina, G.L.*, et*

*al.* (2005). Effects of blocking urokinase receptor signaling by antisense oligonucleotides in a mouse model of experimental prostate cancer bone metastases. Gene Ther *12*, 702-714.

Massion, P.P., Taflan, P.M., Jamshedur Rahman, S.M., Yildiz, P., Shyr, Y., Edgerton, M.E., Westfall, M.D., Roberts, J.R., Pietenpol, J.A., Carbone, D.P*., et al.* (2003). Significance of p63 amplification and overexpression in lung cancer development and prognosis. Cancer Res *63*, 7113-7121.

Masumori, N., Thomas, T.Z., Chaurand, P., Case, T., Paul, M., Kasper, S., Caprioli, R.M., Tsukamoto, T., Shappell, S.B., and Matusik, R.J. (2001). A probasin-large T antigen transgenic mouse line develops prostate adenocarcinoma and neuroendocrine carcinoma with metastatic potential. Cancer Res *61*, 2239-2249.

McDade, S.S., Henry, A.E., Pivato, G.P., Kozarewa, I., Mitsopoulos, C., Fenwick, K., Assiotis, I., Hakas, J., Zvelebil, M., Orr, N*., et al.* (2012). Genome-wide analysis of p63 binding sites identifies AP-2 factors as co-regulators of epidermal differentiation. Nucleic Acids Res *40*, 7190-7206.

McGrath, J.A., Duijf, P.H., Doetsch, V., Irvine, A.D., de Waal, R., Vanmolkot, K.R., Wessagowit, V., Kelly, A., Atherton, D.J., Griffiths, W.A*., et al.* (2001). Hay-Wells syndrome is caused by heterozygous missense mutations in the SAM domain of p63. Hum Mol Genet *10*, 221-229.

McMenamin, M.E., Soung, P., Perera, S., Kaplan, I., Loda, M., and Sellers, W.R. (1999). Loss of PTEN expression in paraffin-embedded primary prostate cancer correlates with high Gleason score and advanced stage. Cancer Res *59*, 4291-4296.

McNeal, J.E. (1981a). Normal and pathologic anatomy of prostate. Urology *17*, 11-16.

McNeal, J.E. (1981b). The zonal anatomy of the prostate. Prostate *2*, 35-49.

McNeal, J.E. (1988). Normal histology of the prostate. Am J Surg Pathol *12*, 619-633.

Mellinger, G.T., Gleason, D., and Bailar, J., 3rd (1967). The histology and prognosis of prostatic cancer. J Urol *97*, 331-337.

Miller, D.C., Hafez, K.S., Stewart, A., Montie, J.E., and Wei, J.T. (2003). Prostate carcinoma presentation, diagnosis, and staging: an update form the National Cancer Data Base. Cancer *98*, 1169-1178.

Mills, A.A., Zheng, B., Wang, X.J., Vogel, H., Roop, D.R., and Bradley, A. (1999). p63 is a p53 homologue required for limb and epidermal morphogenesis. Nature *398*, 708-713.

Minelli, A., Bellezza, I., Conte, C., and Culig, Z. (2009). Oxidative stress-related aging: A role for prostate cancer? Biochim Biophys Acta *1795*, 83-91.

Mulholland, D.J., Xin, L., Morim, A., Lawson, D., Witte, O., and Wu, H. (2009). Lin-Sca-1+CD49fhigh stem/progenitors are tumor-initiating cells in the Pten-null prostate cancer model. Cancer Res *69*, 8555-8562.

Nedelcu, A.M., and Tan, C. (2007). Early diversification and complex evolutionary history of the p53 tumor suppressor gene family. Dev Genes Evol *217*, 801-806.

Nishioka, C., Ikezoe, T., Furihata, M., Yang, J., Serada, S., Naka, T., Nobumoto, A., Kataoka, S., Tsuda, M., Udaka, K*., et al.* (2013). CD34(+)/CD38(-) acute myelogenous leukemia cells aberrantly express CD82 which regulates adhesion and survival of leukemia stem cells. Int J Cancer *132*, 2006-2019.

Ocana, O.H., Corcoles, R., Fabra, A., Moreno-Bueno, G., Acloque, H., Vega, S., Barrallo-Gimeno, A., Cano, A., and Nieto, M.A. (2012). Metastatic colonization requires the repression of the epithelial-mesenchymal transition inducer Prrx1. Cancer Cell *22*, 709-724.

Osada, M., Ohba, M., Kawahara, C., Ishioka, C., Kanamaru, R., Katoh, I., Ikawa, Y., Nimura, Y., Nakagawara, A., Obinata, M*., et al.* (1998). Cloning and functional analysis of human p51, which structurally and functionally resembles p53. Nat Med *4*, 839-843.

Ousset, M., Van Keymeulen, A., Bouvencourt, G., Sharma, N., Achouri, Y., Simons, B.D., and Blanpain, C. (2012). Multipotent and unipotent progenitors contribute to prostate postnatal development. Nat Cell Biol *14*, 1131-1138.

Parsa, R., Yang, A., McKeon, F., and Green, H. (1999). Association of p63 with proliferative potential in normal and neoplastic human keratinocytes. J Invest Dermatol *113*, 1099-1105.

Parsons, J.K., Gage, W.R., Nelson, W.G., and De Marzo, A.M. (2001). p63 protein expression is rare in prostate adenocarcinoma: implications for cancer diagnosis and carcinogenesis. Urology *58*, 619-624.

Passegue, E., Wagner, E.F., and Weissman, I.L. (2004). JunB deficiency leads to a myeloproliferative disorder arising from hematopoietic stem cells. Cell *119*, 431-443.

Pellegrini, G., Dellambra, E., Golisano, O., Martinelli, E., Fantozzi, I., Bondanza, S., Ponzin, D., McKeon, F., and De Luca, M. (2001). p63 identifies keratinocyte stem cells. Proc Natl Acad Sci U S A *98*, 3156-3161.

Petrylak, D.P., Tangen, C.M., Hussain, M.H., Lara, P.N., Jr., Jones, J.A., Taplin, M.E., Burch, P.A., Berry, D., Moinpour, C., Kohli, M.*, et al.* (2004). Docetaxel and estramustine compared with mitoxantrone and prednisone for advanced refractory prostate cancer. N Engl J Med *351*, 1513-1520.

Pignon, J.C., Grisanzio, C., Geng, Y., Song, J., Shivdasani, R.A., and Signoretti, S. (2013). p63-expressing cells are the stem cells of developing prostate, bladder, and colorectal epithelia. Proc Natl Acad Sci U S A *110*, 8105-8110.

Price, D. (1963). Comparative Aspects of Development and Structure in the Prostate. Natl Cancer Inst Monogr *12*, 1-27.

Propping, P., and Zerres, K. (1993). ADULT-syndrome: an autosomal-dominant disorder with pigment anomalies, ectrodactyly, nail dysplasia, and hypodontia. Am J Med Genet *45*, 642-648.

Qin, J., Liu, X., Laffin, B., Chen, X., Choy, G., Jeter, C.R., Calhoun-Davis, T., Li, H., Palapattu, G.S., Pang, S.*, et al.* (2012). The PSA(-/lo) prostate cancer cell population harbors self-renewing long-term tumor-propagating cells that resist castration. Cell Stem Cell *10*, 556-569.

Ratnacaram, C.K., Teletin, M., Jiang, M., Meng, X., Chambon, P., and Metzger, D. (2008). Temporally controlled ablation of PTEN in adult mouse prostate epithelium generates a model of invasive prostatic adenocarcinoma. Proc Natl Acad Sci U S A *105*, 2521-2526.

Richardson, G.D., Robson, C.N., Lang, S.H., Neal, D.E., Maitland, N.J., and Collins, A.T. (2004). CD133, a novel marker for human prostatic epithelial stem cells. J Cell Sci *117*, 3539-3545.

Rocco, J.W., Leong, C.O., Kuperwasser, N., DeYoung, M.P., and Ellisen, L.W. (2006). p63 mediates survival in squamous cell carcinoma by suppression of p73-dependent apoptosis. Cancer Cell *9*, 45-56.

Romano, R.A., Smalley, K., Magraw, C., Serna, V.A., Kurita, T., Raghavan, S., and Sinha, S. (2012). DeltaNp63 knockout mice reveal its indispensable role as a master regulator of epithelial development and differentiation. Development *139*, 772-782.

Rowland, A., Miners, J.O., and Mackenzie, P.I. (2013). The UDP-glucuronosyltransferases: their role in drug metabolism and detoxification. Int J Biochem Cell Biol *45*, 1121-1132.

Senoo, M., Pinto, F., Crum, C.P., and McKeon, F. (2007). p63 Is essential for the proliferative potential of stem cells in stratified epithelia. Cell *129*, 523-536.

Shappell, S.B., Thomas, G.V., Roberts, R.L., Herbert, R., Ittmann, M.M., Rubin, M.A., Humphrey, P.A., Sundberg, J.P., Rozengurt, N., Barrios, R*., et al.* (2004). Prostate pathology of genetically engineered mice: definitions and classification. The consensus report from the Bar Harbor meeting of the Mouse Models of Human Cancer Consortium Prostate Pathology Committee. Cancer Res *64*, 2270-2305.

Shen, M.M., and Abate-Shen, C. (2010). Molecular genetics of prostate cancer: new prospects for old challenges. Genes Dev *24*, 1967-2000.

Signoretti, S., Pires, M.M., Lindauer, M., Horner, J.W., Grisanzio, C., Dhar, S., Majumder, P., McKeon, F., Kantoff, P.W., Sellers, W.R*., et al.* (2005). p63 regulates commitment to the prostate cell lineage. Proc Natl Acad Sci U S A *102*, 11355-11360.

Signoretti, S., Waltregny, D., Dilks, J., Isaac, B., Lin, D., Garraway, L., Yang, A., Montironi, R., McKeon, F., and Loda, M. (2000). p63 is a prostate basal cell marker and is required for prostate development. Am J Pathol *157*, 1769-1775.

Sniezek, J.C., Matheny, K.E., Westfall, M.D., and Pietenpol, J.A. (2004). Dominant negative p63 isoform expression in head and neck squamous cell carcinoma. Laryngoscope *114*, 2063-2072.

Sobel, R.E., and Sadar, M.D. (2005a). Cell lines used in prostate cancer research: a compendium of old and new lines--part 1. J Urol *173*, 342-359.

Sobel, R.E., and Sadar, M.D. (2005b). Cell lines used in prostate cancer research: a compendium of old and new lines--part 2. J Urol *173*, 360-372.

Stanbrough, M., Leav, I., Kwan, P.W., Bubley, G.J., and Balk, S.P. (2001). Prostatic intraepithelial neoplasia in mice expressing an androgen receptor transgene in prostate epithelium. Proc Natl Acad Sci U S A *98*, 10823-10828.

Su, X., Chakravarti, D., Cho, M.S., Liu, L., Gi, Y.J., Lin, Y.L., Leung, M.L., El-Naggar, A., Creighton, C.J., Suraokar, M.B*., et al.* (2010). TAp63 suppresses metastasis through coordinate regulation of Dicer and miRNAs. Nature *467*, 986-990.

Su, X., Paris, M., Gi, Y.J., Tsai, K.Y., Cho, M.S., Lin, Y.L., Biernaskie, J.A., Sinha, S., Prives, C., Pevny, L.H*., et al.* (2009). TAp63 prevents premature aging by promoting adult stem cell maintenance. cell stem cell *5*, 64-75.

Sugimura, Y., Cunha, G.R., and Donjacour, A.A. (1986). Morphogenesis of ductal networks in the mouse prostate. Biol Reprod *34*, 961-971.

Suh, E.K., Yang, A., Kettenbach, A., Bamberger, C., Michaelis, A.H., Zhu, Z., Elvin, J.A., Bronson, R.T., Crum, C.P., and

McKeon, F. (2006). p63 protects the female germ line during meiotic arrest. Nature *444*, 624-628.

Sunahara, M., Ichimiya, S., Nimura, Y., Takada, N., Sakiyama, S., Sato, Y., Todo, S., Adachi, W., Amano, J., and Nakagawara, A. (1998). Mutational analysis of the p73 gene localized at chromosome 1p36.3 in colorectal carcinomas. Int J Oncol *13*, 319-323.

Tang, Y., Hamburger, A.W., Wang, L., Khan, M.A., and Hussain, A. (2009). Androgen deprivation and stem cell markers in prostate cancers. Int J Clin Exp Pathol *3*, 128-138.

Termini, C.M., Cotter, M.L., Marjon, K.D., Buranda, T., Lidke, K.A., and Gillette, J.M. (2014). The membrane scaffold CD82 regulates cell adhesion by altering alpha4 integrin stability and molecular density. Mol Biol Cell *25*, 1560-1573.

Thanos, C.D., and Bowie, J.U. (1999). p53 Family members p63 and p73 are SAM domain-containing proteins. Protein Sci *8*, 1708-1710.

Thurfjell, N., Coates, P.J., Vojtesek, B., Benham-Motlagh, P., Eisold, M., and Nylander, K. (2005). Endogenous p63 acts as a survival factor for tumour cells of SCCHN origin. Int J Mol Med *16*, 1065-1070.

Timms, B.G., Mohs, T.J., and Didio, L.J. (1994). Ductal budding and branching patterns in the developing prostate. J Urol *151*, 1427-1432.

Tsai, J.H., Donaher, J.L., Murphy, D.A., Chau, S., and Yang, J. (2012). Spatiotemporal regulation of epithelial-mesenchymal transition is essential for squamous cell carcinoma metastasis. Cancer Cell *22*, 725-736.

Tucci, P., Agostini, M., Grespi, F., Markert, E.K., Terrinoni, A., Vousden, K.H., Muller, P.A., Dotsch, V., Kehrloesser, S., Sayan, B.S.*, et al.* (2012). Loss of p63 and its microRNA-205 target results in enhanced cell migration and metastasis in prostate cancer. Proc Natl Acad Sci U S A *109*, 15312-15317.

Urist, M.J., Di Como, C.J., Lu, M.L., Charytonowicz, E., Verbel, D., Crum, C.P., Ince, T.A., McKeon, F.D., and Cordon-Cardo, C. (2002). Loss of p63 expression is associated with tumor progression in bladder cancer. Am J Pathol *161*, 1199-1206.

Valkenburg, K.C., and Williams, B.O. (2011). Mouse models of prostate cancer. Prostate Cancer *2011*, 895238.

van Bokhoven, H., Jung, M., Smits, A.P., van Beersum, S., Ruschendorf, F., van Steensel, M., Veenstra, M., Tuerlings, J.H., Mariman, E.C., Brunner, H.G.*, et al.* (1999). Limb mammary syndrome: a new genetic disorder with mammary hypoplasia,

ectrodactyly, and other Hand/Foot anomalies maps to human chromosome 3q27. Am J Hum Genet *64*, 538-546.

Van Keymeulen, A., Rocha, A.S., Ousset, M., Beck, B., Bouvencourt, G., Rock, J., Sharma, N., Dekoninck, S., and Blanpain, C. (2011). Distinct stem cells contribute to mammary gland development and maintenance. Nature *479*, 189-193.

Verhagen, A.P., Ramaekers, F.C., Aalders, T.W., Schaafsma, H.E., Debruyne, F.M., and Schalken, J.A. (1992). Colocalization of basal and luminal cell-type cytokeratins in human prostate cancer. Cancer Res *52*, 6182-6187.

Vigano, M.A., and Mantovani, R. (2007). Hitting the numbers: the emerging network of p63 targets. Cell Cycle *6*, 233-239.

Visvader, J.E. (2011). Cells of origin in cancer. Nature *469*, 314-322.

Visvader, J.E., and Lindeman, G.J. (2012). Cancer stem cells: current status and evolving complexities. Cell Stem Cell *10*, 717-728.

Wang, J., Cai, Y., Ren, C., and Ittmann, M. (2006a). Expression of variant TMPRSS2/ERG fusion messenger RNAs is associated with aggressive prostate cancer. Cancer Res *66*, 8347-8351.

Wang, S., Gao, J., Lei, Q., Rozengurt, N., Pritchard, C., Jiao, J., Thomas, G.V., Li, G., Roy-Burman, P., Nelson, P.S.*, et al.* (2003). Prostate-specific deletion of the murine Pten tumor suppressor gene leads to metastatic prostate cancer. Cancer Cell *4*, 209-221.

Wang, S., Garcia, A.J., Wu, M., Lawson, D.A., Witte, O.N., and Wu, H. (2006b). Pten deletion leads to the expansion of a prostatic stem/progenitor cell subpopulation and tumor initiation. Proc Natl Acad Sci U S A *103*, 1480-1485.

Wang, S.I., Parsons, R., and Ittmann, M. (1998). Homozygous deletion of the PTEN tumor suppressor gene in a subset of prostate adenocarcinomas. Clin Cancer Res *4*, 811-815.

Wang, X., Kruithof-de Julio, M., Economides, K.D., Walker, D., Yu, H., Halili, M.V., Hu, Y.P., Price, S.M., Abate-Shen, C., and Shen, M.M. (2009). A luminal epithelial stem cell that is a cell of origin for prostate cancer. Nature *461*, 495-500.

Wang, Y., Hayward, S., Cao, M., Thayer, K., and Cunha, G. (2001). Cell differentiation lineage in the prostate. Differentiation *68*, 270-279.

Wang, Z.A., Mitrofanova, A., Bergren, S.K., Abate-Shen, C., Cardiff, R.D., Califano, A., and Shen, M.M. (2013). Lineage analysis of basal epithelial cells reveals their unexpected plasticity and supports a cell-of-origin model for prostate cancer heterogeneity. Nat Cell Biol *15*, 274-283.

Weinstein, M.H., Signoretti, S., and Loda, M. (2002). Diagnostic utility of immunohistochemical staining for p63, a sensitive marker of prostatic basal cells. Mod Pathol *15*, 1302-1308.

Whang, Y.E., Wu, X., Suzuki, H., Reiter, R.E., Tran, C., Vessella, R.L., Said, J.W., Isaacs, W.B., and Sawyers, C.L. (1998). Inactivation of the tumor suppressor PTEN/MMAC1 in advanced human prostate cancer through loss of expression. Proc Natl Acad Sci U S A *95*, 5246-5250.

Wu, J., Liang, S., Bergholz, J., He, H., Walsh, E.M., Zhang, Y., and Xiao, Z.X. (2014). DeltaNp63alpha activates CD82 metastasis suppressor to inhibit cancer cell invasion. Cell Death Dis *5*, e1280.

Wu, X., Senechal, K., Neshat, M.S., Whang, Y.E., and Sawyers, C.L. (1998). The PTEN/MMAC1 tumor suppressor phosphatase functions as a negative regulator of the phosphoinositide 3-kinase/Akt pathway. Proc Natl Acad Sci U S A *95*, 15587-15591.

Wu, X., Wu, J., Huang, J., Powell, W.C., Zhang, J., Matusik, R.J., Sangiorgi, F.O., Maxson, R.E., Sucov, H.M., and Roy-Burman, P. (2001). Generation of a prostate epithelial cell-specific Cre transgenic mouse model for tissue-specific gene ablation. Mech Dev *101*, 61-69.

Xin, L., Ide, H., Kim, Y., Dubey, P., and Witte, O.N. (2003). In vivo regeneration of murine prostate from dissociated cell populations of postnatal epithelia and urogenital sinus mesenchyme. Proc Natl Acad Sci U S A *100 Suppl 1*, 11896-11903.

Yang, A., Kaghad, M., Wang, Y., Gillett, E., Fleming, M.D., Dotsch, V., Andrews, N.C., Caput, D., and McKeon, F. (1998). p63, a p53 homolog at 3q27-29, encodes multiple products with transactivating, death-inducing, and dominant-negative activities. Mol Cell *2*, 305-316.

Yang, A., Schweitzer, R., Sun, D., Kaghad, M., Walker, N., Bronson, R.T., Tabin, C., Sharpe, A., Caput, D., Crum, C.*, et al.* (1999). p63 is essential for regenerative proliferation in limb, craniofacial and epithelial development. Nature *398*, 714-718.

Yang, A., Walker, N., Bronson, R., Kaghad, M., Oosterwegel, M., Bonnin, J., Vagner, C., Bonnet, H., Dikkes, P., Sharpe, A.*, et al.* (2000). p73-deficient mice have neurological, pheromonal and inflammatory defects but lack spontaneous tumours. Nature *404*, 99-103.

Ye, X., Lee, Y.C., Choueiri, M., Chu, K., Huang, C.F., Tsai, W.W., Kobayashi, R., Logothetis, C.J., Yu-Lee, L.Y., and Lin, S.H. (2011). Aberrant expression of katanin p60 in prostate cancer bone metastasis. Prostate *72*, 291-300.

Zhang, X.A., Lane, W.S., Charrin, S., Rubinstein, E., and Liu, L. (2003). EWI2/PGRL associates with the metastasis suppressor KAI1/CD82 and inhibits the migration of prostate cancer cells. Cancer Res *63*, 2665-2674.

Zhang, X.H., Jin, X., Malladi, S., Zou, Y., Wen, Y.H., Brogi, E., Smid, M., Foekens, J.A., and Massague, J. (2013). Selection of bone metastasis seeds by mesenchymal signals in the primary tumor stroma. Cell *154*, 1060-1073.

Zucchi, I., Astigiano, S., Bertalot, G., Sanzone, S., Cocola, C., Pelucchi, P., Bertoli, G., Stehling, M., Barbieri, O., Albertini, A.*, et al.* (2008). Distinct populations of tumor-initiating cells derived from a tumor generated by rat mammary cancer stem cells. Proc Natl Acad Sci U S A *105*, 16940-16945.